



POLITECNICO DI TORINO

Faculty of Engineering

Master of Science in Mechanical Engineering

Master Thesis

**Development of a model-based controller
of BMEP and NO_x emissions in a 3.0L
diesel engine and assessment by means
of the HiL methodology**

Supervisors

Prof. Ezio Spessa

Prof. Roberto Finesso

Prof. Stefano D'Ambrosio

Candidate

Alessandro Mancini

April 2018

Contents

1	Classification of Internal Combustion Engines	2
1.1	Spark Ignition Engine	2
1.2	Compression Ignition Engine	4
1.3	Combustion in CI engine	5
1.3.1	Ignition Delay	6
1.3.2	Premixed Phase	7
1.3.3	Mixing Controlled Phase	7
1.3.4	Late Combustion Phase.....	7
2	Pollutant Emissions in CI engine.....	8
2.1	Particulate Matter emissions	8
2.1.1	Nuclei mode particles	9
2.1.2	Accumulation mode particulates	10
2.1.3	Coarse mode particles.....	10
2.2	Nitrogen Oxides emissions	11
2.2.1	Thermal mechanism	12
2.2.2	Prompt mechanism.....	12
2.2.3	NO ₂ /NO Ratio.....	12
2.3	Dependence on Operating Conditions	13
2.3.1	Dependence on Equivalence Ratio	13
2.3.2	Dependence on Injection advance	14
2.3.3	Dependence on Residual gas content	16
2.3.4	Dependence on Injection Pressure	18
3	Heavy-duty Emission Legislative Framework.....	19
3.1	European Union Framework.....	19
3.1.1	ECE R-49 Test Cycles.....	20
3.1.2	ESC Test Cycles.....	21
3.1.3	ELR Test Cycles.....	22
3.1.4	ETC Test Cycles.....	23
3.1.5	WHSC Test Cycles.....	24
3.1.6	WHTC Test Cycles.....	25
4	Combustion Control Techniques	25
4.1	Control Systems Structure	25
4.1.1	Open Loop Control.....	26

4.1.2	Closed Loop Control.....	26
4.2	Model-Based Control	27
5	Model-Based Control of BMEP and Model-Based/Closed Loop Control of NOx.....	28
5.1	Engine Setup.....	28
5.2	Combustion Model Description	29
5.3	Steps to Validate a Control Algorithm	30
5.3.1	The Model in the Loop Phase	30
5.3.2	The Hardware in the Loop Phase.....	35
5.3.3	Rapid Prototyping.....	36
5.4	Hardware and Software related to HiL	37
5.4.1	The Engine Emulator	37
5.4.2	The Rapid Prototyping Device.....	40
6	Model in the Loop Results.....	44
6.1	BMEP Target Profile and Constant NOx Target and Speed	44
6.2	NOx Target Profile and Constant BMEP Target and Speed	48
6.2.1	BMEP Target of 2 bar.....	48
6.2.2	BMEP Target of 8 bar.....	51
6.2.3	BMEP Target of 14 bar.....	54
6.3	BMEP Target Profile, NOx Target Profile and Speed Profile	57
7	Hardware in the Loop Results.....	61
8	Conclusion.....	64
9	Bibliography.....	65

List of Figures

Figure 1.1: Flame front propagation	2
Figure 1.2: Burning velocity without turbulence.....	3
Figure 1.3: Pressure profile without knock, with slight knock and with intensive knock.	3
Figure 1.4: Behaviors of pressure, fuel injected, ignited and burned over time.	5
Figure 1.5: Pressure trend and heat release curve as a function of crank angle.	6
Figure 1.6: Heat Release Rate (HRR).....	7
Figure 2.1: Percentage of combustion products.	8
Figure 2.2: Particulate Matter.	9
Figure 2.3: Composition of Nuclei Mode and Accumulation Mode particles.....	10
Figure 2.4: Mass and Number Distribution of PM particles.	11
Figure 2.5: NO ₂ as percent of total NO _x in Diesel exhaust as function of load and speed.	13
Figure 2.6: NO _x as a function of equivalence ratio.	14
Figure 2.7: NO _x and particulates as the air to fuel ratio varies. NO _x in blue and PM in red.	14
Figure 2.8: NO _x dependence on SOI.....	15
Figure 2.9: NO _x BSFC trade-off.	15
Figure 2.10: PMNO _x trade-off.....	16
Figure 2.11: Flame region increment due to EGR recirculation.	16
Figure 2.12: Effect of EGR versus injection timing retard on BSFC.....	17
Figure 2.13: BSFC according to SOI for different injection pressures.	18
Figure 2.14: NO _x according to SOI for different injection pressures.	18
Figure 3.1: ETC speed profile.	24
Figure 3.2: WHTC torque and speed profiles.	25
Figure 4.1: Open Control Loop.	26
Figure 4.2: Feedforward Control.	26
Figure 4.3: Closed Loop System.	27
Figure 5.1: F1C Engine.....	29
Figure 5.2: Scheme of the real-time combustion model.	30
Figure 5.3: Simulink block containing the control system.	31
Figure 5.4: GT-ISE Fast Running Model	32
Figure 5.5: Connection tool between engine model and control system.....	32
Figure 5.6: Scheme for a model in the loop testing.	33
Figure 5.7: SOI correction coefficient.	33
Figure 5.8: q correction coefficient.....	34
Figure 5.9: Flow chart of the BMEPNO _x controller.	34
Figure 5.10: First-Order Filter.	35
Figure 5.11: Hardware in the Loop Setup.....	36
Figure 5.12: Rapid Prototyping test at Denerg Laboratory.....	37
Figure 5.13: NI-PXIe1082.....	38
Figure 5.14: Build VeriStand Setup.	39
Figure 5.15: VeriStand Interface.....	40
Figure 5.16: ETAS ES910.....	41

Figure 5.17: Build Intecrio Setup.	41
Figure 5.18: Intecrio Interface.	43
Figure 6.1: Model Based Control, BMEP result.	44
Figure 6.2: Model Based Control, NOx result.	45
Figure 6.3: Model Based/Closed Loop Control, BMEP result.	46
Figure 6.4: Model Based/Closed Loop Control, NOx result.	46
Figure 6.5: Model based control compared with Model Based/Closed Loop Control, BMEP results.	47
Figure 6.6: Model based control compared with Model Based/Closed Loop Control, NOx results.	47
Figure 6.7: Model Based Control, BMEP target=2, BMEP result.	48
Figure 6.8: Model Based Control, BMEP target=2, NOx result.	49
Figure 6.9: Model Based/Closed Loop control, BMEP target=2, BMEP result.	49
Figure 6.10: Model Based/Closed Loop control, BMEP target=2, NOx result.	50
Figure 6.11: Model based control compared with Model Based/Closed Loop Control, BMEP target=2, BMEP results.	50
Figure 6.12: Model based control compared with Model Based/Closed Loop Control, BMEP target=2, NOx results.	51
Figure 6.13: Model Based Control, BMEP target=8, BMEP result.	51
Figure 6.14: Model Based Control, BMEP target=8, NOx result.	52
Figure 6.15: Model Based/Closed Loop control, BMEP target=8, BMEP result.	52
Figure 6.16: Model Based/Closed Loop control, BMEP target=8, NOx result.	53
Figure 6.17: Model based control compared with Model Based/Closed Loop Control, BMEP target=8, BMEP results.	53
Figure 6.18: Model based control compared with Model Based/Closed Loop Control, BMEP target=8, NOx results.	54
Figure 6.19: Model Based Control, BMEP target=14, BMEP result.	54
Figure 6.20: Model Based Control, BMEP target=14, NOx result.	55
Figure 6.21: Model Based/Closed Loop control, BMEP target=14, BMEP result.	55
Figure 6.22: Model Based/Closed Loop control, BMEP target=14, NOx result.	56
Figure 6.23: Model based control compared with Model Based/Closed Loop Control, BMEP target=14, BMEP results.	56
Figure 6.24: Model based control compared with Model Based/Closed Loop Control, BMEP target=8, NOx results.	57
Figure 6.25: Model Based Control, BMEP result.	58
Figure 6.26: Model Based Control, NOx result.	58
Figure 6.27: Model Based/Closed Loop Control, BMEP result.	59
Figure 6.28: Model Based/Closed Loop Control, NOx result.	59
Figure 6.29: Model based control compared with Model Based/Closed Loop Control, BMEP results.	60
Figure 6.30: Model based control compared with Model Based/Closed Loop Control, NOx results.	60
Figure 7.1: Simulink Engine Model.	61
Figure 7.2: Model Based/Closed Loop Control, BMEP result.	62
Figure 7.3: Model Based/Closed Loop Control, NOx result.	62

List of Tables

Table 3.1: EU Emission Standards for Heavy-Duty Diesel.	20
Table 3.2: ECE R-49 Test Cycles.	21
Table 3.3: ESC Test Cycles.	22
Table 3.4: ELR Test Cycles.	23
Table 3.5: WHSC Test Cycles.	24
Table 5.1: F1C Engine specifications.	28
Table 7.1: Number of cycle iterations.	63
Table 7.2: NetRunTime.	63
Table 7.3: Average iteration time.	63

Nomenclature

τ	Ignition delay
λ	Air–fuel equivalence ratio
ϕ	Fuel-air equivalence ratio
q	Injected fuel
NO _x	Nitrogen Oxides
Soot	Black carbon
PM	Particulate matter
HRR	Rate of heat released
TDC	Top dead centre
C _x H _y	Hydrocarbons
PAH	Polycyclic aromatic hydrocarbon
SOL	Solid fraction
SOF	Soluble organic fraction
SO ₄	Sulfate particulates
EGR	Exhaust Gas Recirculation
SOI	Start Of Injection
BSFC	Brake specific fuel consumption
GHG	Greenhouse gas
ETC	European Transient Cycle
ESC	European Stationary Cycle
ELR	European Load Response
WHSC	World Harmonized Stationary Cycle
WHTC	World Harmonized Transient Cycle
ECUs	Engine Control Units
CFD	Computational Fluid Dynamics
BMEP	Brake Mean Effective Pressure
FMEP	Friction Mean Effective Pressure
IMEP	Indicated Mean Effective Pressure
PMEP	Pumping Mean Effective Pressure
MIL	Model in the Loop
HIL	Hardware in the Loop

RP	Rapid Prototyping
PXI	PCI eXtensions for Instrumentation
PCI	Peripheral Component Interconnect

Abstract

The increasing computational performance of modern engine control units (ECUs) allows to develop and implement more and more complex combustion control techniques in diesel engines. Special attention has been paid to the development of pollutant emission control systems due to the increasing stringency of regulations especially as regards the emissions of nitrogen oxides and particulate matter.

In general, control algorithms include closed loop approaches, model based techniques, or a combination of the two previous methods. Model based controls follow an open loop logic and consequently do not use a feedback loop to ensure that the output has actually reached the desired target value and therefore do not correct any errors they commit. For this reason, an optimal solution is to add a closed loop control to the model based one in order to correct any errors related to combustion model.

In this work, a feedback NO_x control system was developed and subsequently integrated with a model based control [1] which is based on a zero dimensional real time combustion model and which is able to simulate BMEP and NO_x engine out levels. This model based control is able to correctly estimate BMEP but, on the contrary, it is not very precise in terms of NO_x ; the closed loop part has been implemented in order to correct the NO_x error. The parameters on which we operate to control NO_x and BMEP are the start of injection and the injected fuel quantity, respectively.

The algorithm development procedure followed two phases. During the Model in the loop phase, the algorithm has been tested at different speed and load conditions to prove its validity under different working conditions. During the Hardware in the loop phase, the controller has been implemented onto a rapid prototyping device to simulate its real time behavior and determine its computational time.

In the near future, the controller will be tested on the engine installed at the test bench through rapid prototyping. Furthermore, the controller will be further modified by increasing the number of control variables, for example EGR and boost pressure.

Chapter

1 Classification of Internal Combustion Engines

Internal combustion engines can be classified according to the combustion process:

- Spark ignition engine: whose combustion is triggered by the sparkling of a spark.
- compression ignition engines: in which the fuel, injected into the compressed air inside the cylinder, spontaneously ignites itself.

1.1 Spark Ignition Engine

Low reactivity fuels are used in these engines. In fact, such fuels, mixed with combustion air, although in conditions of high pressure and temperature, do not spontaneously give rise to combustion reactions. Fuels typically used have a similar chemical structure: they have an extremely rigid and compact molecule. The more the molecule is stiff and compact the longer the oxidation processes prior to combustion take time. The only way to start the combustion process is to trigger it from the outside, causing an electric spark between two electrodes. The fuel / air mixture at the spark's location reaches very high temperatures. At these temperatures even low reactivity fuels are able to proceed with oxidation in a rapid almost instantaneous way generating combustion. The process, once triggered in this first nucleus, propagates to the rest of the charge gradually and progressively: the first nucleus transmits heat to the adjacent mixture layer, raising its temperature to such a level that even here the reactions of combustion start. This second layer of mixture, once combustion is achieved, transmits heat to the adjacent mixture which in turn transmits to a third layer and so on. Therefore combustion occurs by flame front propagation.



Figure 1.1: Flame front propagation

The spark ignition engine combustion, which occurs in gaseous and premixed phase, is a process that takes place under turbulent conditions. Turbulent motions are fundamental for the development of the combustion process since the burning velocity of a mixture in stillness is very low, of the order of centimeter per second. This speed is not sufficient and it must be increased through turbulent motions.

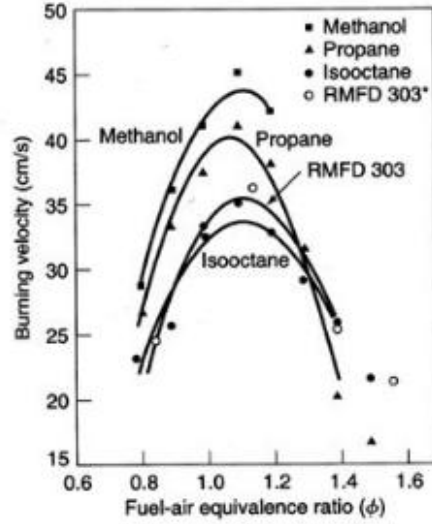


Figure 1.2: Burning velocity without turbulence.

Looking at the diagram, it is clear that it is necessary that the air-fuel ratio must be maintained stoichiometric when the load changes. In this way the burning velocity does not collapse and remains maximum when the load changes. A significant advantage of the combustion process of spark ignition engines is that it adapts to the variation of the engine rotation speed. In fact, the turbulence intensity is directly proportional to this. As the speed of rotation increases, the intensity of turbulence increases and therefore also the flame velocity. This allows ignition engines to have ideally no limits in terms of speed regarding the combustion process. This capacity does not belong to diesel engines. However, the spark ignition engines have a bore limit which is generally of the order of 100 mm. In fact, as the bore increases, the combustion anomalies increase too. The most important anomaly is the detonation or knock. The detonation is the simultaneous self-ignition of the endgas that is the last fraction of mixture that should be reached by the flame. Simultaneous combustion gives rise to an extremely abrupt increase in pressure. This determines the propagation of overpressure waves that generate vibrations and therefore noise and damage the motor members.

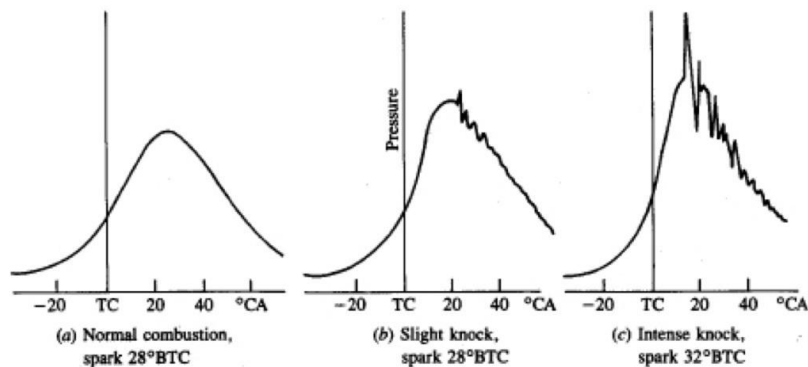


Figure 1.3: Pressure profile without knock, with slight knock and with intensive knock.

The risk of detonation is the most stringent constraint for a spark ignition engine.

1.2 Compression Ignition Engine

High reactivity fuels are used in these engines; they are characterized by a long and flexible molecular structure that allows intermediate reactions to take place very quickly in conditions of high pressure and high temperature. Because of their high reactivity, fuel and oxidizer are mixed only a moment before the combustion process takes place. The fuel is injected liquid into a high density air environment in the form of high pressure sprays. This jet shatters into a myriad of tiny microscopic droplets impacting the wall of air. Such droplets are liquid and are surrounded by hot air. The heat flow of the air surrounding the droplet is extremely intense and leads to its evaporation in an extremely short time. In times of the order of milliseconds, the liquid fuel evaporates and mixes with the surrounding air; since the fuel is extremely reactive, the combustion process is able to start spontaneously without the use of an external primer. There is no longer a flame front propagation inside a homogeneous mixture as in the spark ignition engine; in fact the mixture is heterogeneous: there is a very wide range of air fuel ratio during the combustion process. Since the fuel is very reactive, it is able to burn even with air fuel ratio values relatively far from the stoichiometric. Burning under very low air fuel ratio conditions, we tend to have a process of dehydrogenization of the molecule that leads to the formation of carbon skeletons which give rise to solid carbon particles responsible for particulate emissions and therefore the black smoke characteristic of Diesel engines. A major advantage that diesel engines have over petrol engines is that they can work in variable dosing conditions. In fact the combustion process is not based on flame propagation and therefore it is not necessary to work under stoichiometric conditions in order to obtain the maximum burning velocity. So there is no problem to let the engine draw the same amount of air as the load changes. This allows to avoid bottlenecks, rolling, penalizing for the yield.

1.3 Combustion in CI engine

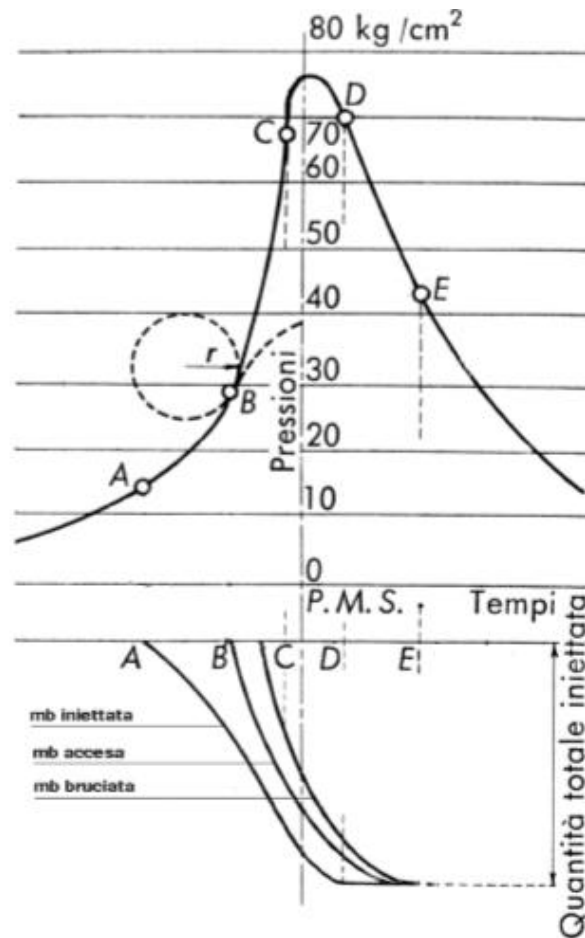


Figure 1.4: Behaviors of pressure, fuel injected, ignited and burned over time.

Combustion does not start exactly when the first droplets of diesel are injected into the cylinder (A), but there is a certain delay (AB) of the order of milliseconds. The time interval between the beginning of the injection (A) and the effective start of the combustion (B) is called ignition delay, τ . This time is necessary for heating, vaporization and mixing of the fuel. During this time an accumulation of diesel particles is generated. Once the self-ignition conditions (B) have been reached, the accumulated fuel burns at the same time following an almost isochoric transformation (positive from the point of view of efficiency), resulting in a sudden increase in pressure in the combustion chamber. This implies an impulsive stress responsible for the onset of noise, vibrations. The phenomenon of accumulation and therefore the characteristic noise of the diesel is very marked in idling conditions after a cold start; in these conditions little fuel is injected and the temperatures in the room are low.

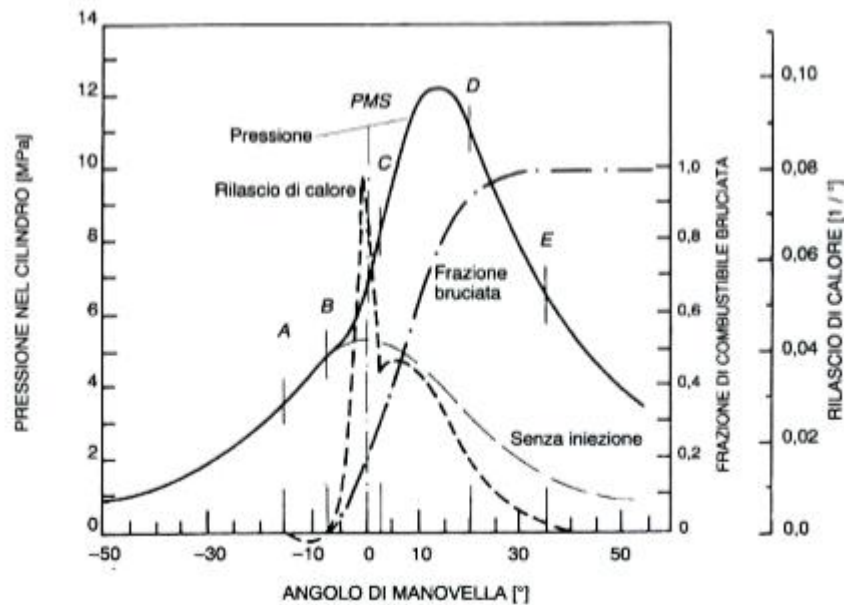


Figure 1.5: Pressure trend and heat release curve as a function of crank angle.

By observing the pressure trend and the heat release curve (HRR) as a function of crank angle, four phases can be identified:

1. Ignition delay (AB).
2. Premixed phase (BC).
3. Mixing controlled phase (CD)
4. Late combustion phase (DE)

1.3.1 Ignition Delay

This delay is due to phenomena of physical and chemical nature.

Physical phenomena are:

- Atomization of the injected fuel jet.
- Evaporation of the droplets.
- Mixing of fuel vapors with the combustion air.

Chemical phenomena are:

- Reactions with formation of intermediate compounds.

Between the two phenomena the physical is more relevant, since the fuel is highly reactive. The jet atomization takes place through a break-up process during which the aerodynamic forces shatter the liquid column into a myriad of microscopic droplets. Atomization improves if:

- Decreases the diameter of the efflux hole and therefore the initial diameter of the liquid jet.
- Increases the injection pressure and therefore the jet speed.
- Decreases the viscosity of the liquid.
- Decreases the surface tension of the liquid.
- Increases air density.

As it has been said previously, the drawback of ignition delay is the simultaneous combustion of accumulation which damages combustion chamber components and causes vibrations and therefore noise. The use of a pilot injection can help to reduce the ignition delay. In fact the main fuel will find high temperature and pressure conditions thanks to the previous combustion of the pilot fuel. This allows to obtain a contained accumulation and a much gentler pressure trend.

1.3.2 Premixed Phase

The premixed phase corresponds to the combustion of the fuel accumulated during the ignition delay. In this phase, NO_x formation does not occur because the mixture is rich, $\lambda=0.25\div0.5$. However, very high temperatures are reached as a result of an almost isochoric combustion favoring the development of NO_x during next phases.

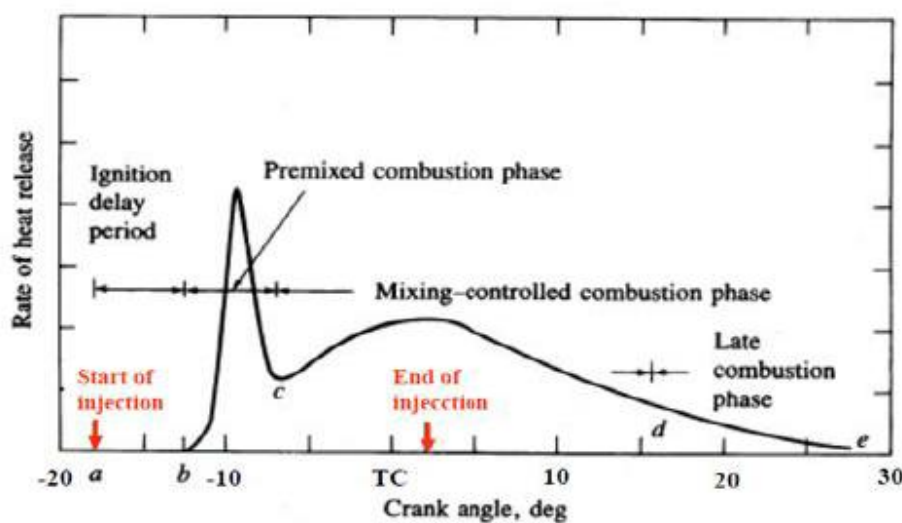


Figure 1.6: Heat Release Rate (HRR).

Observing the heat release diagram, it is easy to notice that the almost simultaneous combustion of the accumulated fuel leads to a peak in HRR.

1.3.3 Mixing Controlled Phase

Only a modest fraction of the fuel burns during the premixed phase. Most of the combustion process occurs during the subsequent diffusion phase (mixing controlled phase) in which the speed of the process is controlled by the rapidity with which the fuel vapors and the oxidising air are mixed. In fact, in this phase, the times necessary for mixing are significantly higher than both those required for evaporation and those required by chemical kinetics. The main problem is to ensure that all the injected fuel will find enough oxygen to react due to the progressive increase of exhaust gases inside the combustion chamber. Therefore, during this phase, unburned carbon nuclei (soot) can be formed for dehydrogenation, condensation and pyrolysis processes.

1.3.4 Late Combustion Phase

The injection is now finished but the chemical reactions are still running out gradually. In this phase the combustion can involve soot formed during the diffusion phase allowing

its oxidation. This phase must not be prolonged too much to avoid reducing the efficiency of the engine; in fact, in order to have high engine performance, it is necessary to concentrate as much as possible the release of heat around the TDC.

Chapter

2 Pollutant Emissions in CI engine

Although ideal combustion reaction of a hydrocarbon fuel C_xH_y should lead to non-toxic combustion products (CO_2, O_2, H_2O, N_2 plus O for lean mixtures), the real combustion process in internal combustion engines produces pollutant emissions (generally about 1% of all combustion products), mainly represented by CO , HC , NO_x and PM . Although CO_2 is not a toxic combustion product, it is greenhouse gas and a major cause of the so called “global warming” and should therefore be kept at a minimum as well.

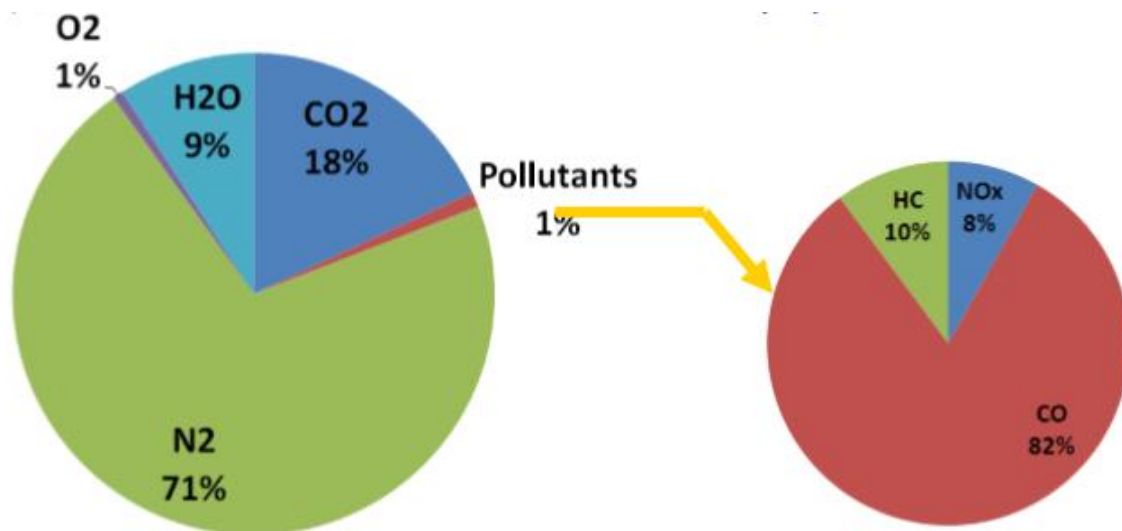


Figure 2.1: Percentage of combustion products.

2.1 Particulate Matter emissions

Particulate Matter is defined as any matter in the exhaust of an internal combustion engine that can be trapped on a sampling filter medium at 125 °F (52°C). Diesel particulates are composed of elemental carbon particles which agglomerate and adsorb other species (mainly unburned hydrocarbons and sulfates) to form structures of complex physical and chemical properties.

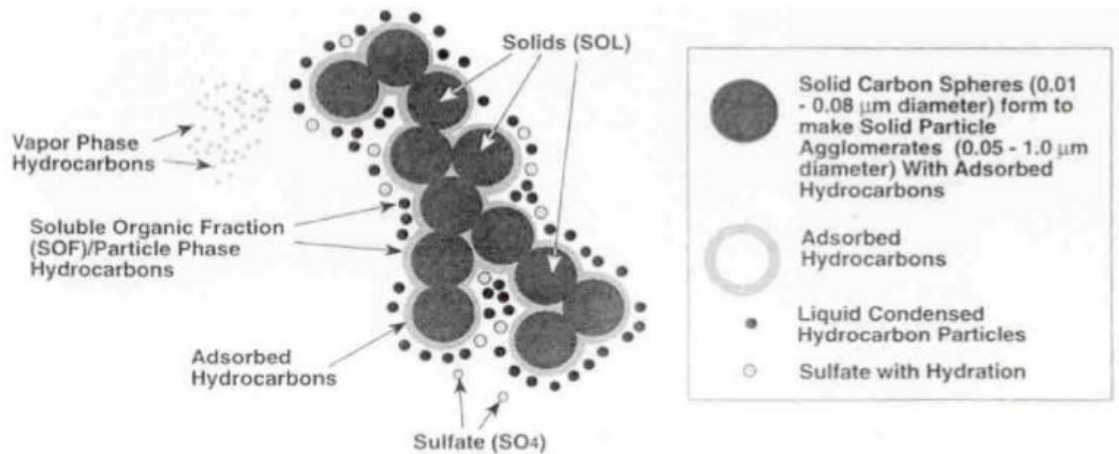


Figure 2.2: Particulate Matter.

Initial soot formation occurs in a very rich environment ($\phi > 4$) at relatively low temperatures (1600K), triggered by premixed burning. In this initial formation process, aromatics condensation reactions dominate, and lead to the formation of the PAH structures that lead to soot. For this reason, PAH are called “soot-precursors”. Then, in the area close to the diffusion flame, where temperature are higher, also aliphatic components may be transformed through pyrolysis and cracking to produce soot with an indirect, slower path. Based on analysis performed by a combination of physical and chemical methods, PM is traditionally divided into three main fractions, which can be further sub-categorized, as follows:

1. Solid fraction (SOL):
 - Elemental carbon.
 - Ash.
2. Soluble organic fraction (SOF) :
 - Organic material derived from engine lubricating oil.
 - Organic material derived from fuel.
3. Sulfate particulates (SO₄) :
 - Sulfuric acid.
 - Water.

Particulate particles can also be classified according to the creation process:

1. Nuclei mode particles.
2. Accumulation mode particulates.
3. Coarse mode particles.

2.1.1 Nuclei mode particles

It is believed that nuclei mode particles (3-40 nm) are primarily volatile and consist mainly of hydrocarbon and hydrated sulfuric acid condensates which are formed from

gaseous precursors as T decreases in the exhaust system and after mixing with cold air. These volatile particles are very unstable; their concentrations strongly depend on dilution conditions such as dilution ratio and residence time. A small amount of nuclei mode particles may consist of solid material, such as carbon or metallic ash from lube oil additives. Nuclei mode particles constitute the majority of particle number but only a few percent of the PM mass. The maximum concentration of nuclei mode particles occurs at 10-20 nm. The nuclei mode, depending on the engine technology and particle sampling technique, typically contains only from 0.1 to 10% of the total PM mass, but it often includes more than 90% of the total particle count. Sometimes the nuclei mode particles present as much as 99% of the total particulate number.

2.1.2 Accumulation mode particulates

Accumulation mode particulates are formed by agglomeration of primary carbon particles and other solid materials, accompanied by adsorption of gases and condensation of vapors. They are composed mainly of solid carbon mixed with condensed heavy hydrocarbons, but may also include sulfur compounds, metallic ash, cylinder wear metals, etc. Diameters of the accumulation mode particles are between approximately 0.03 and 0.5 μm with a maximum concentration between 0.1 and 0.2 μm . Most PM mass emission, but only a small proportion of the total particle number, is composed of agglomerated particles.

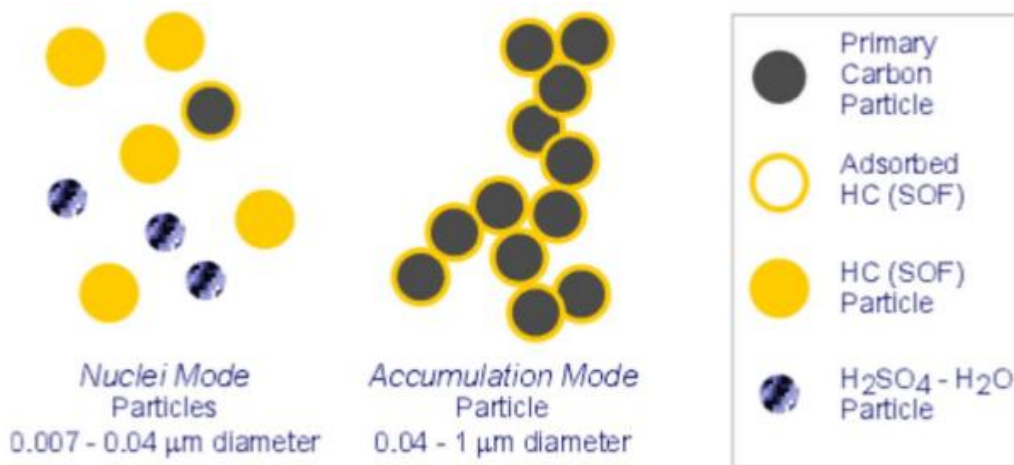


Figure 2.3: Composition of Nuclei Mode and Accumulation Mode particles.

2.1.3 Coarse mode particles

These particles with aerodynamic diameters above 1 μm contain from 5 to 20% of the total PM mass and practically no contribution to particle numbers. The coarse particles are not generated in the diesel combustion process. Rather, they are formed through deposition and subsequent re-entrainment of particulate material from walls of the engine cylinder, exhaust system, or the particulate sampling system.

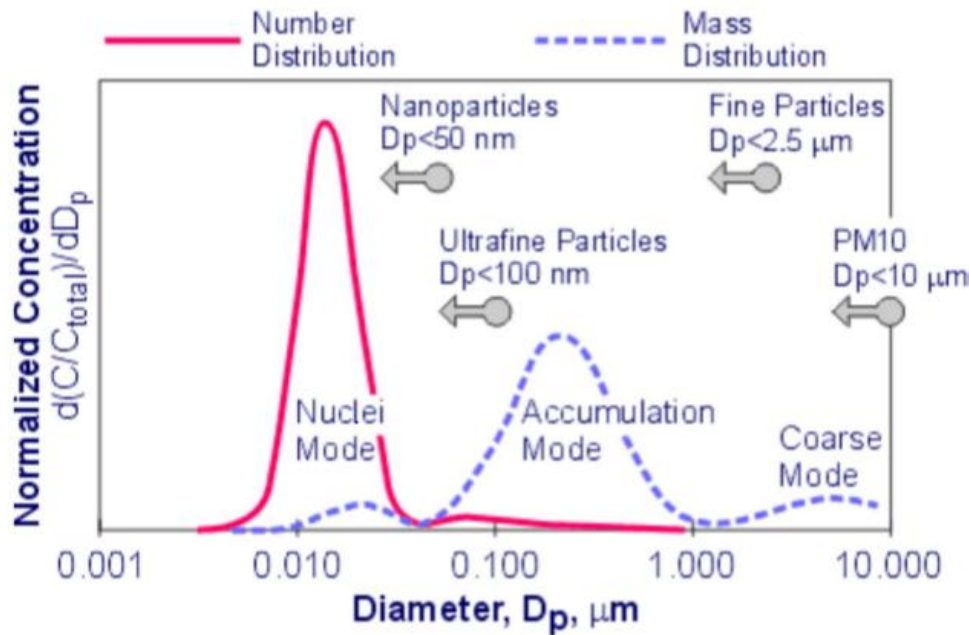


Figure 2.4: Mass and Number Distribution of PM particles.

The nucleation mode becomes even more pronounced when PM after treatment is used. A particulate filter removes the solid fraction efficiently (by more than 99%, if a wall-flow filter is used), while the volatile fraction passes through the filter in the gas phase.

2.2 Nitrogen Oxides emissions

In the past, the portion of charge burned in the initial premixed portion of the heat release profile during diesel combustion was believed to be the principal source of NO_x formation. However, work at General Motors in the 1980s suggested that this was not the case and that the diffusion burning region may be the primary source of NO_x . Work at Sandia later showed that the premixed burning phase of the diesel combustion process occurs under very fuel rich conditions under which very little NO_x actually forms due to low oxygen concentrations and low temperatures and that the diffusion burning region is indeed the primary source of NO_x . Nevertheless, the premixed portion of the fuel, mixed during the ignition delay, which burns before the time of peak cylinder pressure, is particularly important for NO_x formation, because even if NO_x formation during premixed combustion can be not significant, after it has burned, it is compressed to a higher pressure and temperature and so reaches the highest temperature of any portion of the cylinder charge. For this reason, techniques to control NO_x focus on this early phase of combustion. Unfortunately, most of these techniques resort to reducing combustion temperatures. In so doing, they lead to penalties in hydrocarbon emissions, particulate emissions, and fuel consumption.

The mechanisms of formation of nitrogen oxides are:

1. *Thermal mechanism*: during the combustion process the O_2 and N_2 molecules are decomposed into O and N due to the high temperatures. These, in turn, are recombined giving rise to NO and NO_2 .

2. *Prompt mechanism*: a chain reaction mechanism promoted by nitrogen atoms that react with CH radicals that are present in the flame front zone.

Furthermore, in case nitrogen is chemically bound to fuel, part of NO_x can derive from the fuel itself: before fuel enters the flame zone, nitrogen is transformed into radicals or compounds containing the CN group which, in turn, are oxidized to form NO in the flame zone.

2.2.1 Thermal mechanism

Lavoie in 1970 proposed a kinetic model based on 6 equations:

1. $\text{NO} + \text{N} \leftrightarrow \text{N}_2 + \text{O}$
2. $\text{N} + \text{O}_2 \leftrightarrow \text{NO} + \text{O}$
3. $\text{N} + \text{OH} \leftrightarrow \text{NO} + \text{H}$
4. $\text{H} + \text{N}_2\text{O} \leftrightarrow \text{N}_2 + \text{OH}$
5. $\text{O} + \text{N}_2\text{O} \leftrightarrow \text{N}_2 + \text{O}_2$
6. $\text{O} + \text{N}_2\text{O} \leftrightarrow \text{NO} + \text{NO}$

The main mechanism of NO_x formation consists of the first three equations listed above and is called the thermal mechanism of Zeldovich-Keck.

The reaction speed constant varies according to the law:

$$k = aT^b e^{-\left(\frac{A}{RT}\right)}$$

Where a, b, A are constant characteristics of the reaction in question, R is the universal constant of perfect gases and T is the absolute temperature.

2.2.2 Prompt mechanism

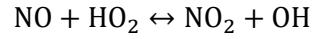
The formation process of NO_x according to this mechanism is extremely rapid (hence the name of prompt mechanism) and is poorly influenced by temperature. Lavoie and Blumberg in 1973 observed that the only thermal mechanism was not able to correctly predict the NO_x levels measured in the motor. It was also necessary to consider the prompting mechanism to contribute to the formation of NO_x , even if to a lesser extent. The equations that regulate the following mechanism are:

7. $\text{CH} + \text{N}_2 \leftrightarrow \text{HCN} + \text{N}$
8. $\text{HCN} \xrightarrow{+\text{O}} \text{NCO} \xrightarrow{+\text{H}} \text{NH} \xrightarrow{+\text{H}} \text{N} \xrightarrow{+\text{O}_2, +\text{OH}} \text{NO}$

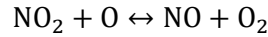
Therefore, the chain reaction mechanism is promoted by nitrogen atoms unlike the mechanism proposed by Zeldovich in which the chain of reactions is promoted by oxygen.

2.2.3 NO_2/NO Ratio

Depending on the chemical equilibrium conditions in the combustion gases, the NO_2/NO ratio should be small and negligible. However, in Diesel engines the NO_2 levels can reach from 10% to 30% of the total NO_x emissions. In fact, NO produced in the flame zone can be rapidly converted into NO_2 :



Later , the conversion from NO_2 to NO should take place:



The latter reaction can be frozen due to mixing with a colder fluid such as excess air and flue gases at lower temperatures. The mechanism is consistent with the fact that the highest NO_2/NO ratios in Diesel are found at low loads, where the colder regions that can freeze the decomposition of NO_2 are more numerous in the chamber.

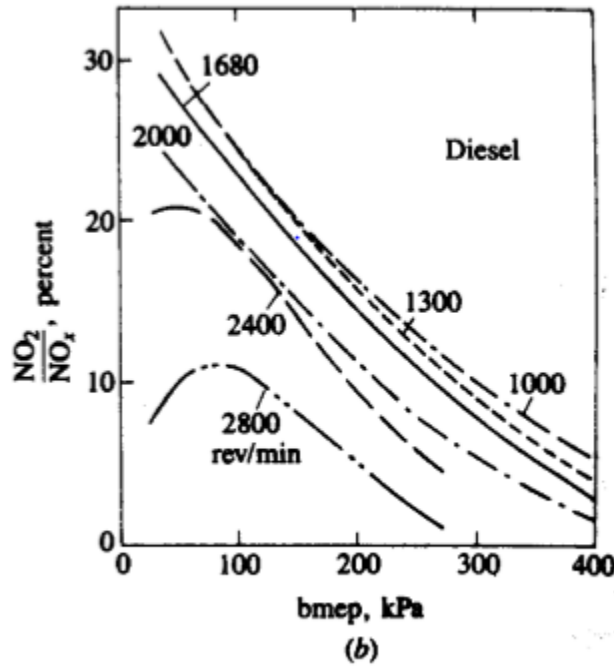


Figure 2.5: NO_2 as percent of total NO_x in Diesel exhaust as function of load and speed.

2.3 Dependence on Operating Conditions

The main operating parameters on which emissions depend are the following:

- Equivalence ratio.
- Injection advance.
- Residual gas content.
- Injection pressure.

2.3.1 Dependence on Equivalence Ratio

The concentration of NO_x decreases as the load decreases, but much less than in the case of spark ignition engines, since their formation depends on the local fuel air ratio. If the temperatures and pressures do not vary too much, the NO_x emitted should be reduced almost proportionally to the amount injected [2].

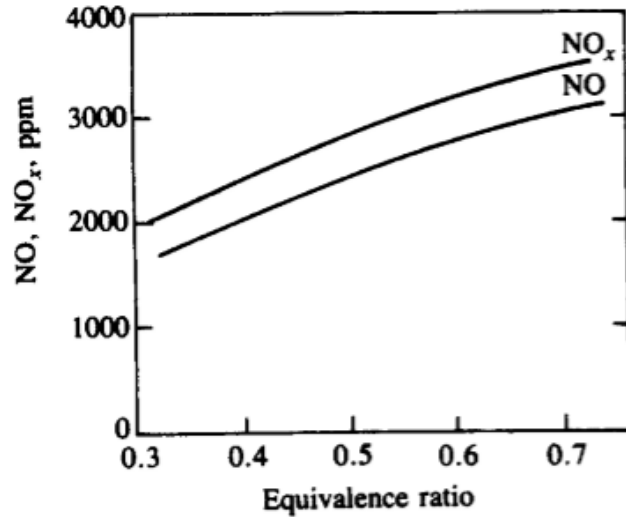


Figure 2.6: NO_x as a function of equivalence ratio.

The particulate emissions are extremely sensitive to the engine load, and show a marked increase as the load increases (i.e. as the air to fuel ratio decreases).

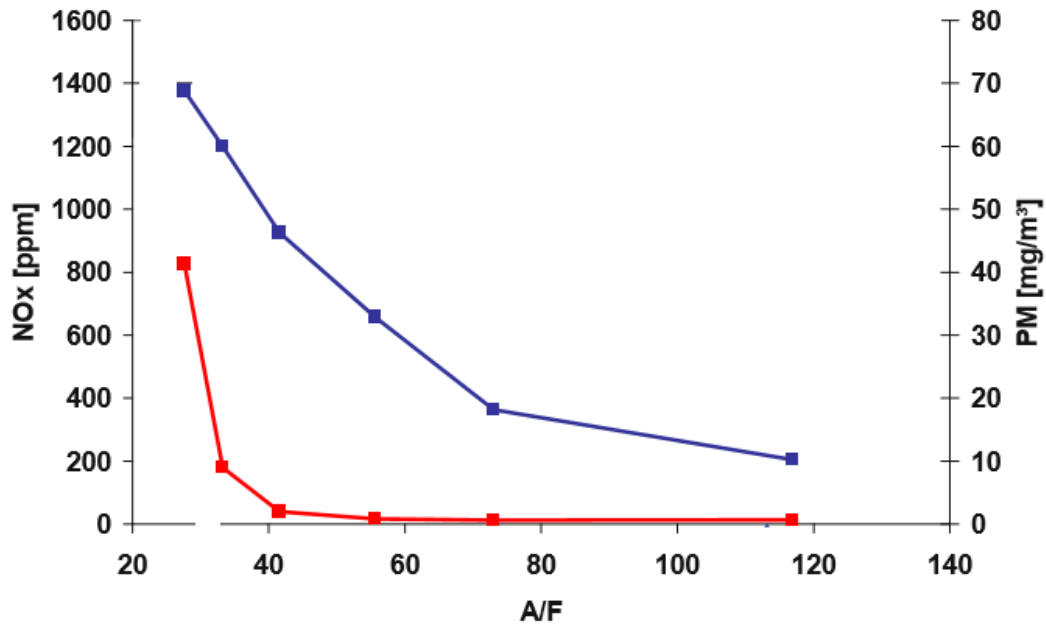


Figure 2.7: NO_x and particulates as the air to fuel ratio varies. NO_x in blue and PM in red.

2.3.2 Dependence on Injection advance

Injection timing advance appears to extend the ignition delay. The reason for this observation is that fuel is injected into a lower pressure medium having lower temperature. The longer the ignition delay, the greater the portion of fuel injected during that period, and the better the chance for it to mix with air. In other words, the earlier the fuel is injected, the longer the ignition delay, and the greater the premixed portion of the fuel prior to ignition. Higher NO_x formation is usually related to the premixed portion of the fuel. As injection timing is retarded, the opposite effect is

experienced. Ignition delay tends to be shorter and ultimately, the premixed portion of the fuel is reduced. Reducing the premixed fuel portion leads to lower NO_x formation. Since retarding injection timing has a desirable effect on NO_x formation, it has become an effective means to control NO_x emissions.

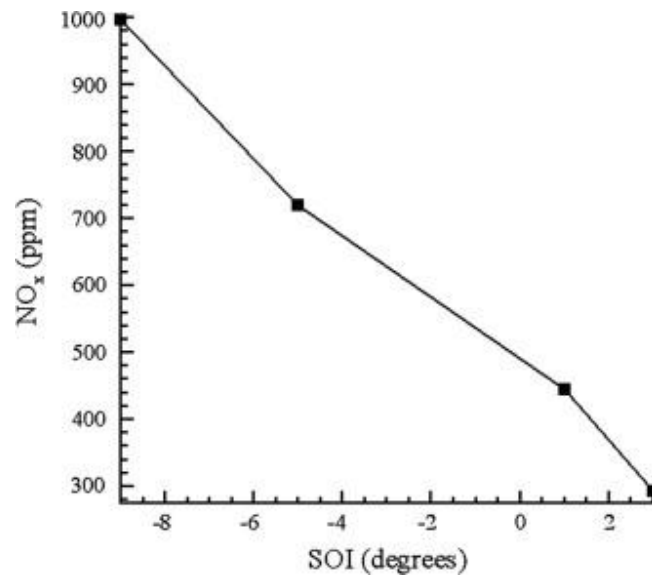


Figure 2.8: NO_x dependence on SOI.

An important side effect to this action is the increase in fuel consumption, as shown in the diagram which shows the NO_x /BSFC trade off, unless other measures are taken to avoid this loss in fuel economy.

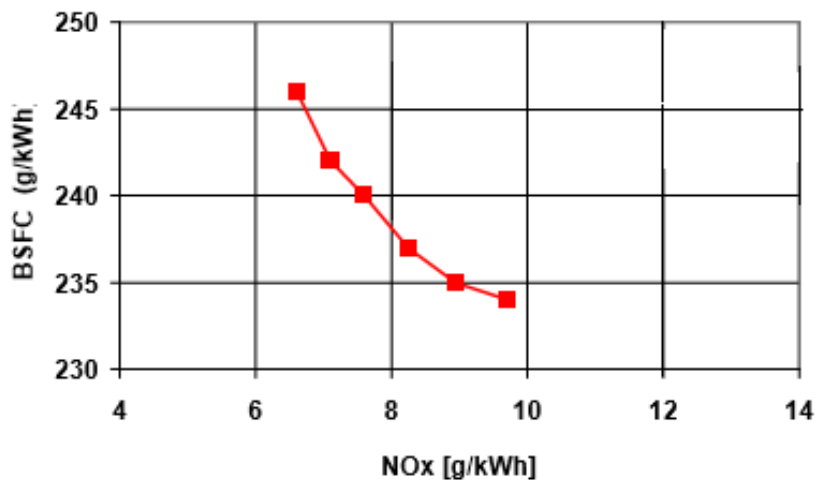


Figure 2.9: NO_x /BSFC trade-off.

Noteworthy is also the dependence of particulate emissions from the injection advance, with a marked increase with the decrease of the advance itself, as opposed to what happens for NO_x : it is necessary to find an optimal injection start value, which allows to contain both polluting emissions within acceptable levels. Significant improvements can be achieved with the use of multiple injections within the same cycle, possible in "common rail" direct injection systems.

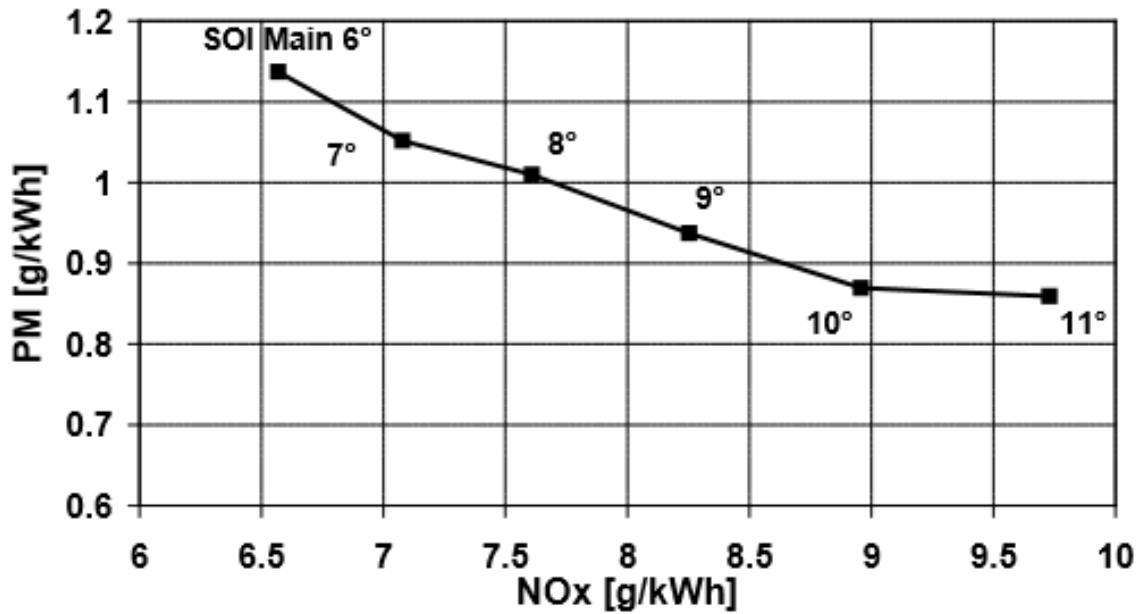


Figure 2.10: PM/NO_x trade-off.

2.3.3 Dependence on Residual gas content

The use of the exhaust gas recirculation (EGR) strategy can be very useful in order to reduce NO_x emissions. This effect is substantially due to a reduction in temperatures reached during the combustion process, a reduction which is expressed by the combined effects of:

1. *Dilution effect* : reduction of temperatures due to the dilution of the charge of fresh air with combustion gases and consequent need to enlarge the amount of charge involved locally by combustion due to the reduction of oxygen concentration during the combustion process.

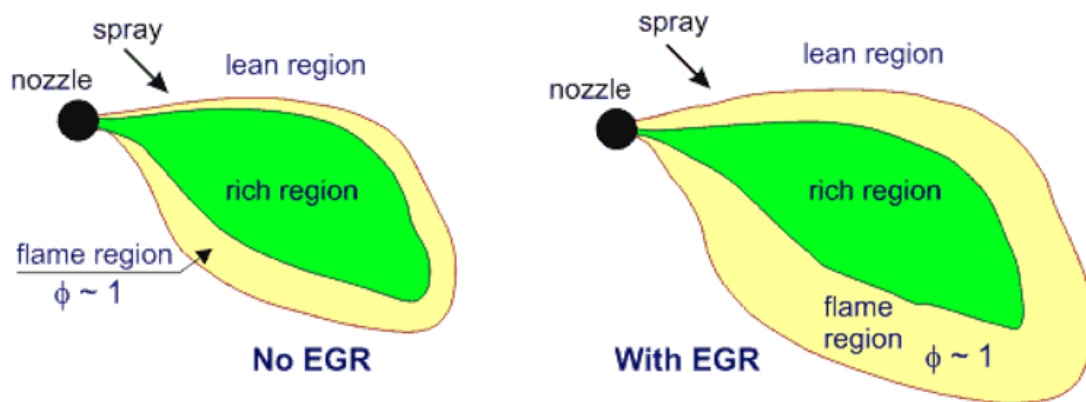


Figure 2.11: Flame region increment due to EGR recirculation.

2. Thermal effect : reduction of maximum temperatures reached thanks to the greater thermal capacity of the combustion gases (in particular CO_2 and H_2O).
3. Chemical effect : reduction of temperatures due to chemical effects.

Among these effects, the prevailing effect is the dilution effect.

Since diesel combustion is always lean, exhaust gases still contain significant amount of oxygen. The oxygen content will vary with engine load, decreasing with increasing loads. Same percentages of recirculated exhaust gases may therefore produce different effects on NO_x emissions, according to the composition of the recirculated exhaust. Therefore EGR %, although commonly used in practise, is not a significant parameter, and should be better replaced by intake oxygen concentration. Test results indicate that high ratios of EGR need to be applied at low load but low ratios of EGR are sufficient for high load. When operating at lower loads, Diesel engines generally tolerate a higher EGR ratio because the exhaust contains a high concentration of O_2 and low concentrations of combustion products CO_2 and H_2O . At high loads, however, the exhaust oxygen becomes scarce and inert constituents become dominating.

As for the SOI, the reduction of NO_x emissions is accompanied by the negative increase in specific consumption and PM emissions although, with the same NO_x reduction, the penalties in terms of fuel consumption are lower with EGR.

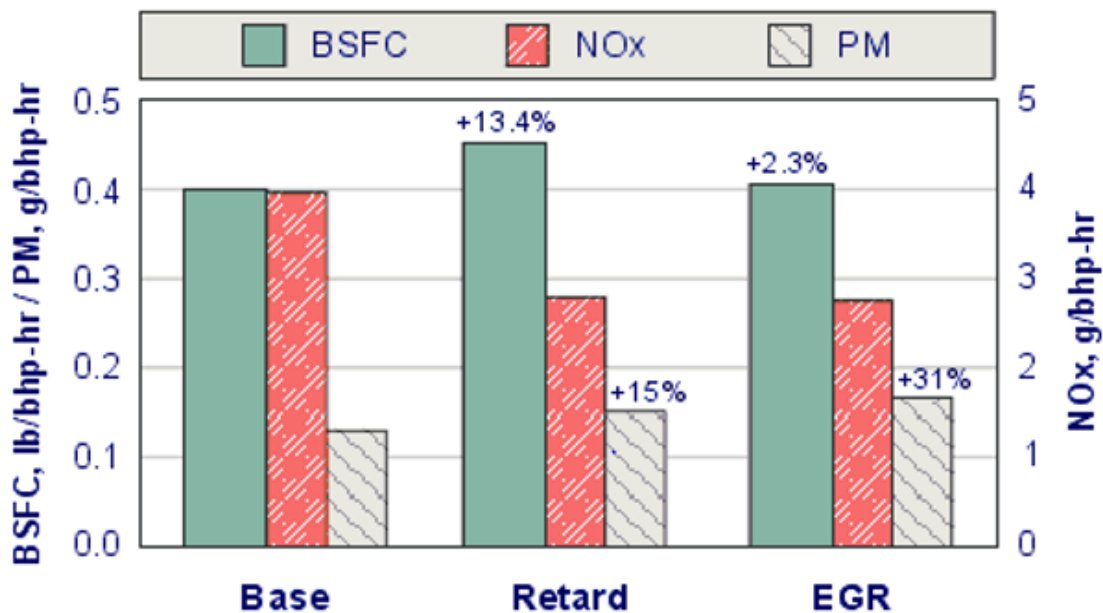


Figure 2.12: Effect of EGR versus injection timing retard on BSFC.

The percentage of maximum EGR is limited by an increase in emissions of particulates, unburned hydrocarbons and carbon monoxide due to a lower availability of oxygen. The increase in PM emissions limits the use of EGR to partial load conditions, making this strategy particularly suitable for automotive engines, whose approval cycles provide operating conditions rather far from full load. On the contrary, the use of the EGR for the containment of NO_x may be less suitable for Heavy Duty engines, for which the homologation cycles also provide for full load operation during which EGR can cause a substantial increase of PM emissions.

2.3.4 Dependence on Injection Pressure

In general, an increase in injection pressure leads to an improvement in performance in terms of specific consumption and particulate emissions, unfortunately accompanied by an increase in NO_x , noise and maximum pressure. In fact, with the increase of injection pressure, the injection speed, the accumulation and the intensity of the premixed phase increase.

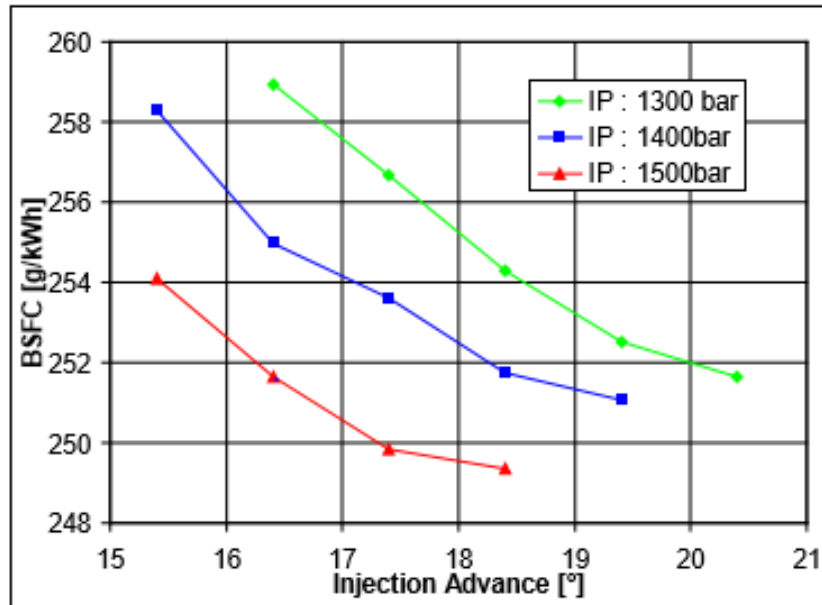


Figure 2.13: BSFC according to SOI for different injection pressures.

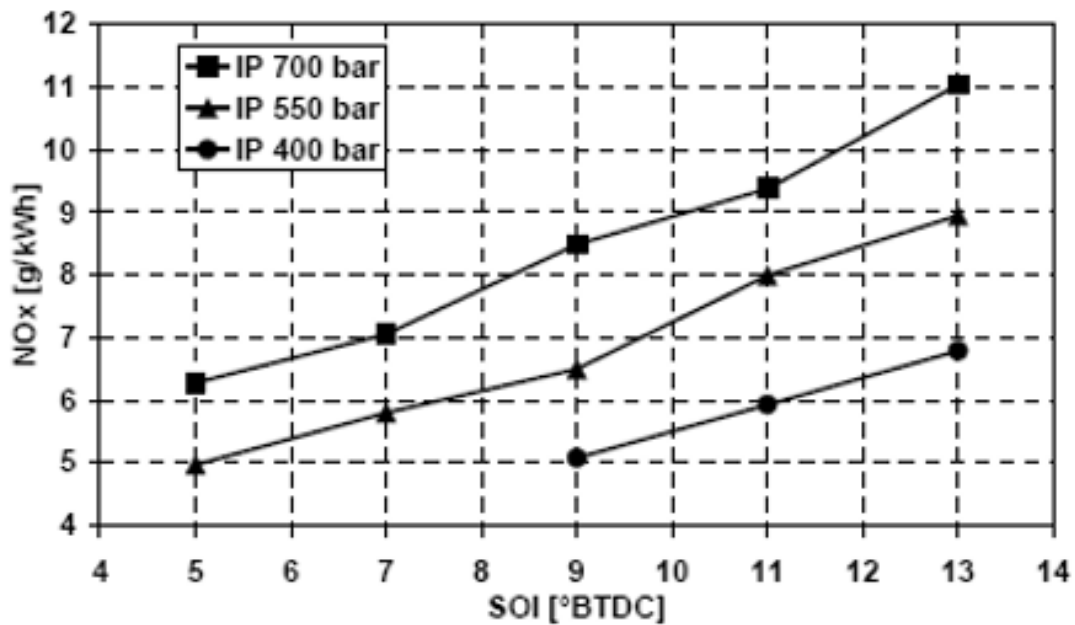


Figure 2.14: NO_x according to SOI for different injection pressures.

Chapter

3 Heavy-duty Emission Legislative Framework

Regulators are concerned about:

- improving local air quality.
- lowering GHG emissions.
- lowering dependence on imported petroleum.
- switching from petroleum to a more sustainable fuel.

In road transport the search for new technologies and fuels has been driven by regulators, which have been mandating increasingly stringent standards for emissions of air pollutants, fuel economy and the ability to use alternative fuels. The air quality deterioration caused by motor vehicle traffic have been the subject of attention and monitoring since the end of the '60s, at least in the three main areas where economic development was accompanied by a significant increase in the number of vehicles on the road: North America, Europe and Japan. The CO concentrations that could be measured in many urban centres and the NO₂ level sampled in metropolitan areas were particularly critical in those years. Therefore, the process of defining test procedures to detect levels of pollution of motor vehicles was started. Emissions of pollutants from vehicles are closely related to operating conditions of the engine. The goal of emission test procedures is:

- to reproduce, in a controlled and repetitive way, the statistically most frequent conditions of use of a powertrain, depending on its application.
- to establish sampling systems and instrumentation to be used to measure with accuracy and precision the amount of pollutants emitted.

The development of these procedures involved both the authorities responsible for environmental protection and the industry. International panels of experts from different countries have also been involved in the process in order to promote the harmonization of test procedures. Cost-benefit analysis has also to be taken into account [3].

3.1 European Union Framework

European emission regulations for new heavy-duty diesel engines are commonly referred to as Euro I ... VI. Sometimes Arabic numerals are also used (Euro 1 ... 6). As shown in the figure below, there are two sets of emission standards, with different type of testing requirements:

- Steady-State Testing.
- Transient Testing.

EU Emission Standards for Heavy-Duty Diesel Engines: Steady-State Testing								
Stage	Date	Test	CO	HC	NOx	PM	PN	Smoke
			g/kWh				1/kWh	1/m
Euro I	1992, ≤ 85 kW	ECE R-49	4.5	1.1	8.0	0.612		
	1992, > 85 kW		4.5	1.1	8.0	0.36		
Euro II	1996.10		4.0	1.1	7.0	0.25		
	1998.10		4.0	1.1	7.0	0.15		
Euro III	1999.10 <i>EEV only</i>	ESC & ELR	1.5	0.25	2.0	0.02		0.15
	2000.10		2.1	0.66	5.0	0.10 ^a		0.8
Euro IV	2005.10		1.5	0.46	3.5	0.02		0.5
Euro V	2008.10		1.5	0.46	2.0	0.02		0.5
Euro VI	2013.01	WHSC	1.5	0.13	0.40	0.01	8.0×10 ¹¹	

a – PM = 0.13 g/kWh for engines < 0.75 dm³ swept volume per cylinder and a rated power speed > 3000 min⁻¹

EU Emission Standards for Heavy-Duty Diesel and Gas Engines: Transient Testing								
Stage	Date	Test	CO	NMHC	CH ₄ ^a	NOx	PM ^b	PN ^c
			g/kWh				1/kWh	1/kWh
Euro III	1999.10 <i>EEV only</i>	ETC	3.0	0.40	0.65	2.0	0.02	
	2000.10		5.45	0.78	1.6	5.0	0.16 ^c	
Euro IV	2005.10		4.0	0.55	1.1	3.5	0.03	
Euro V	2008.10		4.0	0.55	1.1	2.0	0.03	
Euro VI	2013.01	WHTC	4.0	0.16 ^d	0.5	0.46	0.01	6.0×10 ¹¹

a – for gas engines only (Euro III-V: NG only; Euro VI: NG + LPG)
b – not applicable for gas fueled engines at the Euro III-IV stages
c – PM = 0.21 g/kWh for engines < 0.75 dm³ swept volume per cylinder and a rated power speed > 3000 min⁻¹
d – THC for diesel engines
e – for diesel engines; PN limit for positive ignition engines TBD

Table 3.1: EU Emission Standards for Heavy-Duty Diesel.

The regulatory emission test cycles have been changed several times, as indicated in the previous tables. Since the Euro III stage (2000), the earlier steady-state engine test ECE R-49 has been replaced by two cycles: the European Stationary Cycle and the European Transient Cycle. Smoke opacity was measured over the European Load Response test. Since the Euro VI stage, diesel engines are tested over the WHSC + WHTC tests [3].

3.1.1 ECE R-49 Test Cycles

The R49 is a 13-mode steady-state diesel engine test cycle introduced by ECE Regulation No. 49 and then adopted by Directive 88/77/EEC [EU 1988]. It had been used for type approval emission testing of heavy-duty highway engines through the Euro II emission standard. Since the Euro III stage (October 2000), the R49 cycle has been replaced by the ESC schedule. The R49 test remains a regulatory testing procedure in countries that still accept Euro II or earlier emission standards. The R49 test is performed on an engine dynamometer operated through a sequence of 13 speed and load conditions. Exhaust emissions measured at each mode are expressed in g/kWh. The final test result is a weighted average of the 13 modes [3].

Mode No.	Speed	Load, %	Weighting Factors	
			R49	US
1	idle	-	0.25/3	0.20/3
2	maximum torque speed	10	0.08	0.08
3		25	0.08	0.08
4		50	0.08	0.08
5		75	0.08	0.08
6		100	0.25	0.08
7	idle	-	0.25/3	0.20/3
8	rated power speed	100	0.10	0.08
9		75	0.02	0.08
10		50	0.02	0.08
11		25	0.02	0.08
12		10	0.02	0.08
13	idle	-	0.25/3	0.20/3

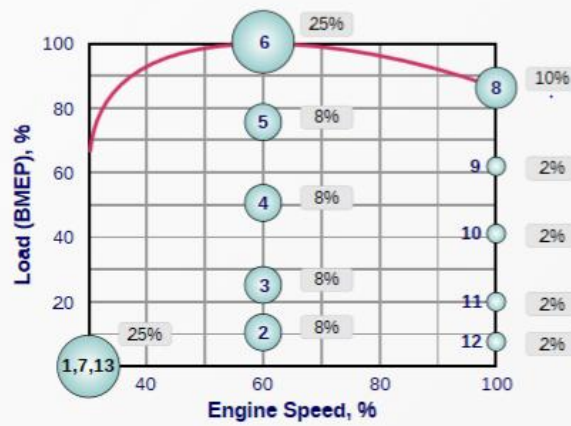


Table 3.2: ECE R-49 Test Cycles.

3.1.2 ESC Test Cycles

The ESC test cycle was introduced together with the ETC and the ELR tests by the Euro III emission regulation for emission measurement from heavy-duty diesel engines. The ESC is a 13-mode steady-state procedure that replaced the R-49 test. The engine is tested on an engine dynamometer over a sequence of steady-state modes. The engine must be operated for the prescribed time in each mode. The specified speed shall be held to within ± 50 rpm and the specified torque shall be held to within $\pm 2\%$ of the maximum torque at the test speed. Emissions are measured during each mode and averaged over the cycle using a set of weighting factors. Particulate matter emissions are sampled on one filter over the 13 modes. The final emission results are expressed in g/kWh [3].

Mode	Engine Speed	Load, %	Weight, %	Duration
1	Low idle	0	15	4 minutes
2	A	100	8	2 minutes
3	B	50	10	2 minutes
4	B	75	10	2 minutes
5	A	50	5	2 minutes
6	A	75	5	2 minutes
7	A	25	5	2 minutes
8	B	100	9	2 minutes
9	B	25	10	2 minutes
10	C	100	8	2 minutes
11	C	25	5	2 minutes
12	C	75	5	2 minutes
13	C	50	5	2 minutes

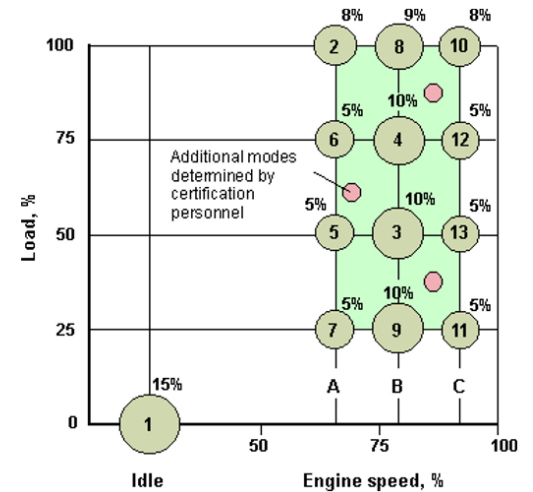


Table 3.3: ESC Test Cycles.

During emission certification testing, the certification personnel may request additional random testing modes within the cycle control area. Maximum emission at these extra modes are determined by interpolation between results from the neighboring regular test modes [3].

3.1.3 ELR Test Cycles

The European Load Response engine test has been introduced by the Euro III emission regulation for the purpose of smoke opacity measurement from heavy-duty diesel engines. The test consists of a sequence of three load steps at each of the three engine speeds A (cycle 1), B (cycle 2) and C (cycle 3), followed by cycle 4 at a speed between speed A and speed C and a load between 10% and 100%, selected by the certification personnel. The final smoke value is determined as a weighted average from the mean values at speeds A (weighting factor 0.43), B (0.56), and C (0.01) [3].

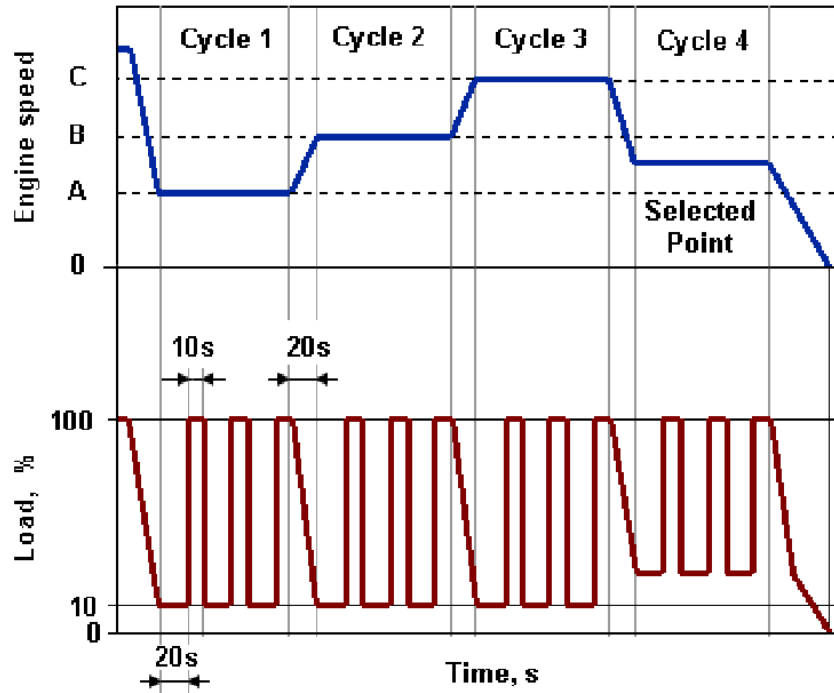


Table 3.4: ELR Test Cycles.

3.1.4 ETC Test Cycles

The ETC test cycle has been introduced, together with the ESC, for emission certification of heavy-duty diesel engines in Europe starting in the year 2000. The ETC cycle has been developed by the former FIGE Institute, Aachen, Germany, based on real road cycle measurements of heavy duty vehicles. Different driving conditions are represented by three parts of the ETC cycle, including urban, rural and motorway driving. The duration of the entire cycle is 1800s. The duration of each part is 600s.

- Part one represents city driving with a maximum speed of 50 km/h, frequent starts, stops, and idling.
- Part two is rural driving starting with a steep acceleration segment. The average speed is about 72 km/h.
- Part three is motorway driving with average speed of about 88 km/h.

FIGE Institute developed the cycle in two variants: as a chassis and an engine dynamometer test. For the purpose of engine certification and type approval, the ETC cycle is performed on an engine dynamometer [3].

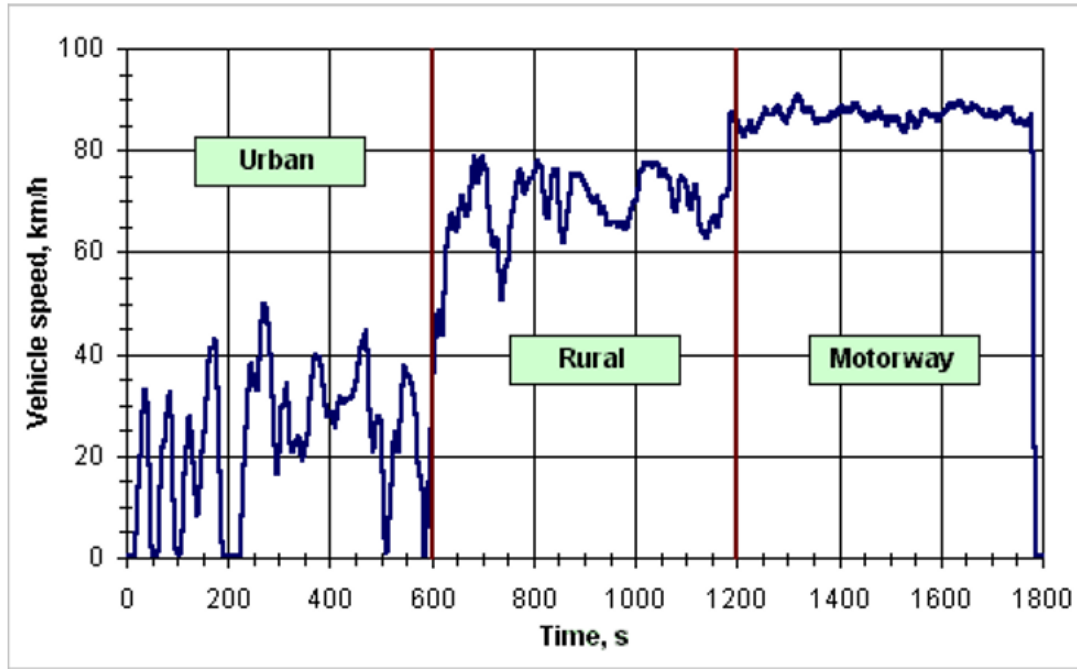


Figure 3.1: ETC speed profile.

3.1.5 WHSC Test Cycles

The WHSC is a ramped steady-state test cycle, with a sequence of steady-state engine test modes with defined speed and torque criteria at each mode and defined ramps between these modes. The WHSC is run from a hot start. The idle mode is separated in two modes, mode 1 at the beginning and mode 13 at the end of the test cycle. Mode 0 is not run, but is only accounted for mathematically by a weighting factor of 0.24 and zero emissions and power [3].

Mode	Speed	Load	Weighting Factor	Mode Length †
–	%	%	–	s
0	Motoring	–	0.24	–
1	0	0	0.17/2	210
2	55	100	0.02	50
3	55	25	0.10	250
4	55	70	0.03	75
5	35	100	0.02	50
6	25	25	0.08	200
7	45	70	0.03	75
8	45	25	0.06	150
9	55	50	0.05	125
10	75	100	0.02	50
11	35	50	0.08	200
12	35	25	0.10	250
13	0	0	0.17/2	210
Total			1	1895
† Including 20 s ramp				

Table 3.5: WHSC Test Cycles.

3.1.6 WHTC Test Cycles

The WHTC test is a transient engine dynamometer schedule of 1800 s duration, with several motoring segments and both cold and hot start requirements. A chassis dynamometer version of the test, the World Harmonized Vehicle Cycle (WHVC), has also been developed, but is not a part of standard international testing procedures [3].

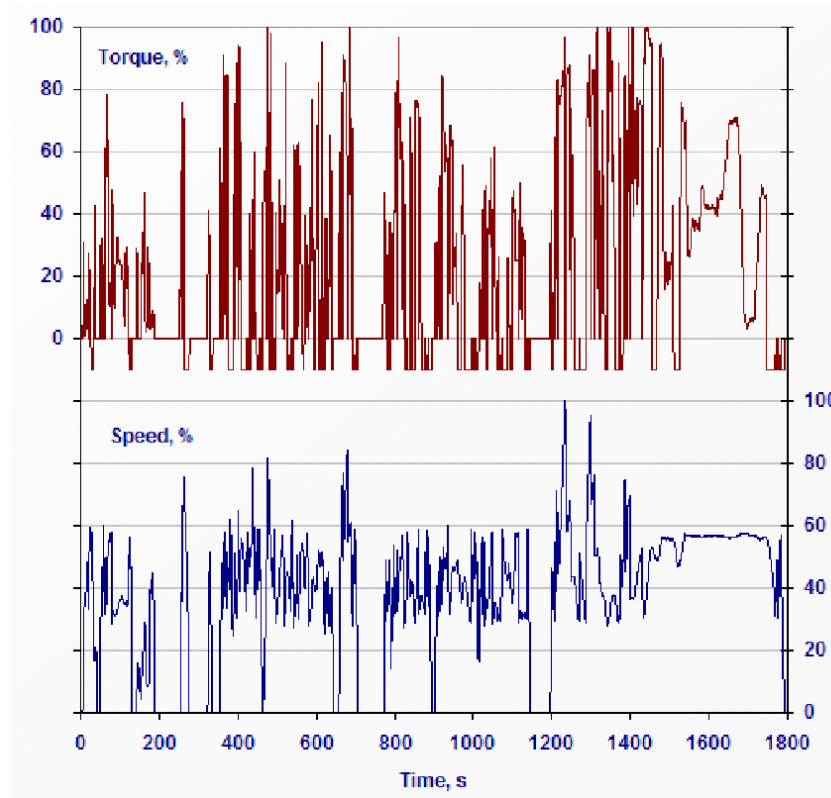


Figure 3.2: WHTC torque and speed profiles.

Chapter

4 Combustion Control Techniques

The increasing computational performance of modern engine control units (ECUs) allows to develop and implement more and more complex combustion control techniques in diesel engines. In general, control algorithms include closed-loop approaches, model-based techniques, or a combination of the two previous methods.

4.1 Control Systems Structure

The goal of a control system is to optimize a signal output, trying to bring it closer to a desired value, by acting on certain operating parameters. The logic of control systems follows one of the following control loops:

1. Open loop control.
2. Closed loop control.

4.1.1 Open Loop Control

In an open-loop controller, also called a non-feedback controller, the control action from the controller is independent of the "process output", which is the process variable that is being controlled. It does not use feedback to determine if its output has achieved the desired goal of the input command or process "set point".



Figure 4.1: Open Control Loop.

However, an open-loop system cannot correct any errors that it makes or correct for outside disturbances, and cannot engage in machine learning. In order to compensate for the limits of an open loop control system, the Feedforward control has been developed. "This control, also called predictive control, aims to measure or predict any potential open loop disturbances and solve them before the controlled variable deviates too far from the target value. In a feed-forward system, the control variable adjustment is not error based, but it is based on the knowledge about the process to be controlled and on the knowledge about the process disturbances. The knowledge about the process derived from a mathematical model" [4].

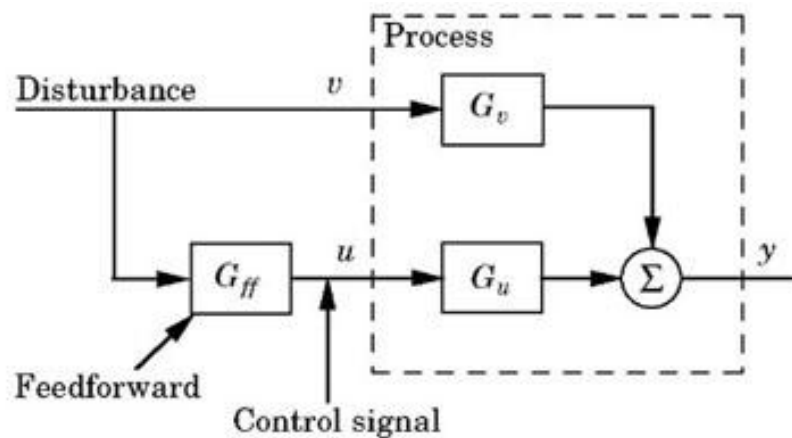


Figure 4.2: Feedforward Control.

4.1.2 Closed Loop Control

A Closed-loop Control System, also known as a feedback control system, is a control system which has one or more feedback loops (hence its name). The reference to "feedback" means that some portion of the output is returned back to the input to form part of the systems excitation. Closed-loop systems are designed to automatically achieve and maintain the desired output condition by comparing it with the actual condition. It does this by generating an error signal which is the difference between the output and the reference input. Therefore, a closed loop system is a fully automatic control system in which its control action depends on the output.

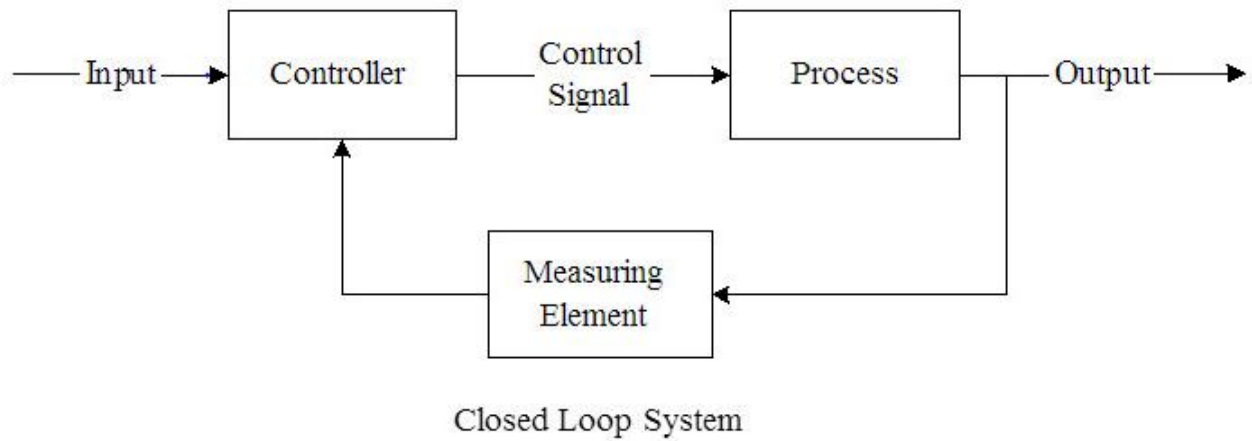


Figure 4.3: Closed Loop System.

4.2 Model-Based Control

Interest in model-based combustion control has increased in recent years . A model-based approach for engine control has in fact several advantages in comparison to the traditional map-based one. Moreover, a model-based control can optimize the combustion process onboard, and overhaul the main calibration parameters in real time. In addition, a model-based approach is able to consider the effects, on the combustion process, of the variability of environmental conditions (humidity, temperature, pressure) or those associated to engine transient operation (turbo-lag, EGR delays, ...), without the need of implementing correction maps. Development of model-based controls has been made possible, recently, thanks to the increasing computational performance of modern ECUs. In general, engine simulation can have different degrees of detail. The main simulation approaches are made up of multidimensional, one-dimensional or zero-dimensional methods, that are characterized by different degrees of detail and computational effort. Mean-value engine and combustion models are capable of simulating the combustion and emission formation processes with a good level of detail, guaranteeing a good predictive capability at steady-state and transient engine operating conditions and, at the same time, offer the possibility to reduce the computational time compared to 1D-CFD approaches. They do not require a high calibration effort because they are physically consistent and, moreover, their accuracy is still acceptable outside the calibration range. Therefore, mean-value models are among the best candidates for the development of model-based combustion control algorithms, as they are physically consistent, and generally require a low calibration effort and a low computational time [1]. Model based controls follow an open loop logic and consequently do not use a feedback loop to ensure that the output has actually reached the desired target value and therefore do not correct any errors they commit. For this reason, an optimal solution is to add a closed loop control to the model based control that corrects any errors related to combustion model.

Chapter

5 Model-Based Control of BMEP and Model-Based/Closed Loop Control of NO_x

In a previous work [1], a model-based approach to control BMEP and NO_x emissions has been developed and assessed on a FPT F1C 3.0L Euro VI diesel engine for heavy-duty applications. The controller is based on a zero-dimensional real-time combustion model, which is able to simulate the HRR, in-cylinder pressure, BMEP and NO_x engine out levels. This type of model-based control is able to correctly estimate BMEP; in fact during simulation, this, within a certain fixed tolerance, efficiently follows BMEP target. On the contrary, this combustion model is not very precise in terms of NO_x. In fact, it has been verified that the real NO_x values do not coincide with those estimated by the model and therefore are far from the desired target values. In this study, we tried to improve the control of nitrogen oxides, adding a closed loop part to the model based one. In fact, a feedback loop has been implemented in order to compare NO_x actual with NO_x target; in case of NO_x estimation error the retraction control is able to correct it. The parameters on which we operate to control NO_x emissions and BMEP are respectively the start of injection and the amount of injected fuel.

5.1 Engine Setup

The reference engine is the FPT F1C 3.0 L Euro VI diesel engine. The main engine features are reported in Table 5.1.

Engine Specifications	
Engine type	FPT F1C Euro VI diesel engine
Number of cylinders	4
Displacement	2998 cm ³
Bore × stroke	95.8 mm × 104 mm
Rod length	160 mm
Compression ratio	17.5
Valves per cylinder	4
Turbocharger	VGT type
Fuel injection system	High pressure Common Rail

Table 5.1: F1C Engine specifications.

The engine is shown in Figure 1. There is a short-route EGR system equipped with a cooler on the engine and the EGR valve is located upstream of the EGR cooler. A flap is installed in the exhaust pipe downstream the turbine, in order to control the temperature of the exhaust gas going to the after-treatment system and to increase EGR rate if necessary [5].

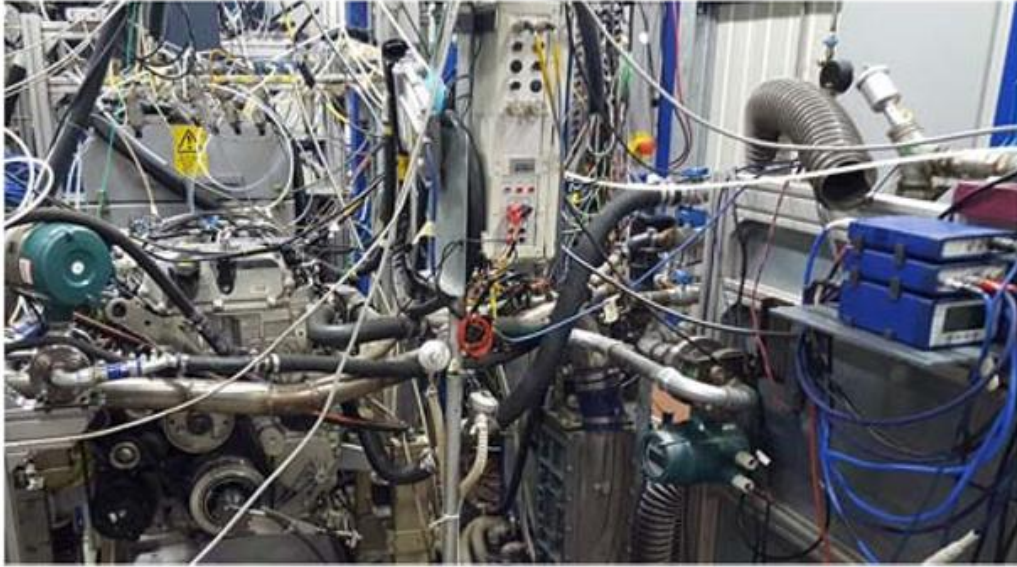


Figure 5.1: F1C Engine.

5.2 Combustion Model Description

“The real-time combustion model that has been used for the development of the NO_x and BMEP model-based controller includes the simulation of:

- Chemical energy release: the approach is based on a model described on the "HRR and MFB50 Estimation in a Euro 6 Diesel Engine by Means of Control-Oriented Predictive Models" article [6]. The input data of the model are the injection parameters, as well as the main thermodynamic conditions in the intake manifold and the engine operating parameters.
- In-cylinder pressure: the approach is based on the inversion of a single-zone heat release model [7] which requires the net energy release as input; the latter is derived starting from the predicted chemical energy release and estimating the heat transfer between the charge and the walls. Polytopic evolutions are assumed during the compression and expansion phases.
- Friction losses: FMEP is evaluated on the basis of the engine speed and peak firing pressure; the simulation of friction losses allows BMEP to be evaluated starting from IMEP.
- Pumping losses: PMEP were simulated on the basis of a semi-empirical correlation which takes into account the intake and exhaust manifold pressure levels, as well as engine speed.
- NO_x emission levels: the approach is based on an improved version of the semi-empirical correlation previously developed by the authors for a 2.0L Euro 5 diesel engine [8] and adapted to the 3.0 L F1C Euro VI engine.

The detailed description of the combustion model and the calibration methodology is reported in [9].” [1]

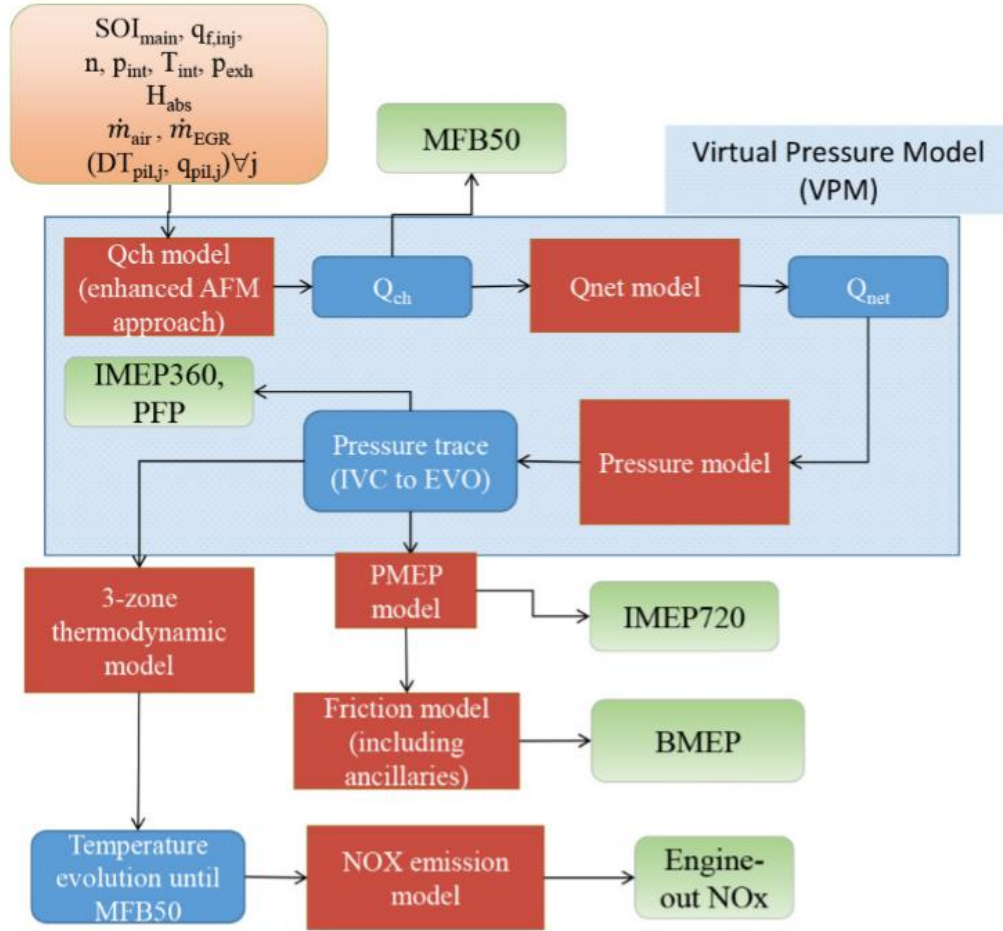


Figure 5.2: Scheme of the real-time combustion model.

5.3 Steps to Validate a Control Algorithm

The development of the electronic control unit is a very complex operation. One of the main obstacles is the definition of the computational time necessary for the heavy control's strategies. This parameter must be taken into account during the development of the code because it must be compared with the hardware computational power available. The right procedure to verify the correct functioning of a control algorithm involves the following steps:

1. *Model in the Loop.*
2. *Hardware in the Loop.*
3. *Rapid Prototyping.*

5.3.1 The Model in the Loop Phase

The first step in order to verify control algorithm is the *Model in the Loop*. This phase, at first, requires the development of a control code, generally realized with the Simulink program, and the development of a model that emulates engine performance.

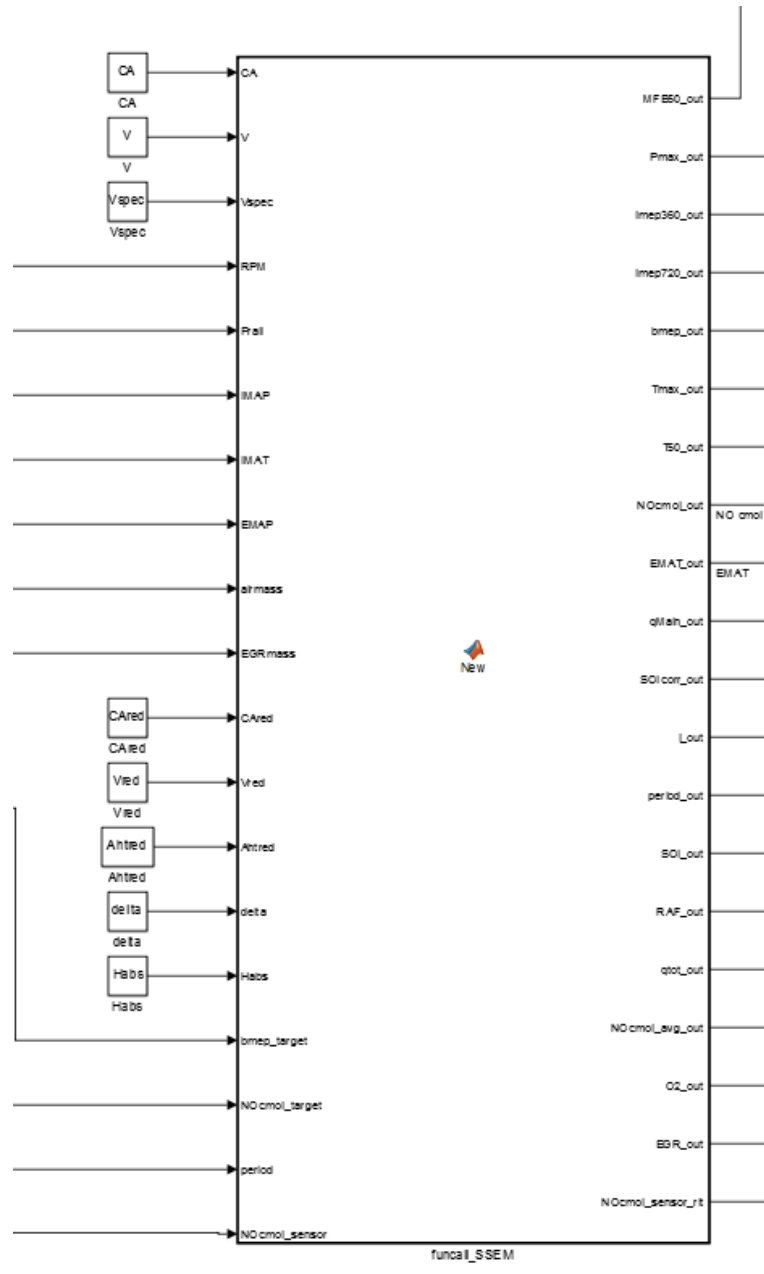


Figure 5.3: Simulink block containing the control system.

The creation of the engine model normally takes place through the use of the GT-Power program. Then, the engine model and the control code are interfaced and the simulation can start. The motor model can be classified according to its level of complexity. Below, different types of models are listed in descending order of complexity:

1. Full Model: model is complete.
2. Fast running Model: fluid dynamics in ducts are simplified.
3. Mean value Model: fluid dynamics in ducts are simplified; cylinders and injectors are respectively reduced to a medium cylinder and to a single injector. Instead of a combustion model, neural networks are used.

During the MIL phase, the fast-running model is used.

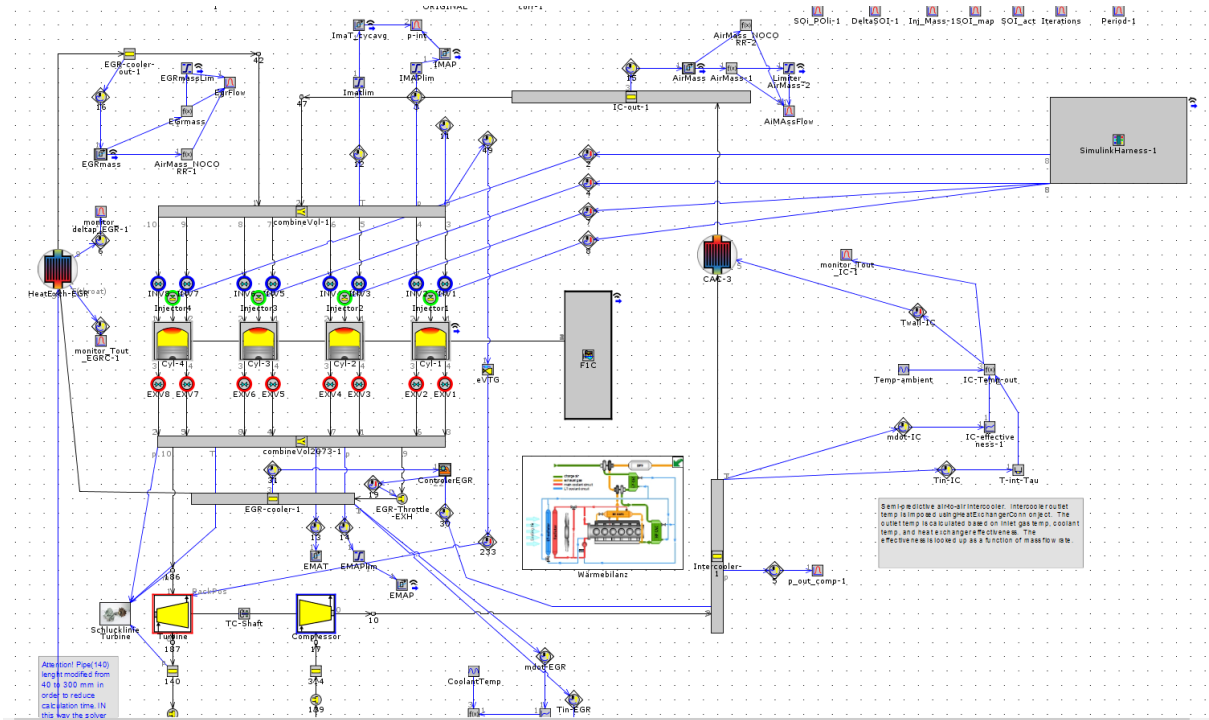


Figure 5.4: GT-ISE Fast Running Model

On GT-ISE the interfacing of the engine model with Simulink occurs by means of the Simulink Harness block, as shown in Figure 5.4. On Simulink the connection between the control system and the engine model is via GT SUITE block, shown in Figure 5.5.

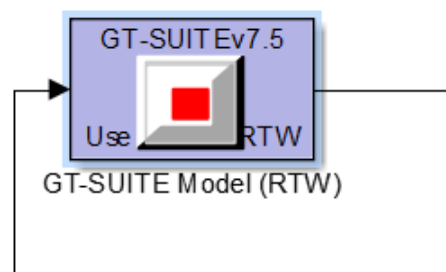


Figure 5.5: Connection tool between engine model and control system.

The MIL phase, in testing the engine controller, is really important in terms of cost-saving and safety issues. In fact, the control system is tested in a virtual environment and so it is possible to verify the controller reliability and implement corrections before the physical test, saving in terms of costs. Moreover, at this stage, there is no risk of damaging the real plant by making changes to control system.



Figure 5.6: Scheme for a model in the loop testing.

5.3.1.1 Model-Based Description

This control, which was developed in the study [1], provides for the inversion of the combustion model, previously described, with the aim of defining the injected quantity and the start of injection that allow the target values of BMEP and NO_x to be reached. On the other hand, the EGR rate is not used for NO_x control and so it is kept constant. An iterative procedure was used to reverse the model. This provides for an initial assumption of the value of q and SOI and a cycle based-integral control which adjust the control variable values in order to attain convergence of the target variables. The end of the iterative process takes place as soon as the difference between the estimated value and the target value is lower than the pre-established tolerances ε_{BMEP} and ε_{NO_x} . More in detail, initially the values of q and SOI are defined starting from a map. The predicted values of BMEP and NO_x associated with them are compared with the target values to determine the error:

$$Err_{BMEP} = BMEP_{target} - BMEP_{estimated}$$

$$Err_{NO_x} = NO_{x,target} - NO_{x,estimated}$$

SOI is then corrected on the basis of NO_x error, while q is corrected on the basis of BMEP error. Then the values of BMEP and NO_x relative to the new values of q and SOI are evaluated and if the tolerances are not yet respected, the values of SOI and q are further corrected. Correction coefficient values of q and SOI are limited to a range [0.15-2] and vary as a function of the sign of the error between two consecutive iterations, as described in the figures below:

$$K_{NO_x,i}^j \in [0.15, 2]$$

$$\text{if } \text{sign}(Err_{NO_x,i}^j) = \text{sign}(Err_{NO_x,i-1}^j): K_{NO_x,i}^j = K_{NO_x,i-1}^j \cdot 2$$

$$\text{if } \text{sign}(Err_{NO_x,i}^j) \neq \text{sign}(Err_{NO_x,i-1}^j): K_{NO_x,i}^j = \frac{K_{NO_x,i-1}^j}{2}$$

Figure 5.7: SOI correction coefficient.

$$K_{BMEP,i}^j \in [0.1, 1]$$

$$\text{if } \text{sign}(Err_{BMEP,i}^j) = \text{sign}(Err_{BMEP,i-1}^j): K_{BMEP,i}^j = K_{BMEP,i-1}^j \cdot 2$$

$$\text{if } \text{sign}(Err_{BMEP,i}^j) \neq \text{sign}(Err_{BMEP,i-1}^j): K_{BMEP,i}^j = \frac{K_{BMEP,i-1}^j}{2}$$

Figure 5.8: q correction coefficient.

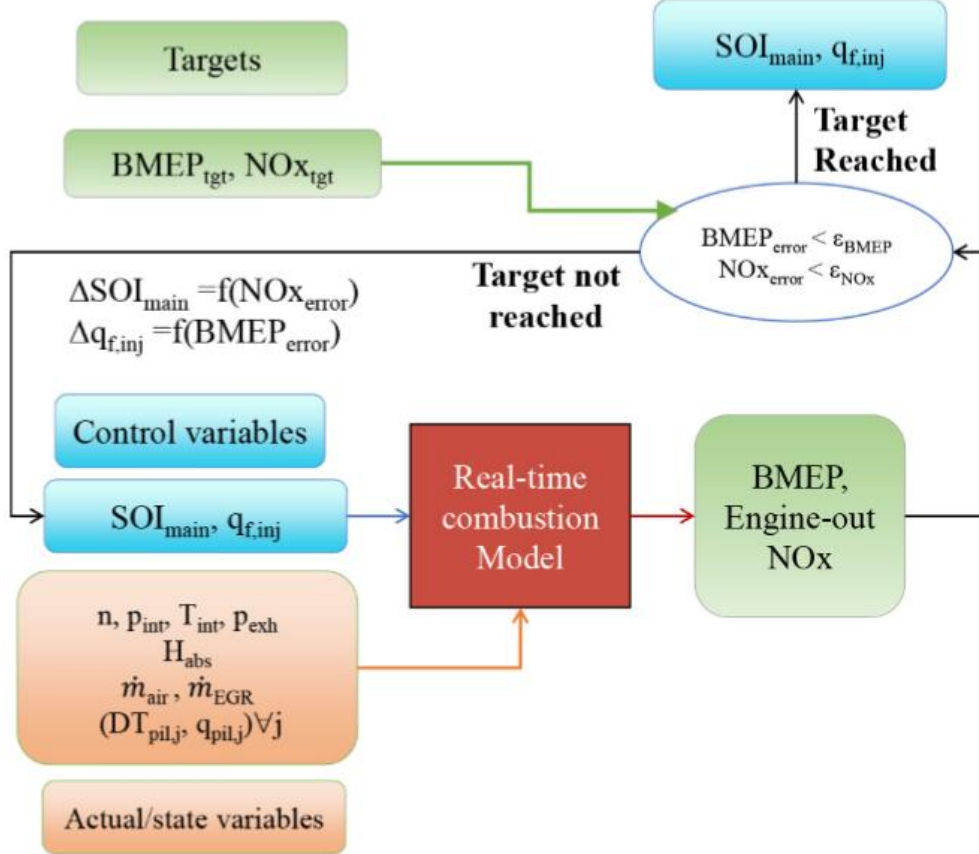


Figure 5.9: Flow chart of the BMEP/NO_x controller.

5.3.1.2 Feedback Control Description

The need to add a closed loop system to the model based control arises from the error that combustion model commits in estimating nitrogen oxides. Therefore, NO_x actual value is expected to enter the control system; this value is then compared to the desired target one. The resulting error is compared to a tolerance and if the tolerance is not met then the start of injection, evaluated by the model based control, is corrected. The correction of SOI is proportional to the error:

$$SOI = SOI_{MB} + k * (NO_{x,target} - NO_{x,actual})$$

SOI = start of injection out of the control.

SOI_{MB} = start of injection defined by model based algorithm.

$NO_{x_{target}}$ = desired nitric oxide.

$NO_{x_{actual}}$ = real nitric oxide.

A series of simulations were carried out in order to determine the correction coefficient, k . The result of these tests led to:

$$k=0.001$$

Actually this is a starting value which varies as a function of the sign of the error between two consecutive iterations. The operating range of the k coefficient is as follows:

$$0.0008 < k < 0.002$$

During experimental tests it came out that NO_x sensor shows a slight delay in returning the measurement, of the order of one second. In this study, results were obtained by interfacing BMEP and NO_x control system not directly with the engine itself but with an engine model realized through the GT Power program. As a consequence, NO_x actual values, entering the control, do not take into account the delay that would actually occur during a real motor test. In order to consider this delay it was decided to filter NO_x actual signal with a discrete filter called "First Order Filter":

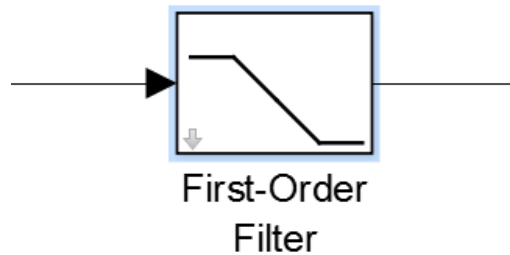


Figure 5.10: First-Order Filter.

5.3.2 The Hardware in the Loop Phase

The *Hardware in the Loop* aims to test the real-time behavior of the controller. The control system is no longer tested in a virtual environment but in a physical one. The procedure linked to this phase involves:

1. Conversion of the engine model from fast running to mean value, that is a simplified model able to run in real time on a specific machine named PXI (PCI eXtensions for Instrumentation), which represents a real-time engine simulator.
2. Insertion of the engine control developed with Simulink on the rapid prototyping device (ETAS ES910).
3. Insertion of the mean value engine model on the PXI.
4. Interfacing the rapid prototyping device with the PXI.

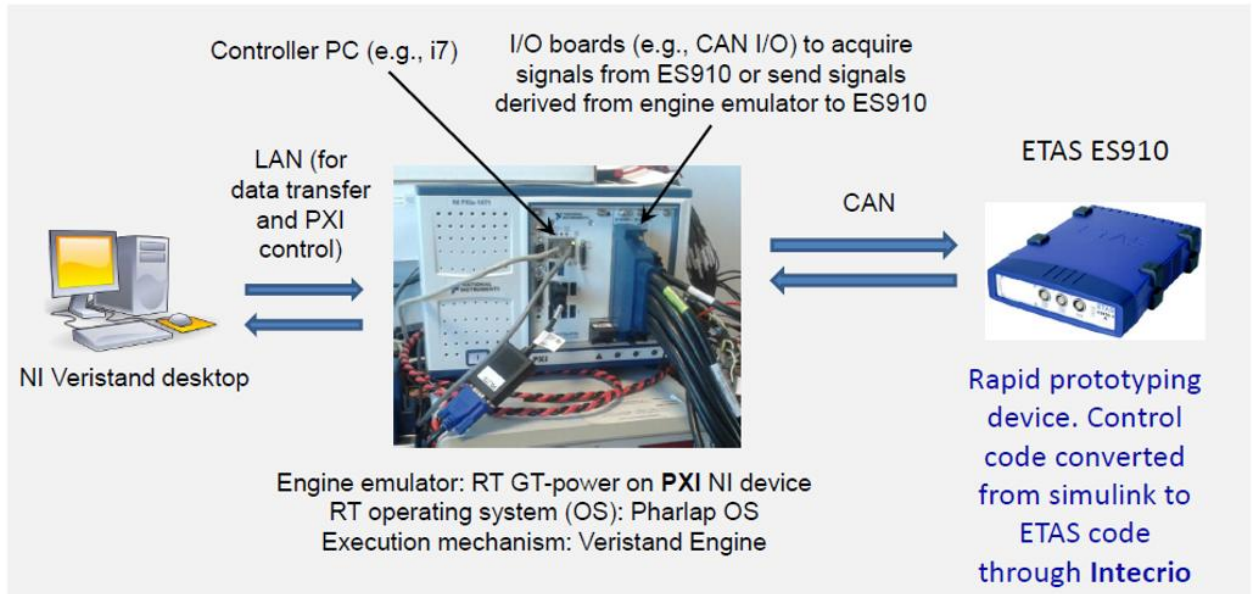


Figure 5.11: Hardware in the Loop Setup.

5.3.2.1 Mean Value Model

Fast running model is able to simulate well the performance of the engine but at the same time it requires a considerable computational effort, not allowing to obtain real time results. It is therefore necessary to pass to a simplified model to reduce simulation times. As mentioned earlier the mean value model is characterized by simplified fluid dynamics, a medium cylinder and a single injector. Moreover neural networks are used instead of the combustion model. These are like a data warehouse that, depending on the input, returns an output. Neural networks require a self-learning phase during which they create first-order relationships between inputs in order to obtain specific outputs.

5.3.3 Rapid Prototyping

The aim of the Rapid Prototyping phase is to verify the functionality of the controller on the real engine. As a result, the engine emulator is no longer necessary and the real engine is used. The control system developed on Simulink is downloaded to the rapid prototyping device which is then connected to the motor in order to allow the start of the test.

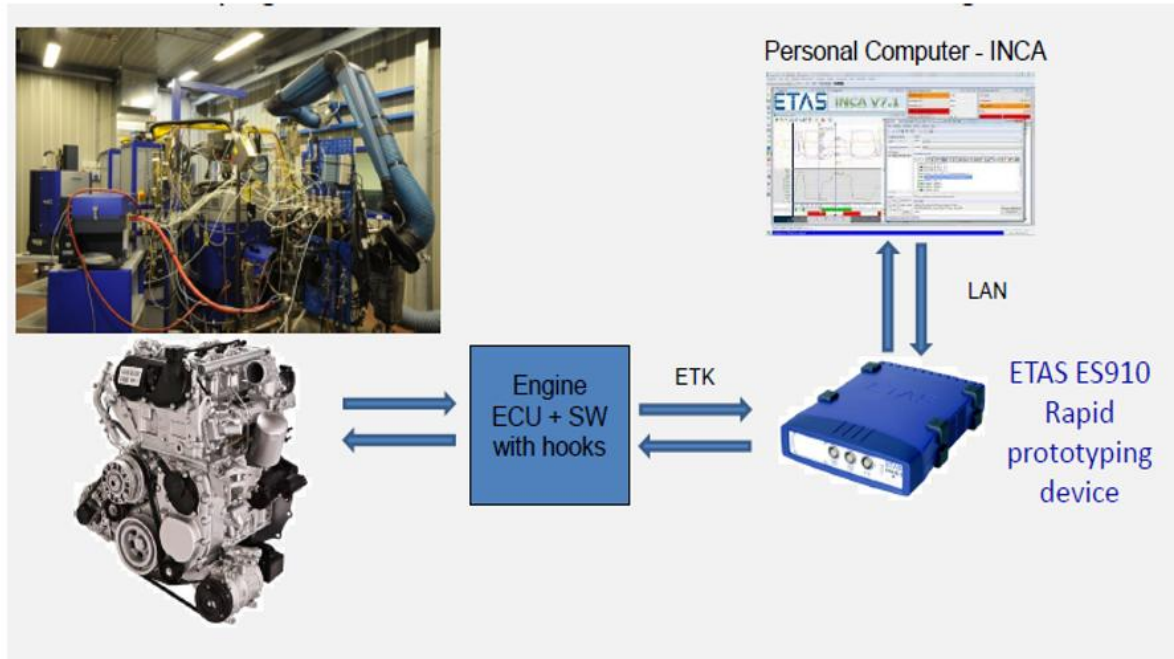


Figure 5.12: Rapid Prototyping test at Dennerg Laboratory.

5.4 Hardware and Software related to HiL

Physical tools necessary for the development of the HiL phase are:

1. An Engine Emulator.
2. A Rapid Prototyping Device.
3. Cable Can used to transfer data between the NI-PXLe1082 and the ETASes910.

5.4.1 The Engine Emulator

The engine emulator is used to perform real time tests. The one used in this study is the NI-PXLe1082 in which it is inserted the controller e-8135. “PXI stands for PCI eXtensions for Instrumentation that is a rugged PC-based platform that offers a high-performance, low-cost deployment solution for measurement and automation systems. PXI combines the Peripheral Component Interconnect (PCI) electrical bus with the rugged, modular Euro-card mechanical packaging of Compact PCI and adds specialized synchronization buses and key software features” [4]. The operating system we used to runs the NI-PXLe1082 is Phar Lap.



Figure 5.13: NI-PXIE1082.

The correct procedure to load the engine model on the NI-PXIE1082 is as follows:

1. Generate the file .dat of the engine model.

GT ISE → RUN → RUN Simulation utilities → generate.dat

2. Load the engine model .dat file and the neural network .nno file on the NI-PXIE1082 using NI-MAX software.

NI MAX → Remote System → NI PXI → file transfer → ni rt → system
→ to add .nno and .dat files

Once the motor model is loaded on the PXI it is necessary to use the NI-VeriStand software to manage the engine emulator. In this case the right procedure is as follows:

1. Generate the code of the control system, comprising of the GT-suite block. This is possible by running the build once correct parameters have been set in "Code Generation" section under "Model configuration parameters" as shown in Figure 5.13. The format that derives from the build operation is the .dll, in accordance with Phar Lap operating system.

Target selection

System target file: NIVeriStand.tlc Browse...

Language: C

Description: NI Phar Lap Real-Time & Windows Targets

Build process

Makefile configuration

☒ Generate makefile

Make command: make_rtw OPTS="-DNAGWARE"

Template makefile: NIVeriStand_vc.tmf

Code Generation Advisor

Select objective: Unspecified

Check model before generating code: On (proceed with warnings) Check Model...

☐ Generate code only Build

☐ Package code and artifacts Zip file name:

Figure 5.14: Build VeriStand Setup.

2. Create a new project on VeriStand.

Open VeriStand → Creat New Project → Project Name → ok

3. Define the hardware on VeriStand.

System definitions → .nivssdf → system explore → controller → PXI → target → hardware
→ name operation system → Phar Lap

System definitions → .nivssdf → system explore → controller → NI PXI → target → hardware
→ IP address → PXI address

4. Define the model on VeriStand.

Simulation models → add simulation → file.dll

5. Initialize input variables on VeriStand.

System Explorer → Models → inports → initialize inports

6. Create frame database using NI-XNET software.

Open NI XNET Database Editor → create new clauster → protocol CAN → give the name
→ ok

7. Create Can port on VeriStand.

System Explore → PXI → Hardware → chassie → NI XNET → CAN
→ Hardware discovery wizard → create CAN port

8. Import frame database on VeriStand.

System Explorer → CAN → XNET database

9. Define input and output frames on VeriStand.

CAN → Incoming → Single Point → import frames

CAN → Outgoing → Event Triggered → import frames

10. Associate frames with variables using “Configuration Mappings” button on VeriStand.

11. Open the project control window with “User Interface” on Project Explorer.

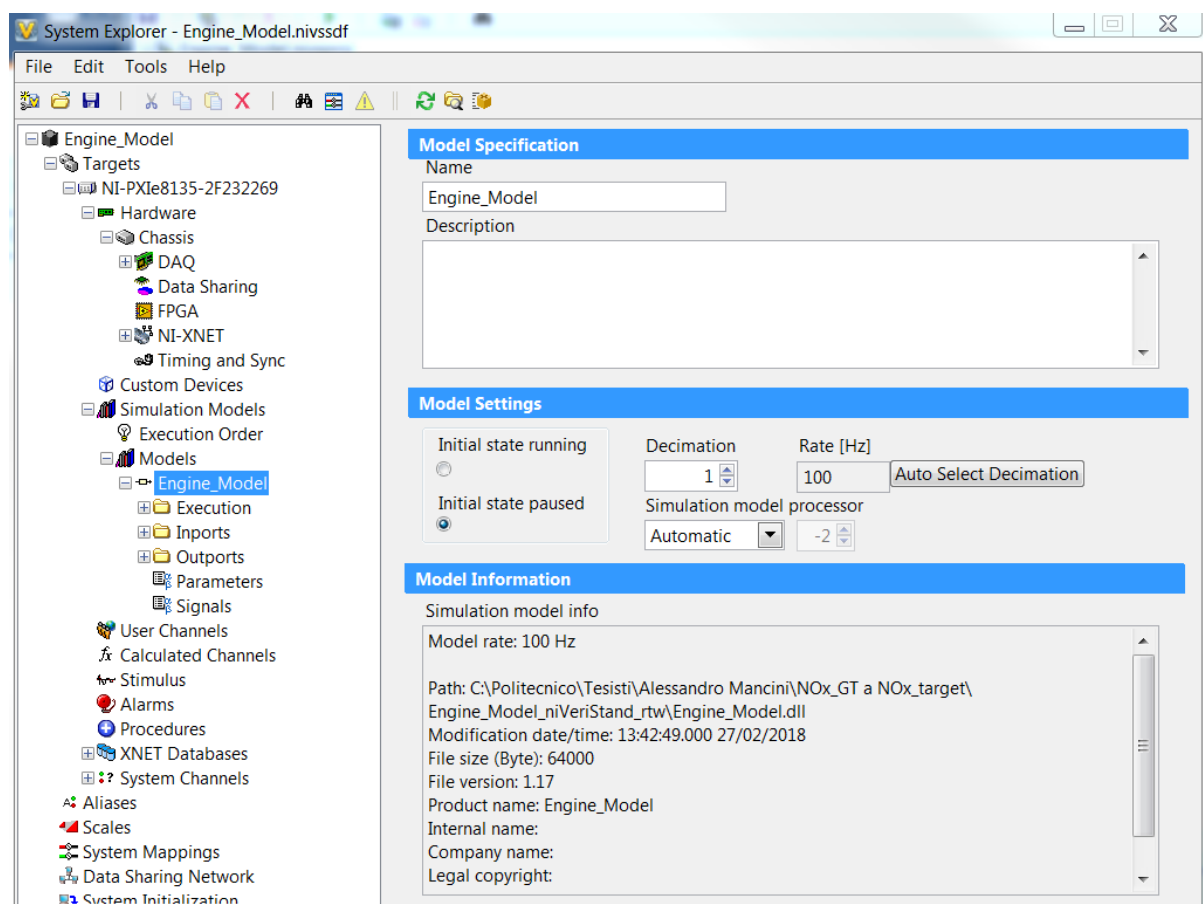


Figure 5.15: VeriStand Interface.

5.4.2 The Rapid Prototyping Device

“The prototyping interface module used in hardware in the loop tests is an ETAS es910. The ETASes910 combines high computing performance with all common ECU interfaces, in practices is a component that enables the exchange of information built inside different software’s environments. The considered device is provided with Can and Lin interfaces for the connection of the ES910 module to vehicle and PXI buses.” [4]



Figure 5.16: ETAS ES910.

Intecrio is the prototyping software-tool that performs the configuration of the ES910 module. The configuration of the rapid prototyping device involves the following steps:

1. Generate the code of the control system, excluding the GT-suite block. This is possible by running the build once correct parameters have been set in "Code Generation" section under "Model configuration parameters" as shown in Figure 5.16. The format that derives from the build operation is the .six.

Figure 5.17: Build Intecrio Setup.

2. Create a new project on Intecrio.

Open Intecrio → generate model .iow

3. Define the hardware on Intecrio.

Hardware Systems → ES900 → insert target → ES910

4. Create Can port on Intecrio.

Hardware Systems → ES900 → insert target → ES910 → insert CAN Controller
→ CAN_IO

5. Create signals.

CAN IO → signals → create signals

6. Create frames and associate signals.

CAN IO → frames → create frames → insert item → associate desired signal

7. Distinguish input signals from output signals.

frame → direction → send or receive

8. Define the model on Intecrio.

modules → import module → file .six

9. Create function and import module on it.

function → create function → drag the module into the created function

10. Create software system and import module on it.

Software systems → create software system
→ drag the module on the created software system

11. Connect variables to input and output ports both for the function and for the software system.

Created function or software system → open in view
→ create input and output ports on the window that appears
→ connect them to variables

12. Create System with hardware and software.

Systems → create system → add hardware and software

13. Connect variables to input and output ports on the created System.

Systems → open in view → drag inputs and outputs into the window that appears
→ connect them to the variables

Drag inputs and outputs to the window dragging the CAN_IO section on the window itself.

Systems → ES910 → CAN → CAN IO → drag CAN IO into the window

14. Download the operating system on ETAS.

Systems → ES900 → ES910 → open OS configuration → User Mapp Mode
→ add timer task

Once the timer task is created, drag imports, model and outputs on actions following this order:

Hardware → drag imports into actions

Software → drag model into actions

Hardware → drag outputs into actions

Moreover, make sure you have dragged to Init and Exit sections respectively “ier_Stant_Modelname” and “ier_Terminate_Modelname”.

15. Build the Intecrio model.

16. Open the project control window with “Open Experiment”.

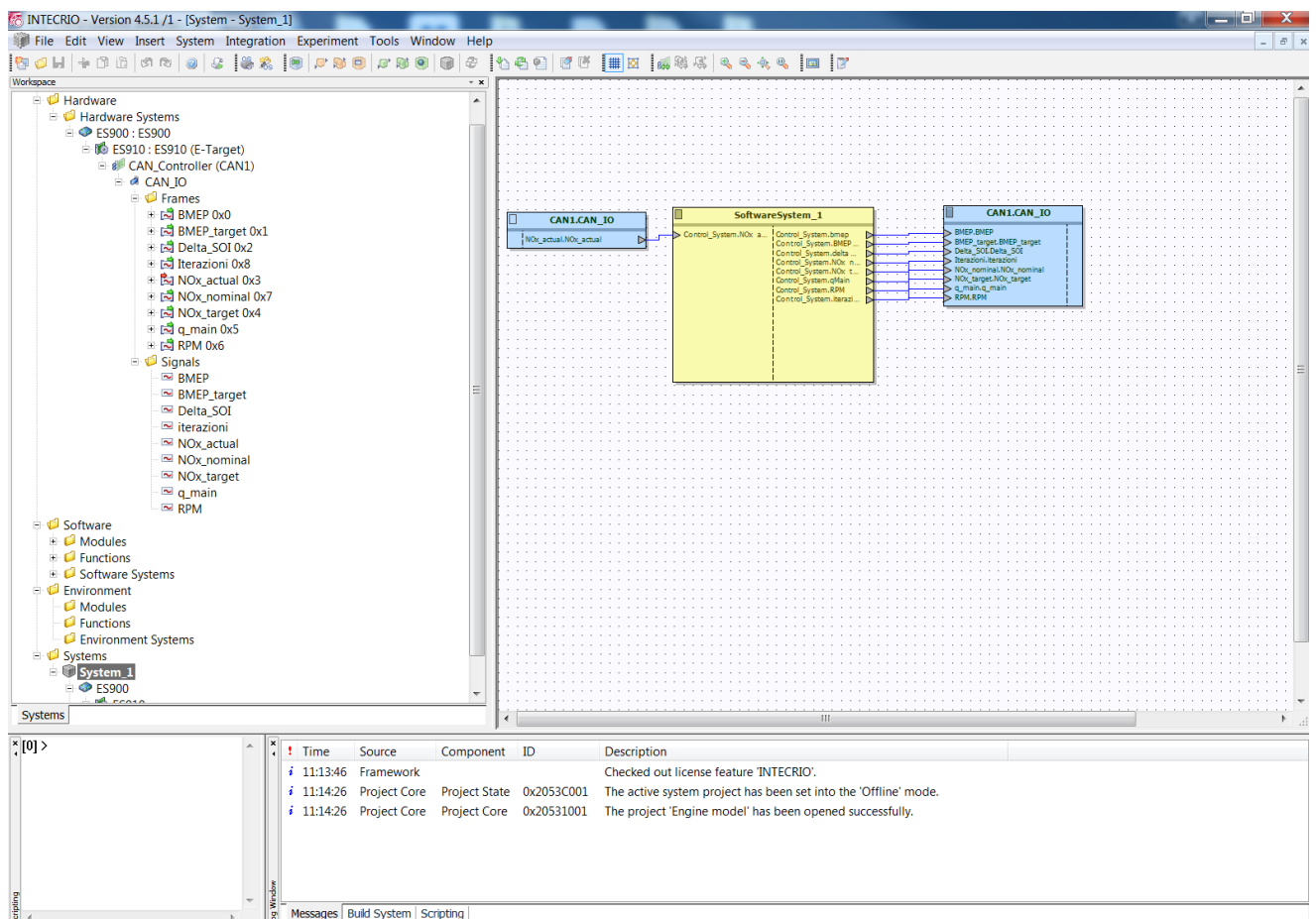


Figure 5.18: Intecrio Interface.

Chapter

6 Model in the Loop Results

In this phase we want to verify the effectiveness of the feedback control on NO_x by comparing the results of the model based control of BMEP and NO_x developed in [1] with those obtained by adding a closed loop part to the control of NO_x . For this purpose several tests were carried out:

- Simulation with BMEP target profile and constant NO_x target and speed.
- Simulation with NO_x target profile and constant BMEP target and speed.
- Simulation with BMEP target profile, NO_x target profile and speed profile.

6.1 BMEP Target Profile and Constant NO_x Target and Speed

During this test NO_x target is kept at 350 ppm, the speed at 3250 rpm while BMEP target follows a fixed profile. The results of BMEP and NO_x related to the model based control are shown respectively in Figure 6.1 and in Figure 6.2.

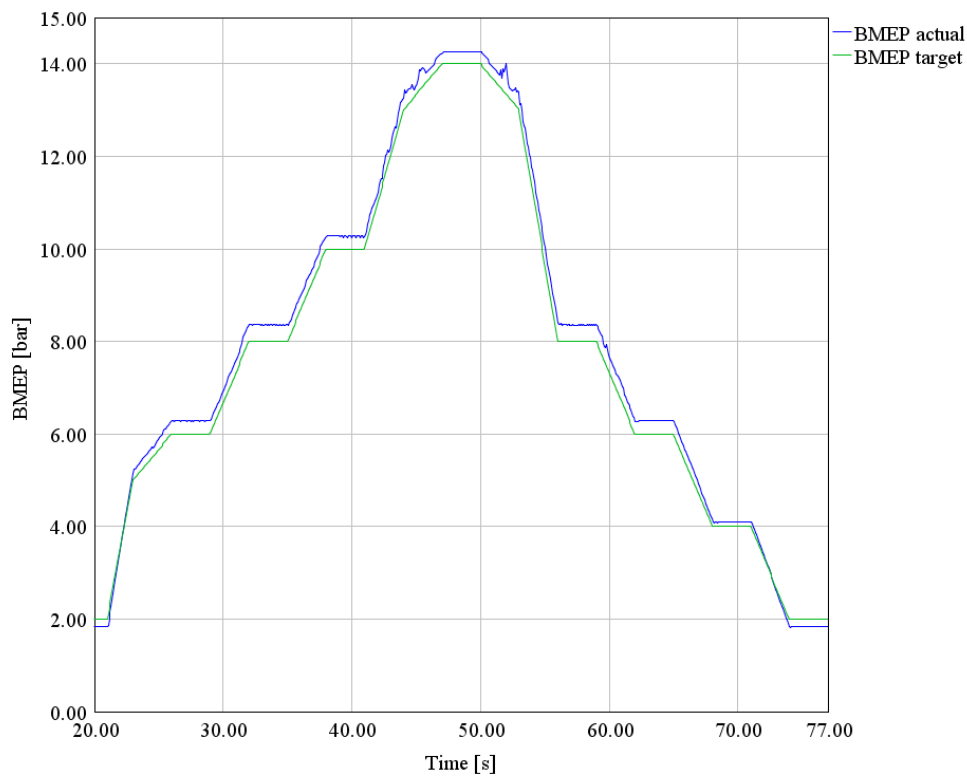


Figure 6.1: Model Based Control, BMEP result.

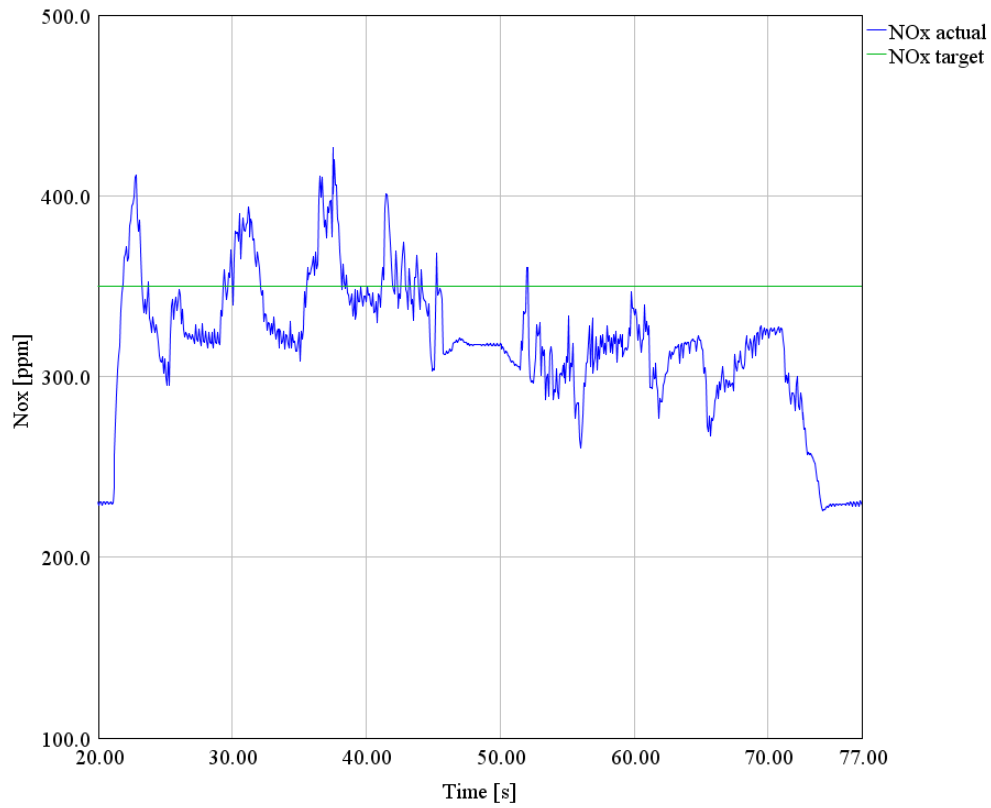


Figure 6.2: Model Based Control, NO_x result.

It is noted that model based control is able to correctly estimate BMEP; indeed, BMEP actual does not deviate excessively from BMEP target. On the contrary, it is not able to accurately predict NO_x ; in fact, NO_x actual is often far from the desired target value.

The results of the model based control combined with the closed loop system are shown in Figure 6.3 and 6.4. By comparing them with the results obtained using only the model based control, it can be verified that the integration of the closed loop NO_x control does not significantly affect the BMEP, which remains almost the same, while it positively modifies nitrogen oxides trend: NO_x actual is now closer to the target value.

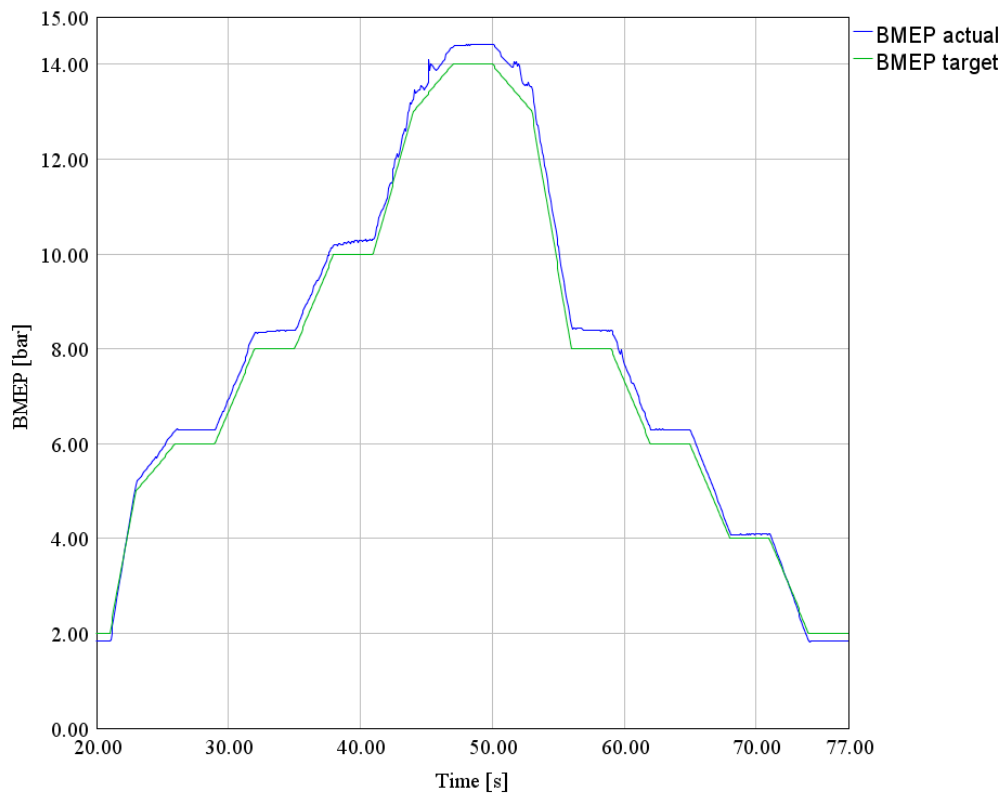


Figure 6.3: Model Based/Closed Loop Control, BMEP result.

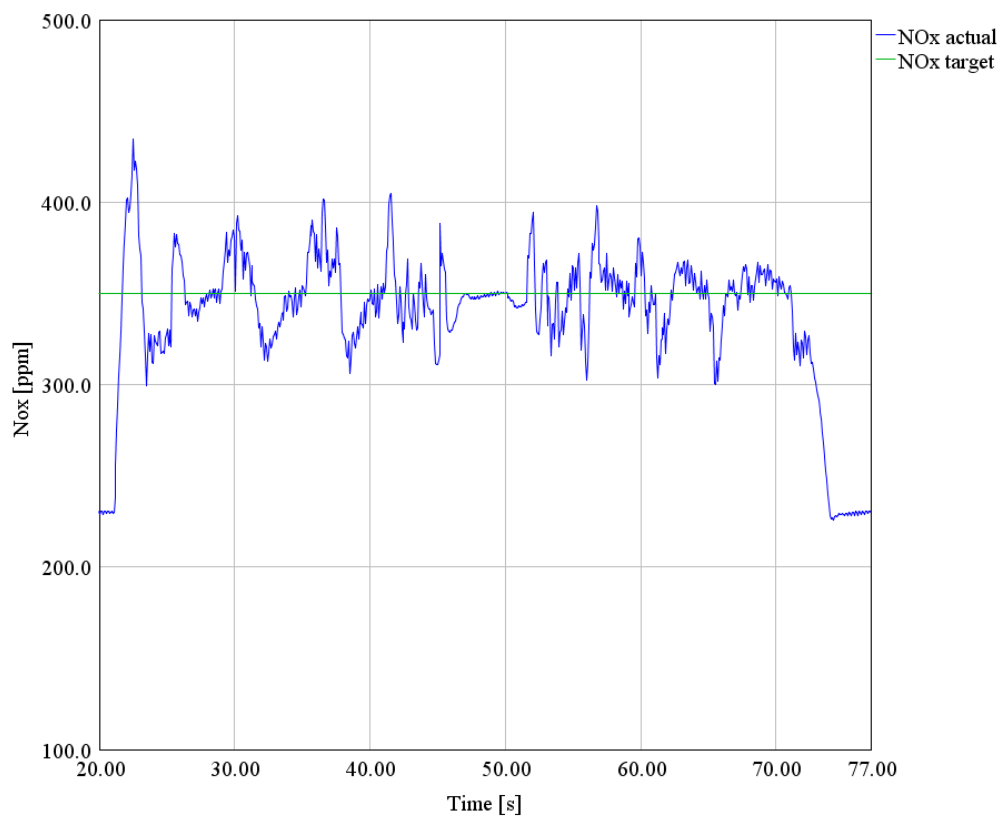


Figure 6.4: Model Based/Closed Loop Control, NO_x result.

In the figures below, the results of the model based control integrated with the feedback loop are compared with those of the controller without the closed loop system.

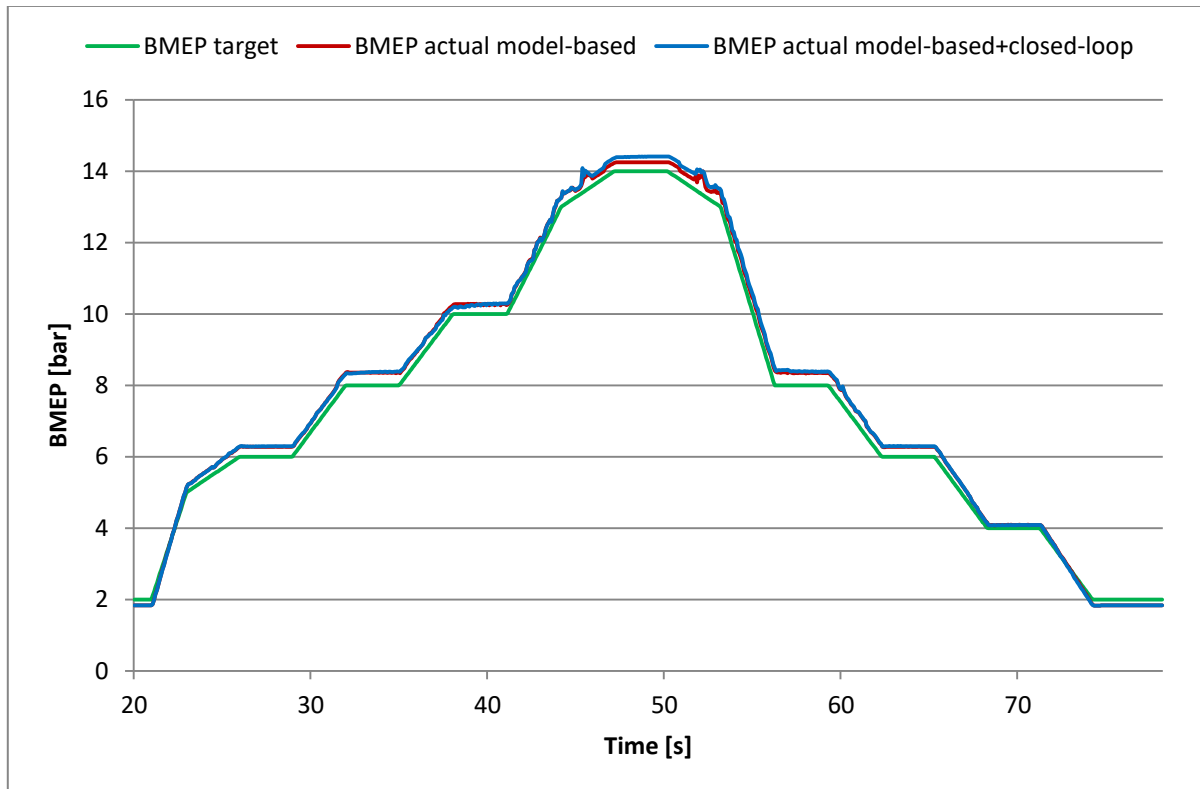


Figure 6.5: Model based control compared with Model Based/Closed Loop Control, BMEP results.

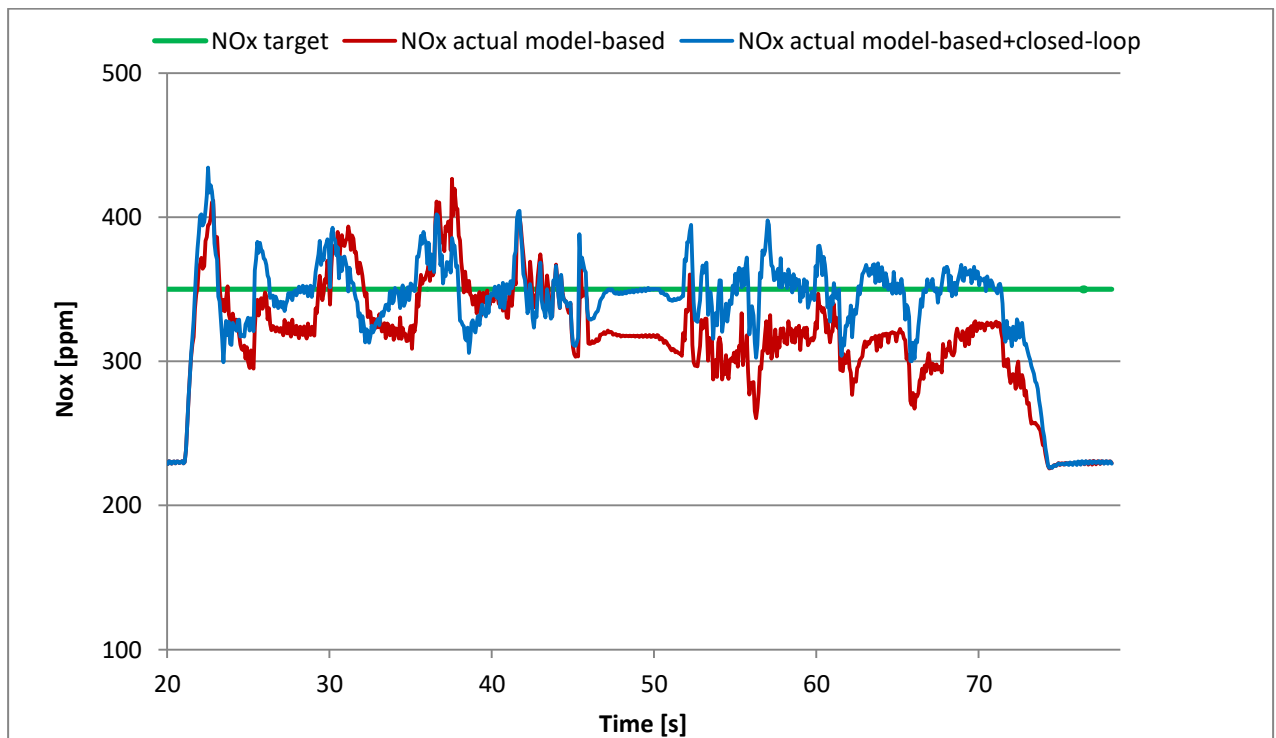


Figure 6.6: Model based control compared with Model Based/Closed Loop Control, NO_x results.

6.2 NO_x Target Profile and Constant BMEP Target and Speed

During these tests speed and BMEP target are kept constant while NO_x target follows a fixed profile. Three tests were performed with the same NO_x target profile and the same speed of 2000 rpm but with different BMEP target values, i.e. 2,8 and 14 bar.

Below are the results of BMEP and NO_x obtained with and without the NO_x closed loop control for the different cases. Analyzing them we deduce what already stated previously that is that the NO_x feedback control significantly improves NO_x behavior and does not significantly affect BMEP.

It is important to note that sometimes the control is not able to satisfy NO_x target value because SOI, which is the NO_x control parameter, has reached its limit value and can not be further modified.

6.2.1 BMEP Target of 2 bar

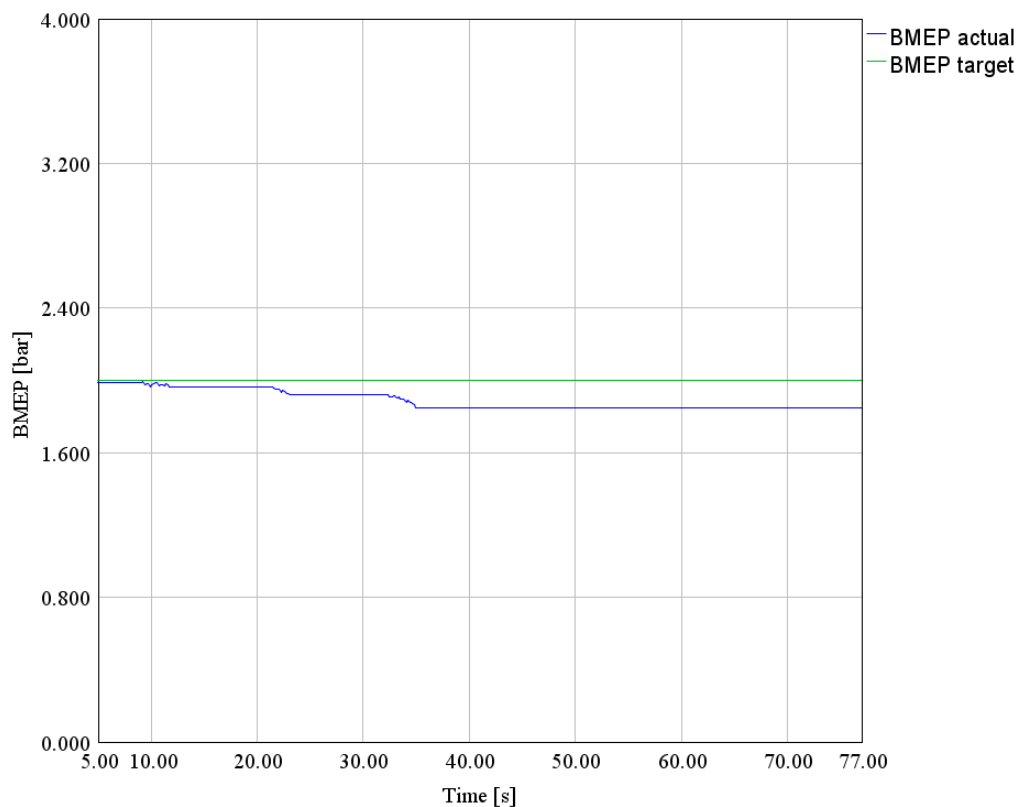


Figure 6.7: Model Based Control, BMEP target=2, BMEP result.

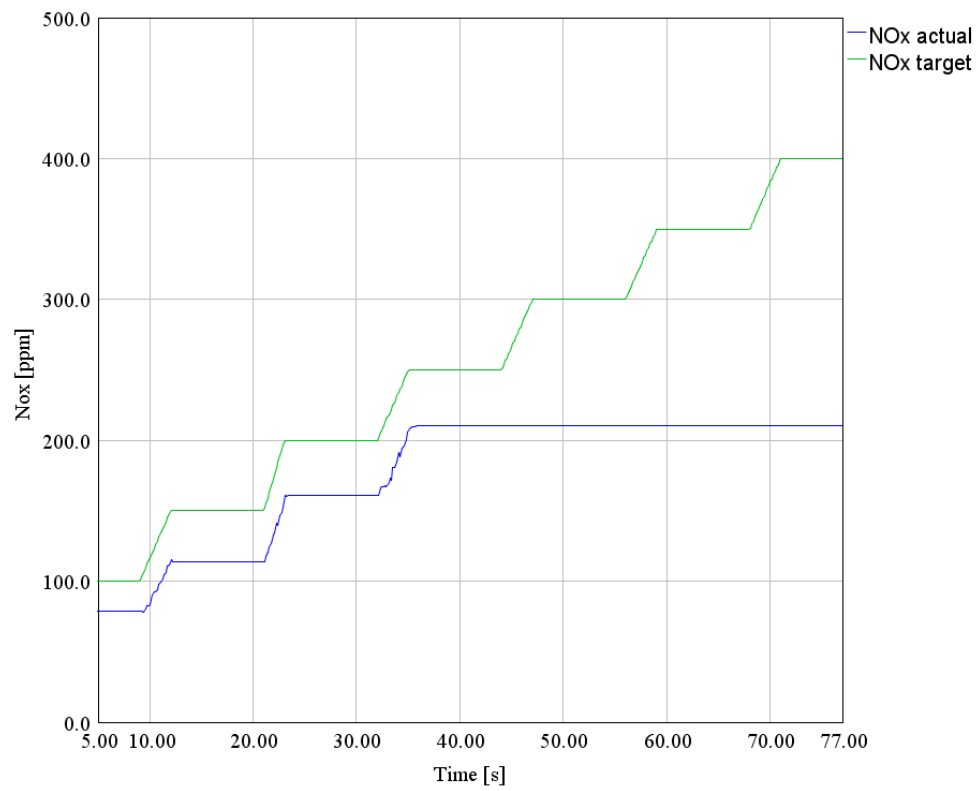


Figure 6.8: Model Based Control, BMEP target=2, NO_x result.

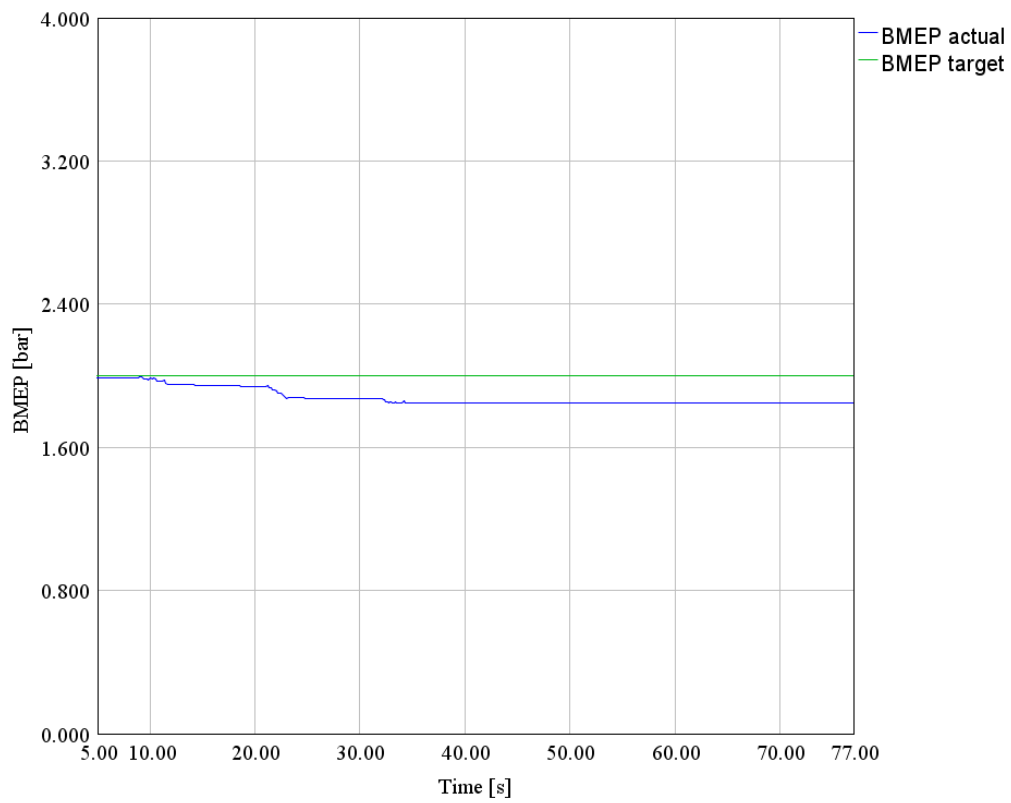


Figure 6.9: Model Based/Closed Loop control, BMEP target=2, BMEP result.

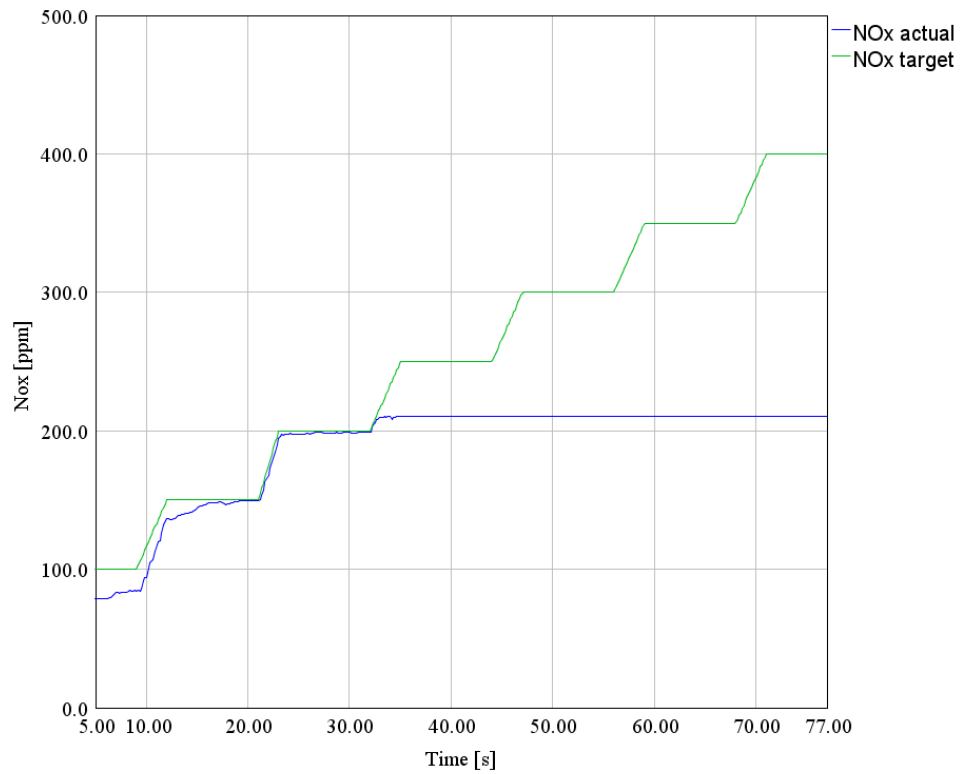


Figure 6.10: Model Based/Closed Loop control, BMEP target=2, NO_x result.

In the figures below, the results of the model based control integrated with the feedback loop are compared with those of the controller without the closed loop system.

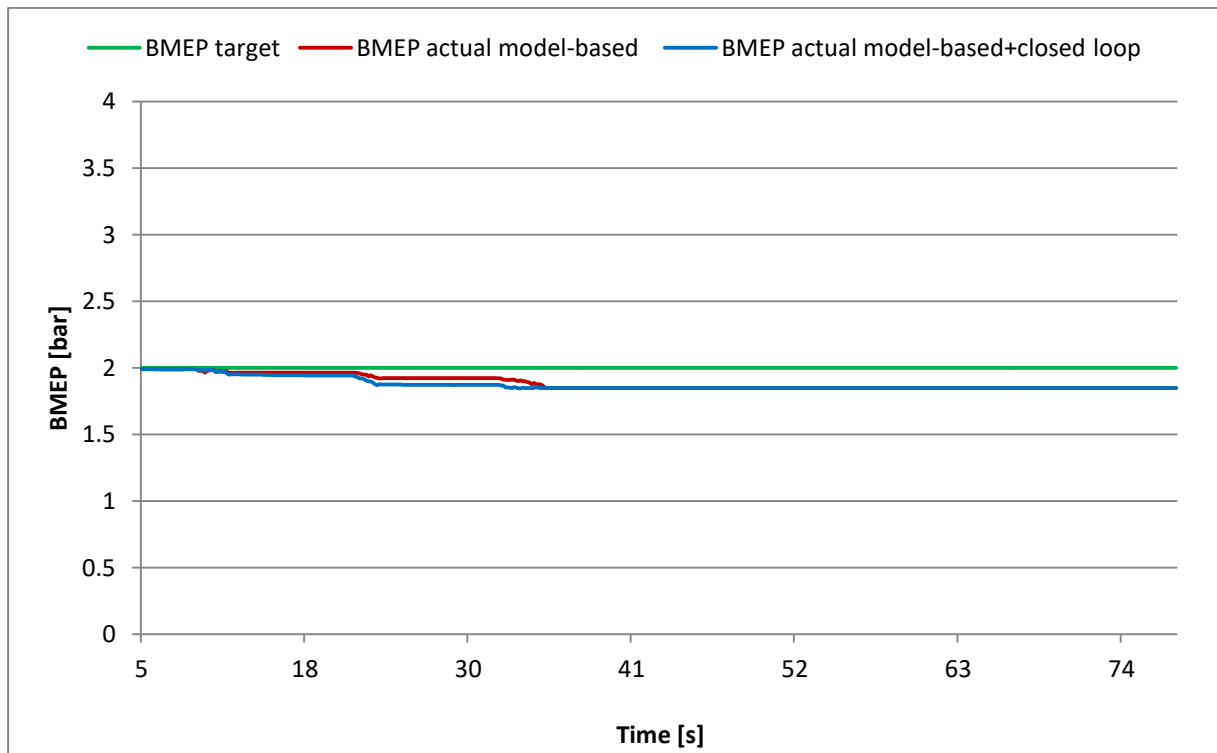


Figure 6.11: Model based control compared with Model Based/Closed Loop Control, BMEP target=2, BMEP results.

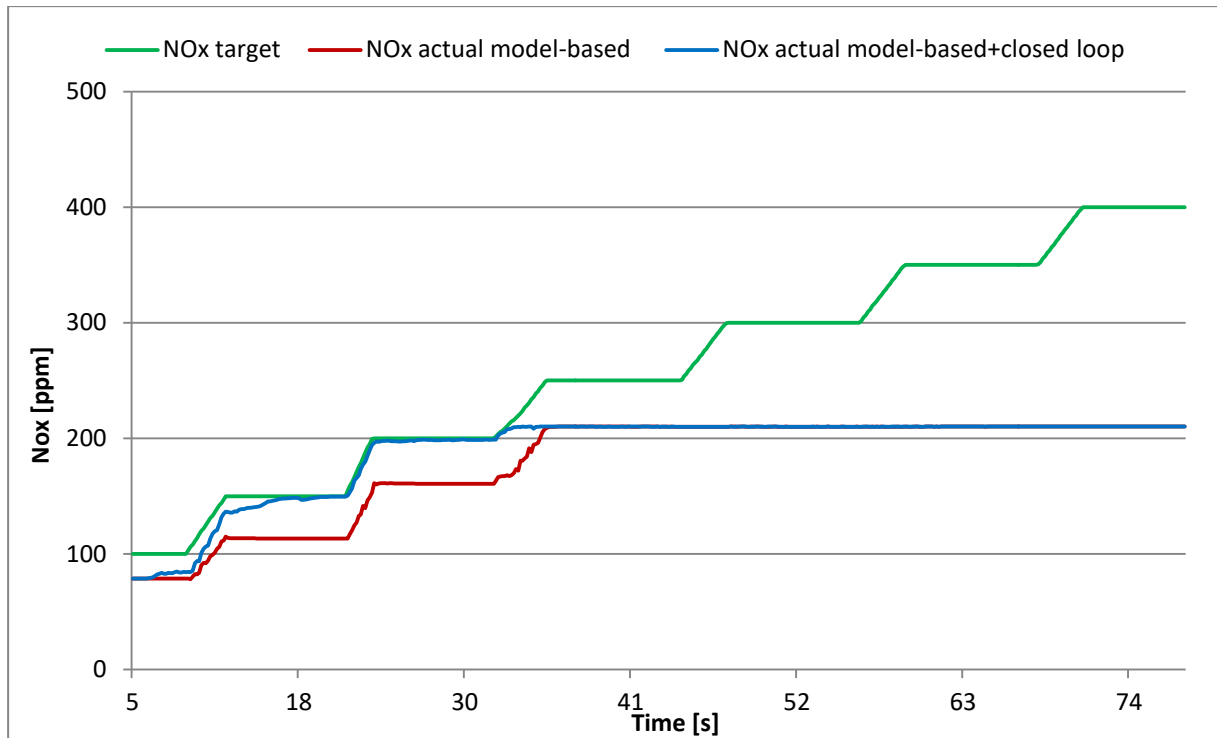


Figure 6.12: Model based control compared with Model Based/Closed Loop Control, BMEP target=2, NO_x results.

6.2.2 BMEP Target of 8 bar

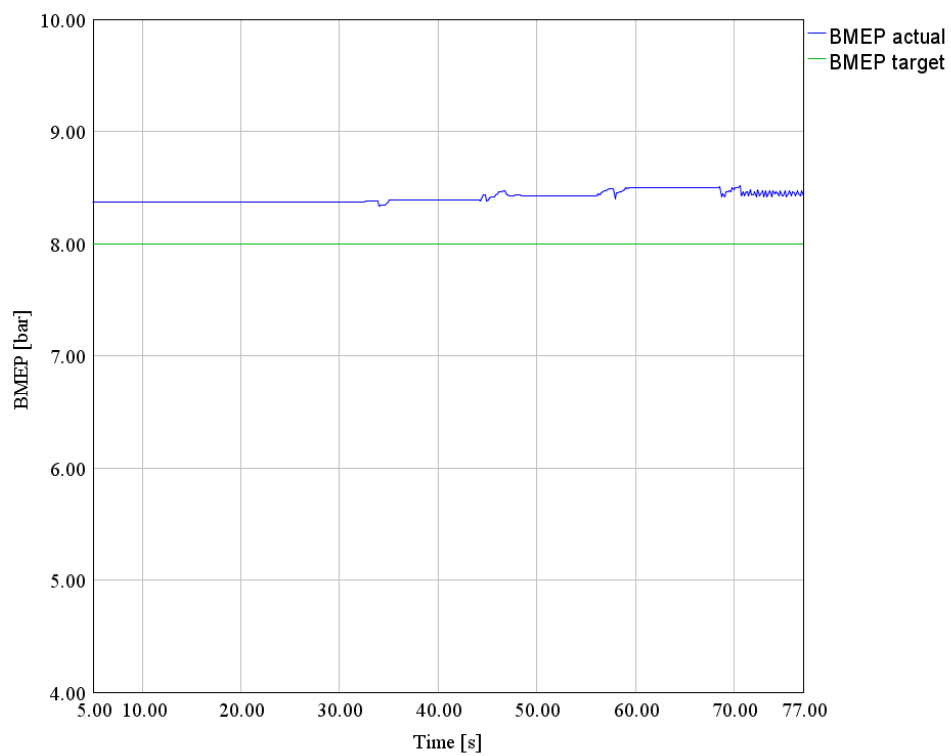


Figure 6.13: Model Based Control, BMEP target=8, BMEP result.

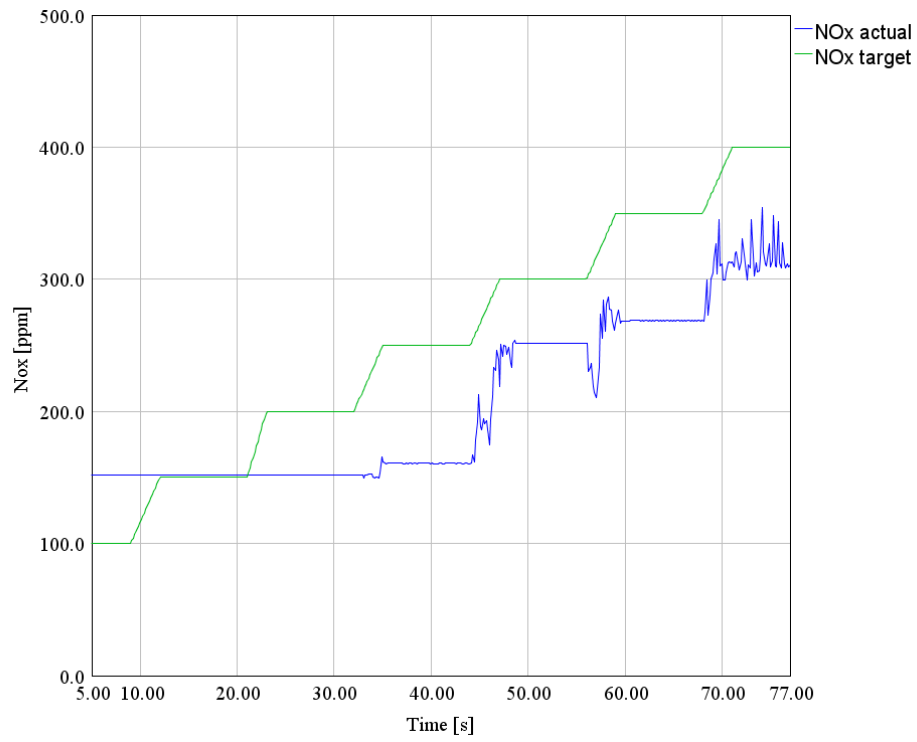


Figure 6.14: Model Based Control, BMEP target=8, NO_x result.

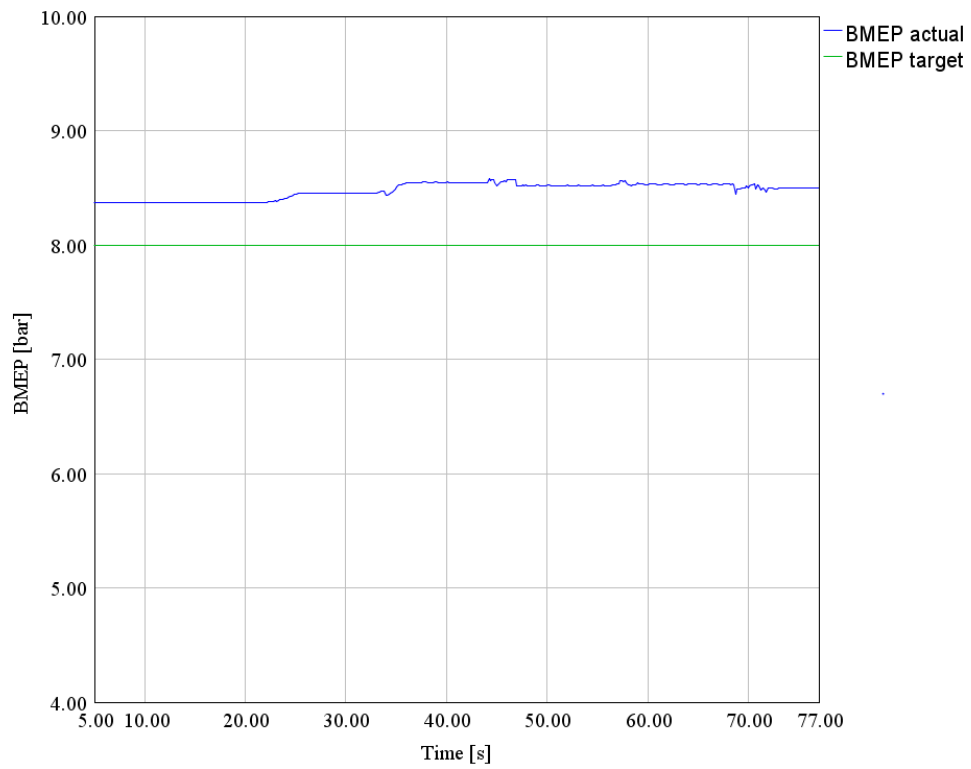


Figure 6.15: Model Based/Closed Loop control, BMEP target=8, BMEP result.

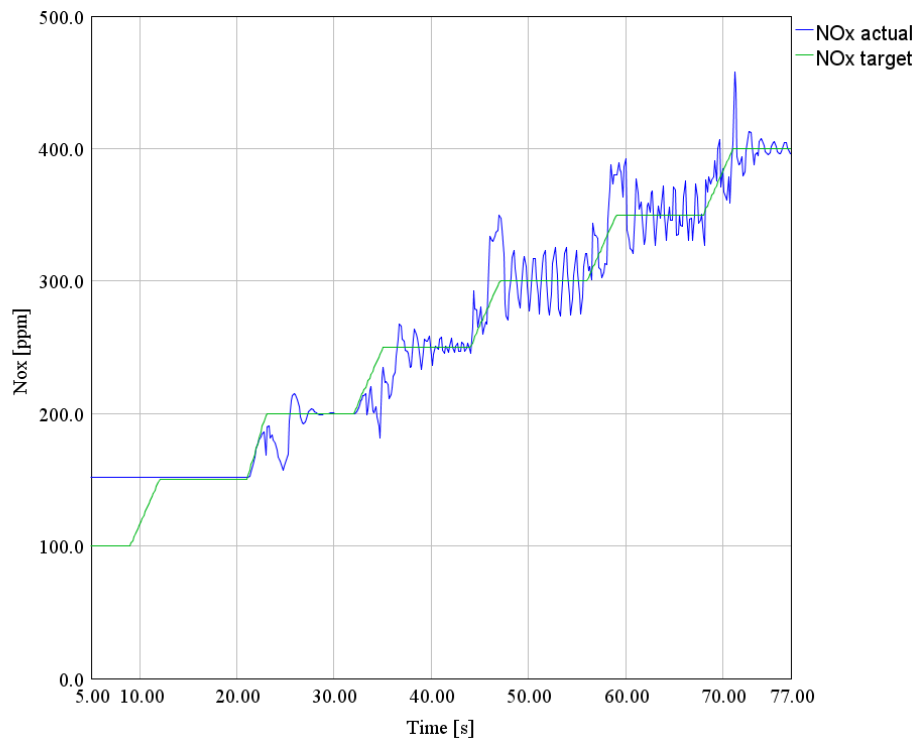


Figure 6.16: Model Based/Closed Loop control, BMEP target=8, NO_x result.

In the figures below, the results of the model based control integrated with the feedback loop are compared with those of the controller without the closed loop system.

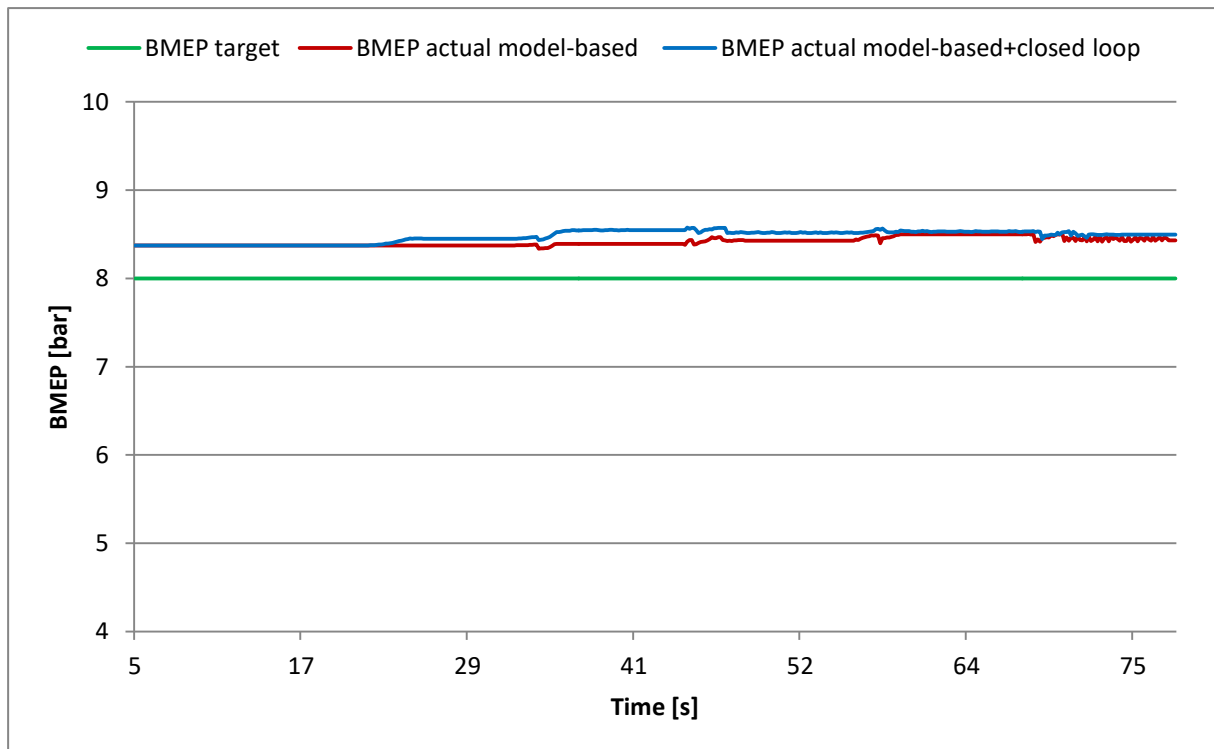


Figure 6.17: Model based control compared with Model Based/Closed Loop Control, BMEP target=8, BMEP results.

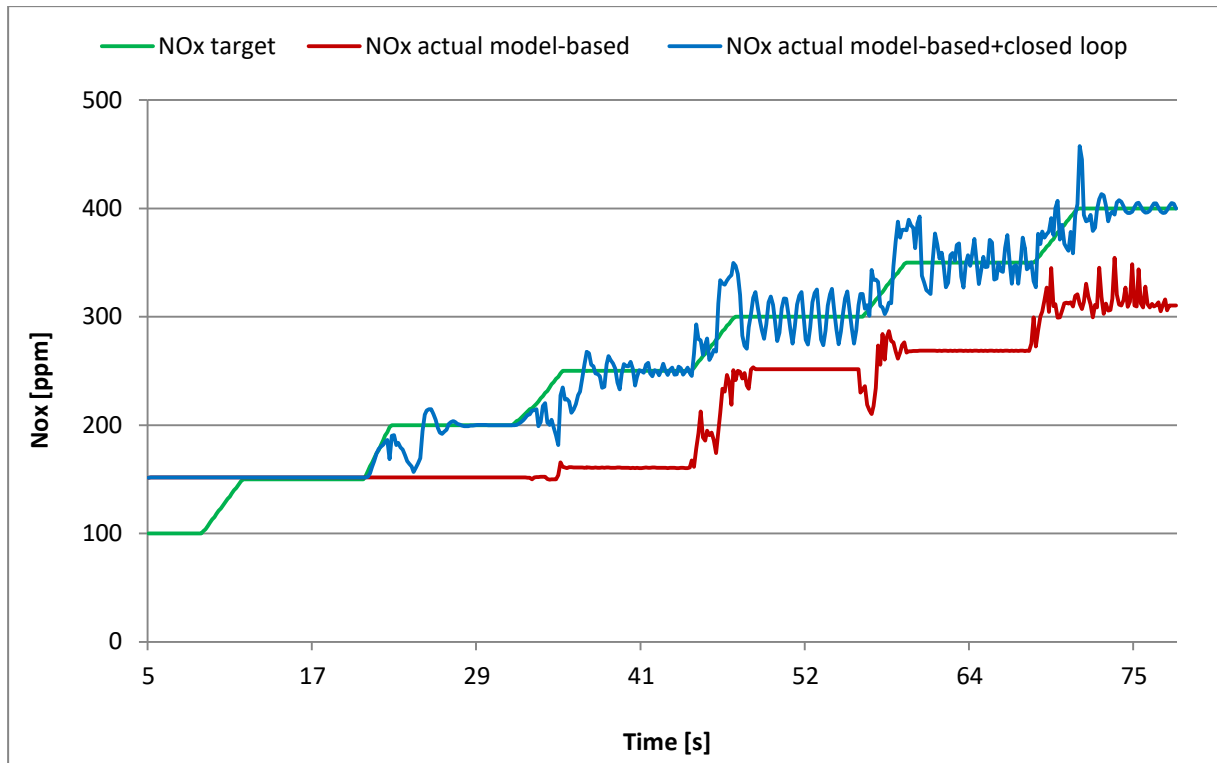


Figure 6.18: Model based control compared with Model Based/Closed Loop Control, BMEP target=8, NO_x results.

6.2.3 BMEP Target of 14 bar

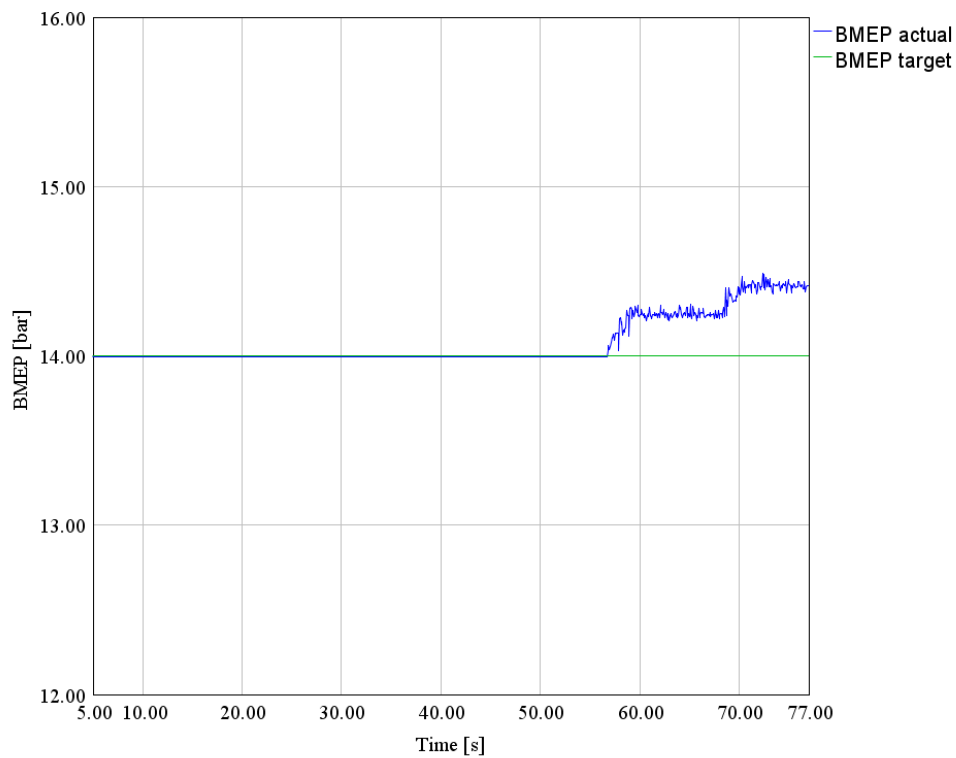


Figure 6.19: Model Based Control, BMEP target=14, BMEP result.

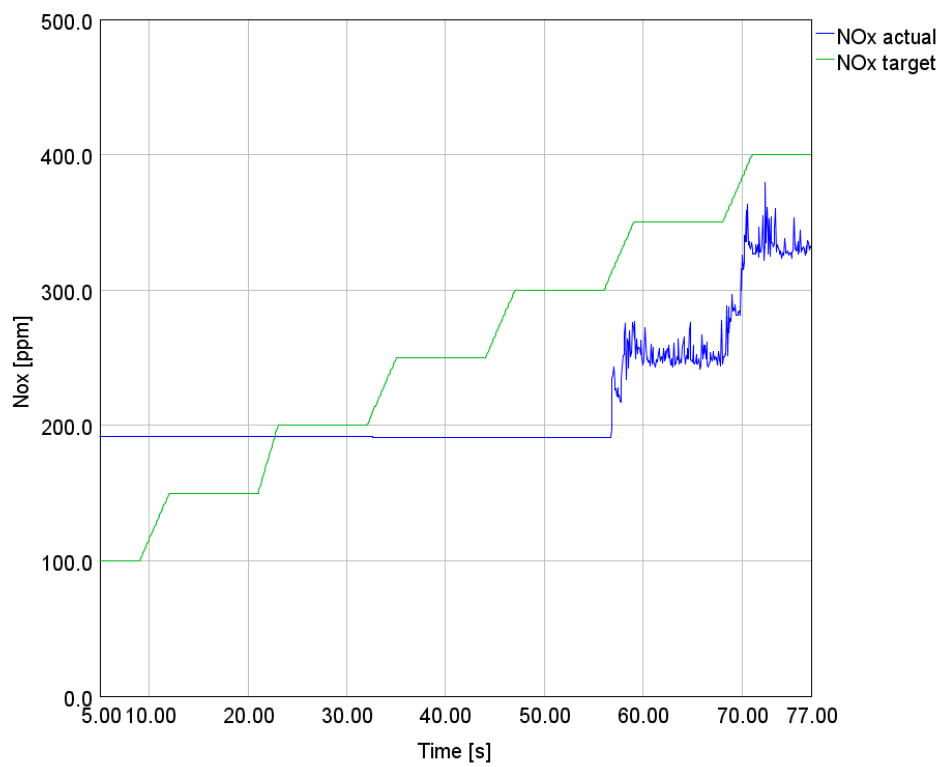


Figure 6.20: Model Based Control, BMEP target=14, NO_x result.

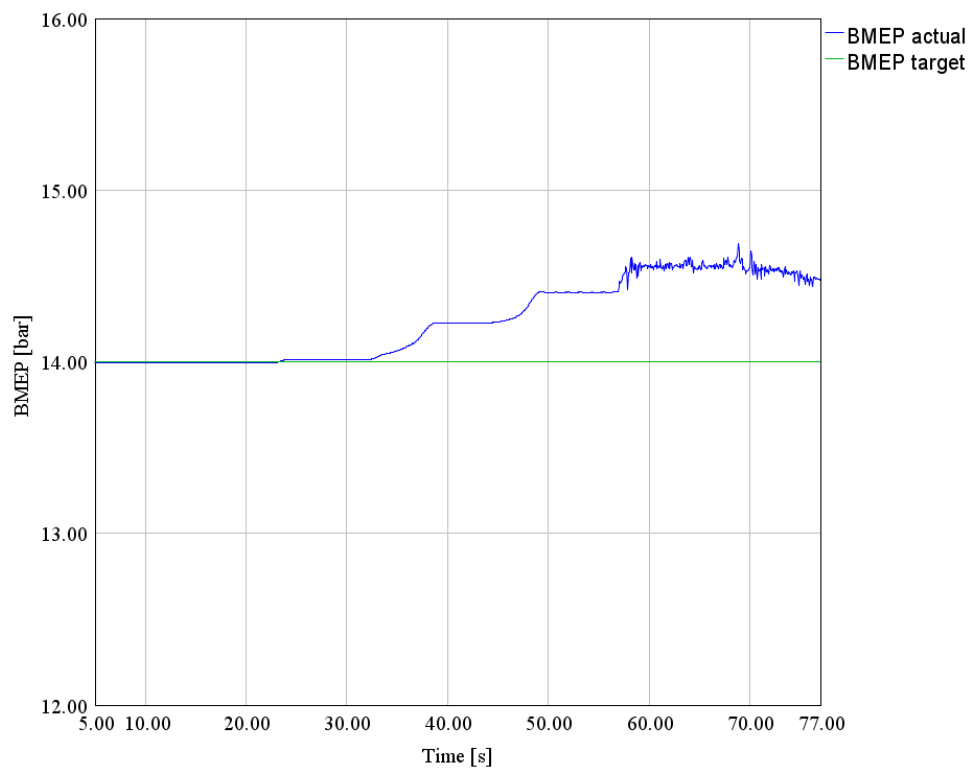


Figure 6.21: Model Based/Closed Loop control, BMEP target=14, BMEP result.

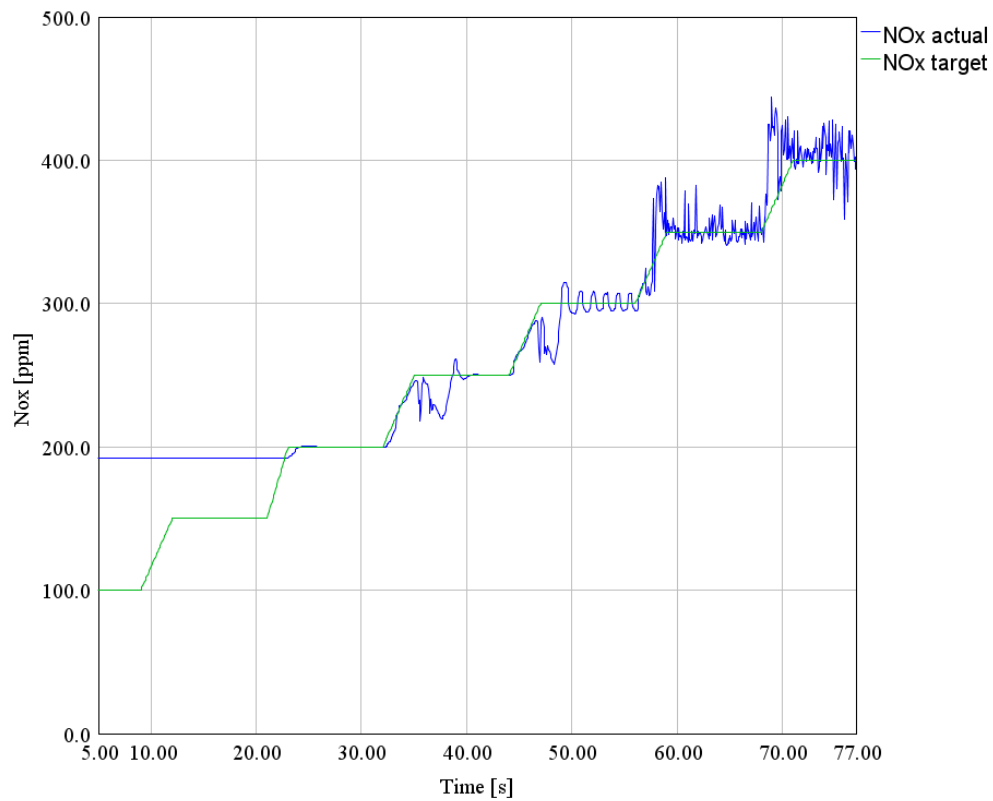


Figure 6.22: Model Based/Closed Loop control, BMEP target=14, NO_x result.

In the figures below, the results of the model based control integrated with the feedback loop are compared with those of the controller without the closed loop system.

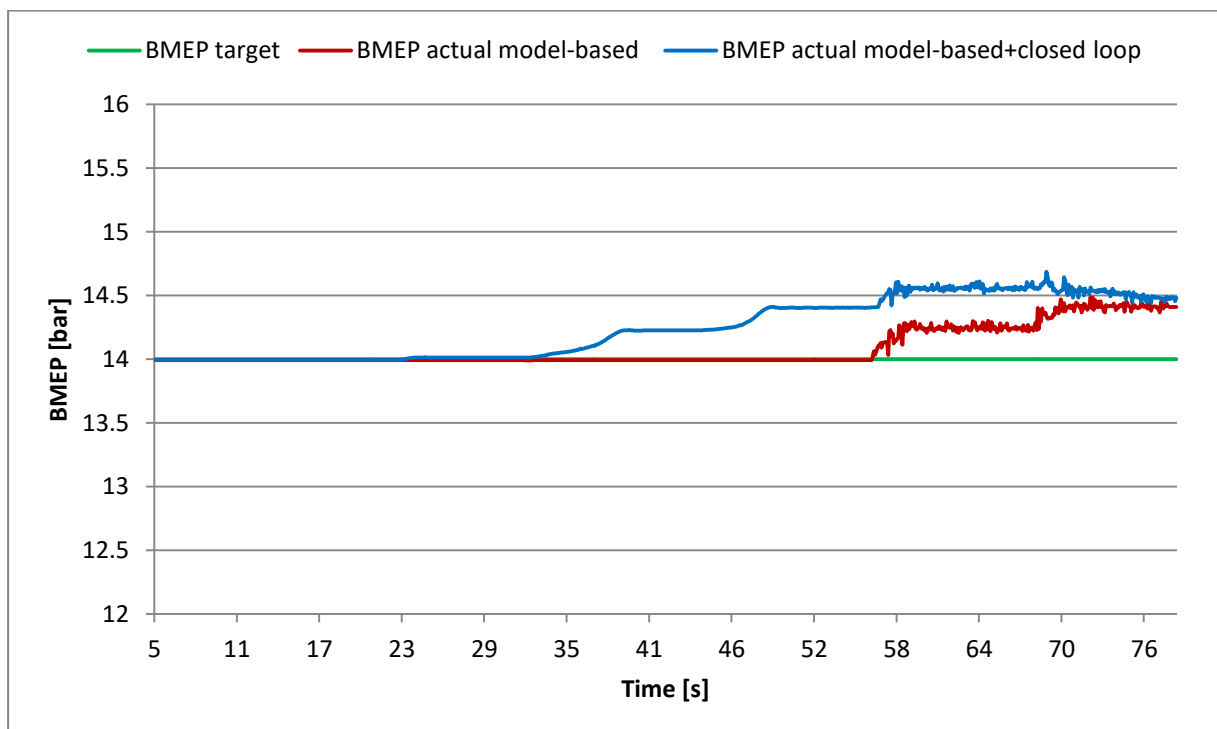


Figure 6.23: Model based control compared with Model Based/Closed Loop Control, BMEP target=14, BMEP results.

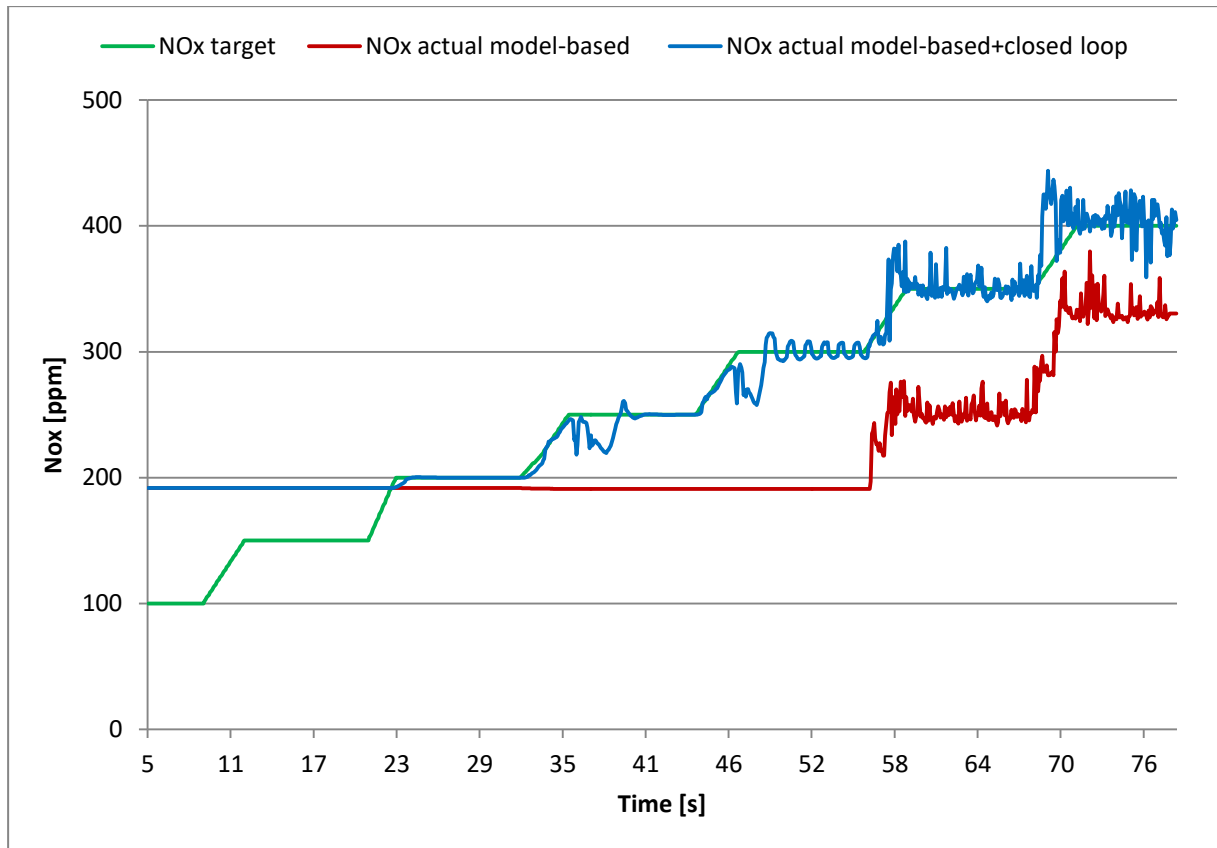


Figure 6.24: Model based control compared with Model Based/Closed Loop Control, BMEP target=8, NO_x results.

6.3 BMEP Target Profile, NO_x Target Profile and Speed Profile

The improvement in NO_x emissions obtained with the addition of the feedback control is further highlighted by the results of this test. This simulation was performed with a BMEP target profile, a speed profile and a NO_x target profile generated as a speed and load function.

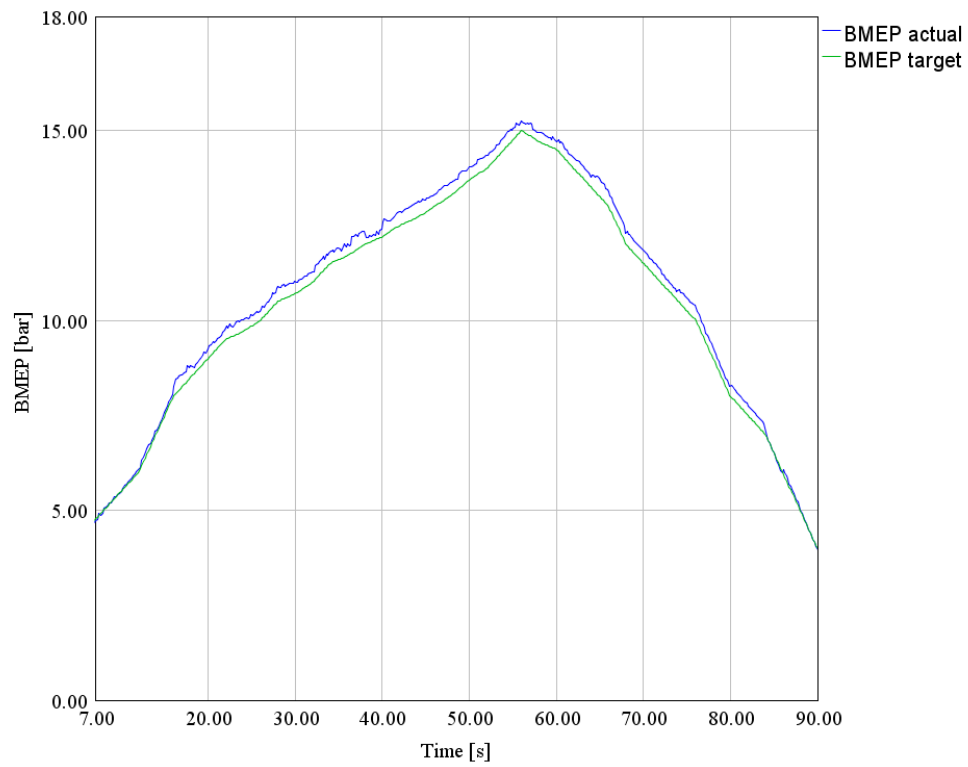


Figure 6.25: Model Based Control, BMEP result.

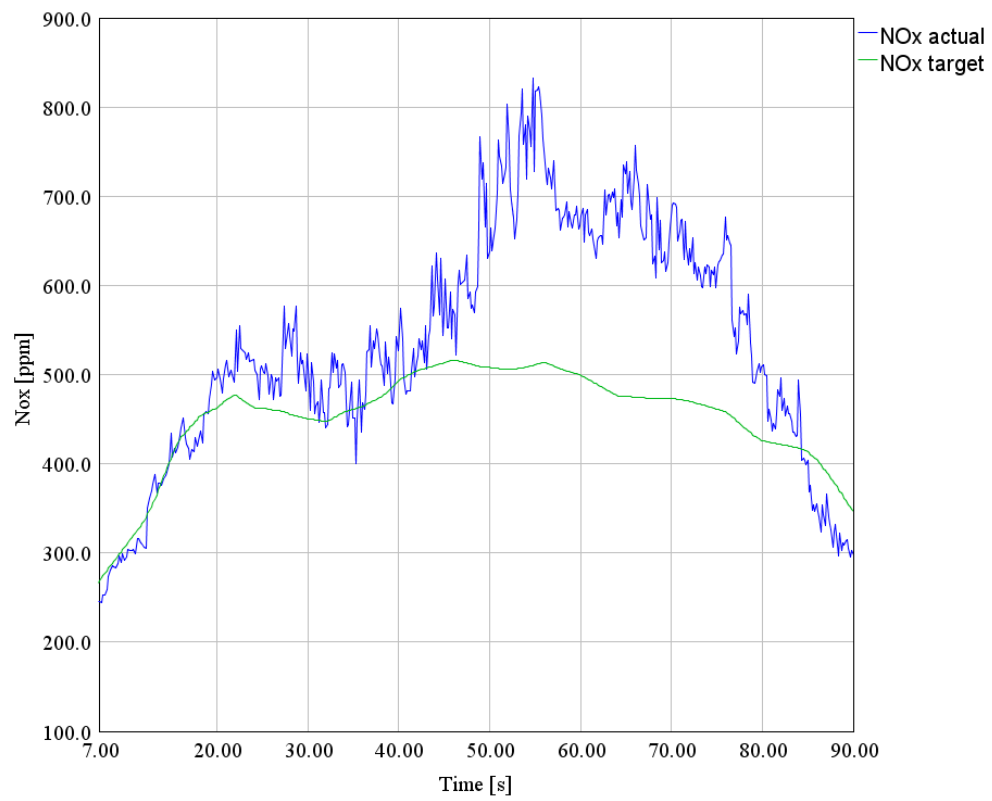


Figure 6.26: Model Based Control, NO_x result.

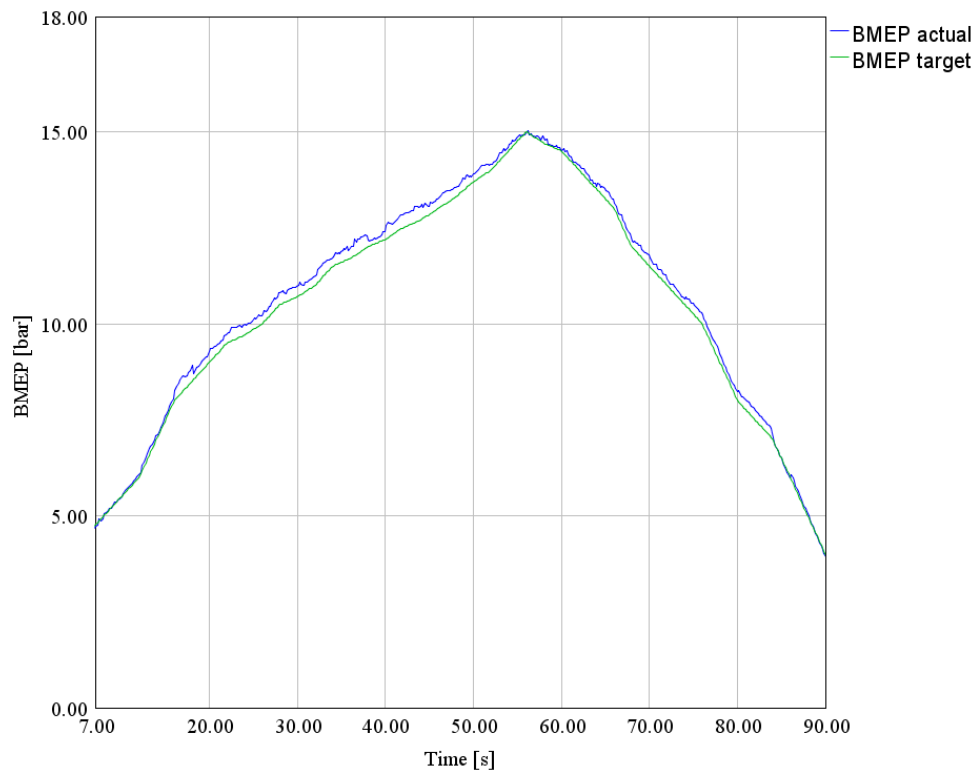


Figure 6.27: Model Based/Closed Loop Control, BMEP result.

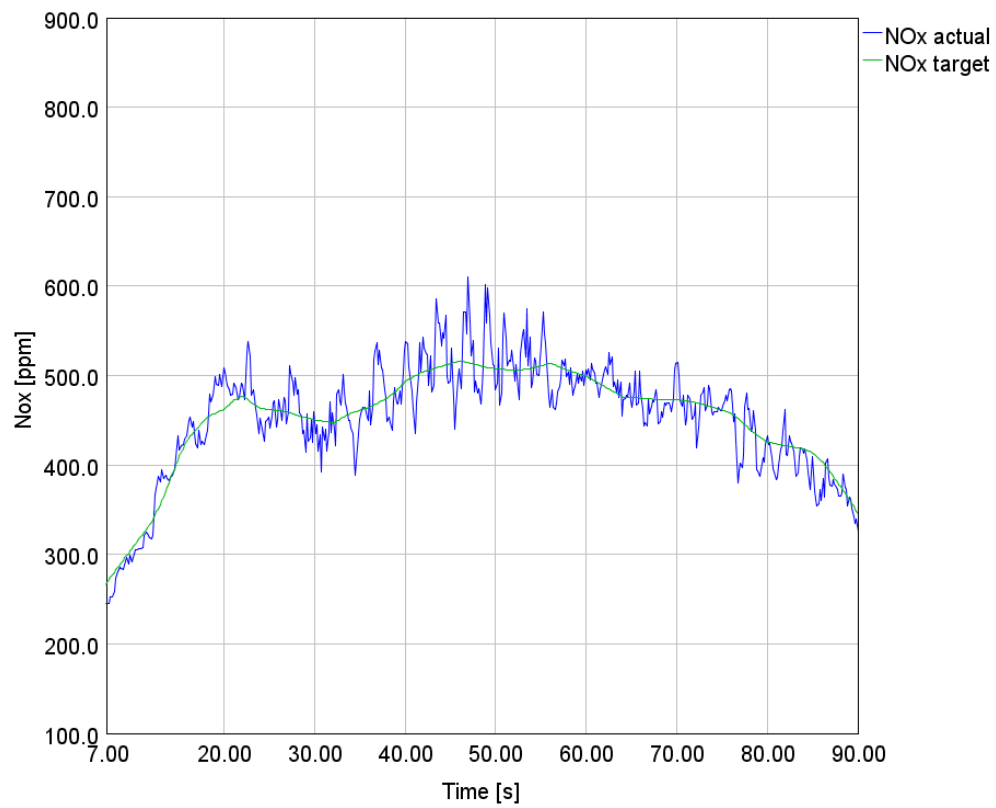


Figure 6.28: Model Based/Closed Loop Control, NO_x result.

In the figures below, the results of the model based control integrated with the feedback loop are compared with those of the controller without the closed loop system.

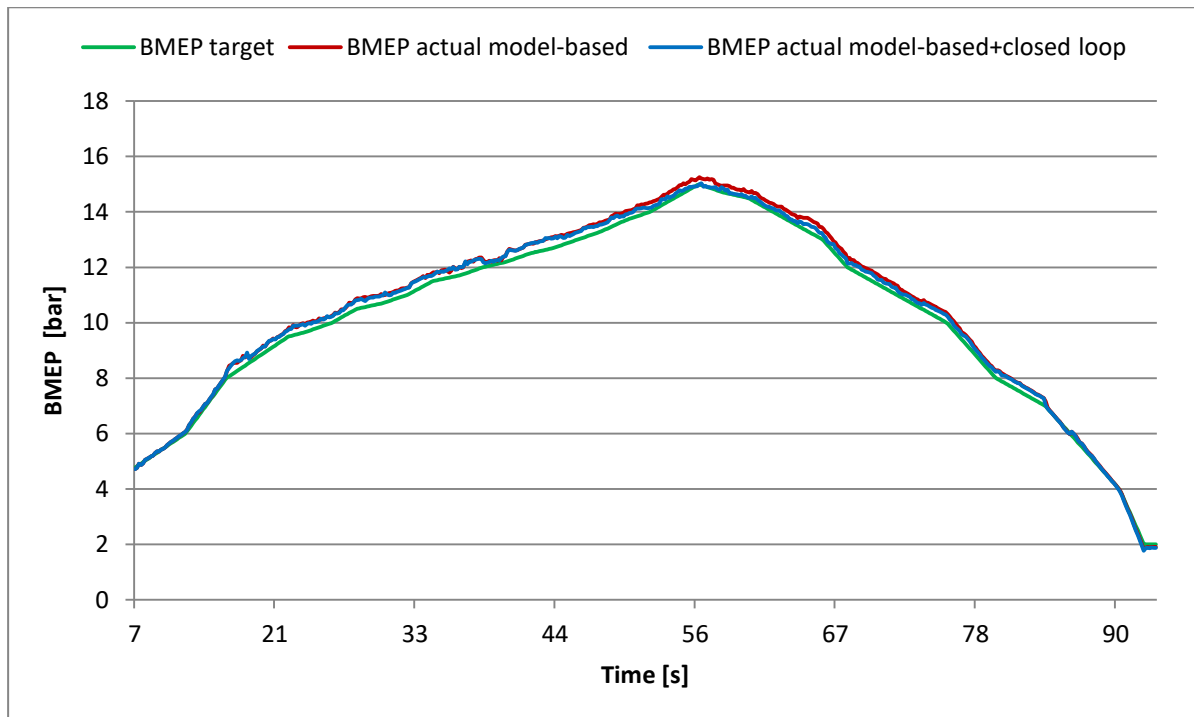


Figure 6.29: Model based control compared with Model Based/Closed Loop Control, BMEP results.

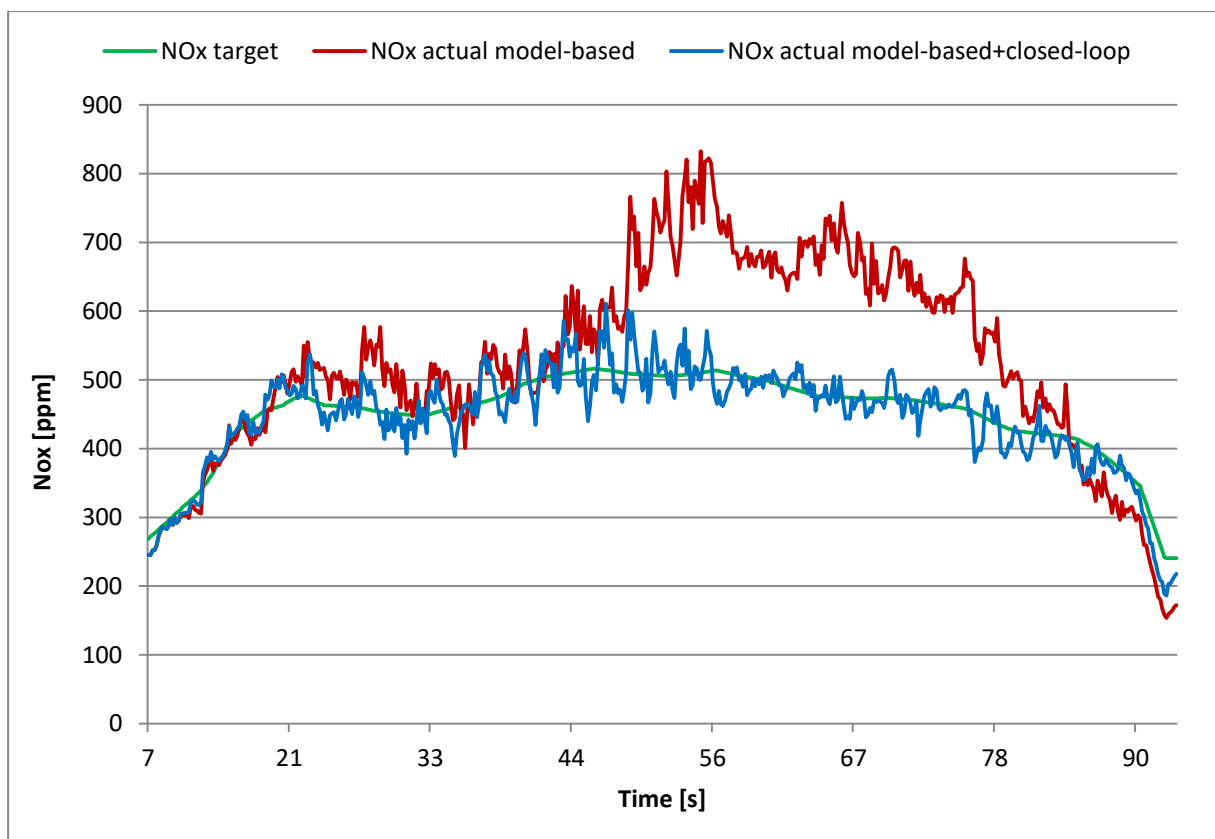


Figure 6.30: Model based control compared with Model Based/Closed Loop Control, NO_x results.

Chapter

7 Hardware in the Loop Results

The Hardware in the Loop phase aims at testing the real-time behavior of the integrated model base control with the closed loop one. This requires the conversion of the engine model, realized with GT Power, from fast running to mean value which uses neural networks instead of combustion model. In this study, the neural network model of the NO_x emissions was not available and consequently an alternative solution was developed to test the controller: in fact, a Simulink model was used in place of the mean value one. This model is able to estimate NO_x actual as a function of the start of injection variation, i.e. ΔSOI , according to the equation that follows:

$$NO_x \text{ actual} = NO_x \text{ nominal} + k * \Delta SOI$$

The coefficient k is determined by means of maps that depend on speed, BMEP and ΔSOI .

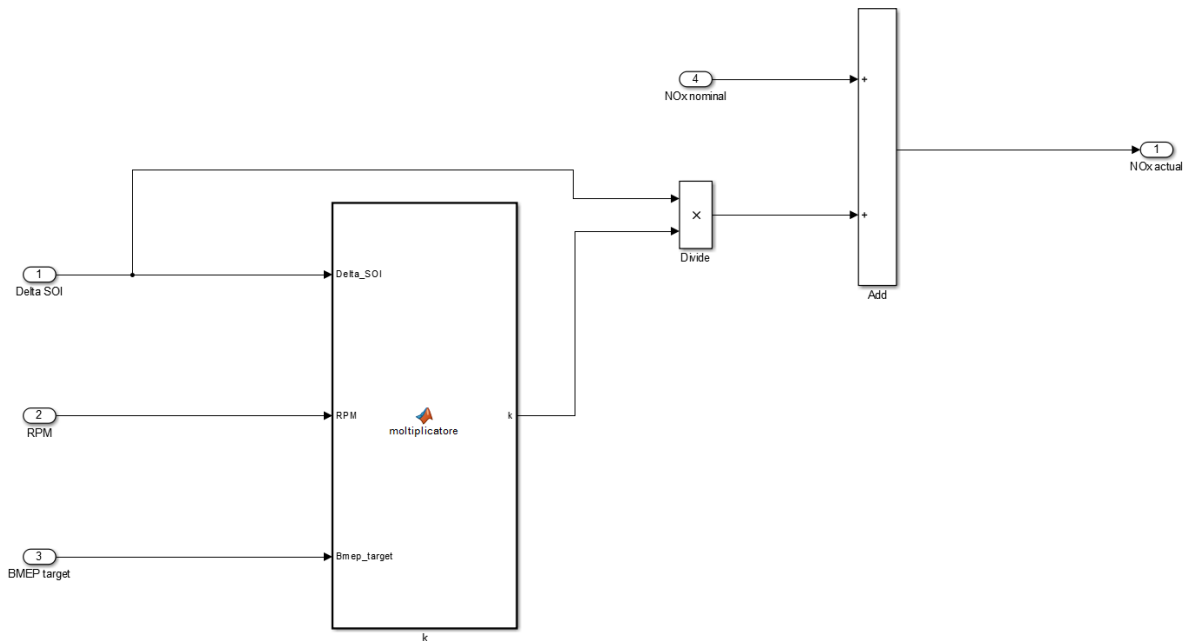


Figure 7.1: Simulink Engine Model.

As shown in figure 7.1, the only output is NO_x actual and consequently it is also the only input to the control system coming from the engine model. The remaining inputs, necessary for the control system, are passed as profiles acquired during the MiL tests. The procedure to perform the HiL test is the same as explained in paragraph 5.4; in this case, however, there is no .dat file to be downloaded to the PXI and the VeriStand project uses the model in figure 7.1 instead of the mean value one. The results obtained by this procedure are useful for understanding overall the real time behavior of the control system, but they do not fully reflect it, since the reference engine model is too simplified. Accurate results will be achieved once the neural networks have been developed.

The test carried out in this phase used the same BMEP target, speed and NO_x target profiles as the test described in paragraph 6.3. Therefore, the results of this test are expected to be similar to those obtained previously during the MiL phase.

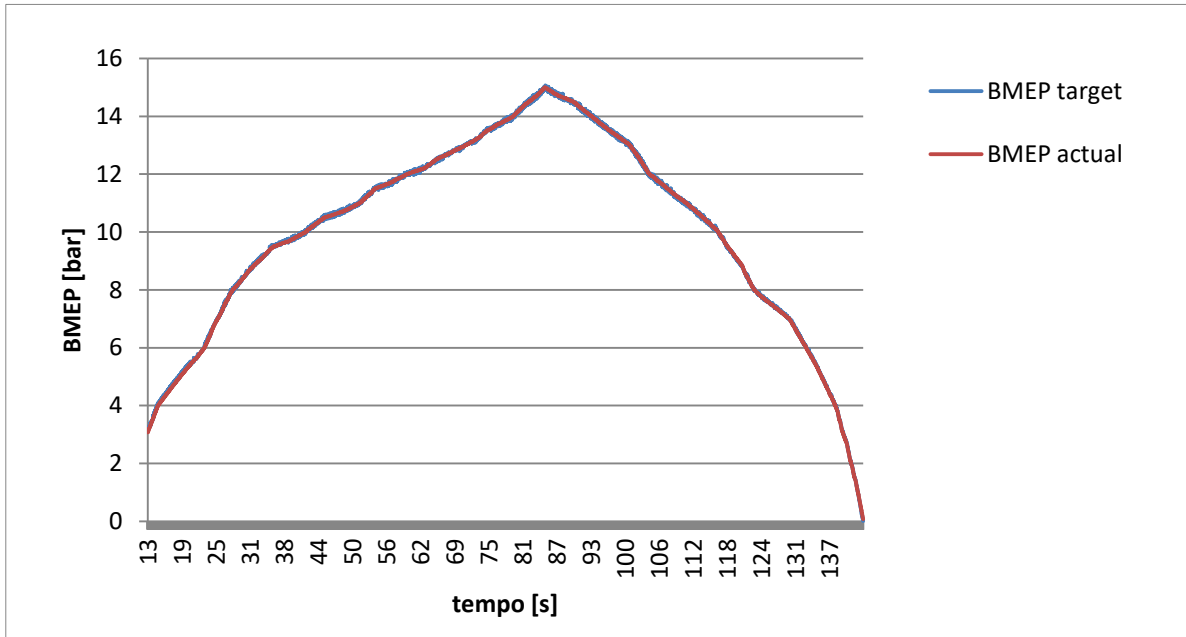


Figure 7.2: Model Based/Closed Loop Control, BMEP result.

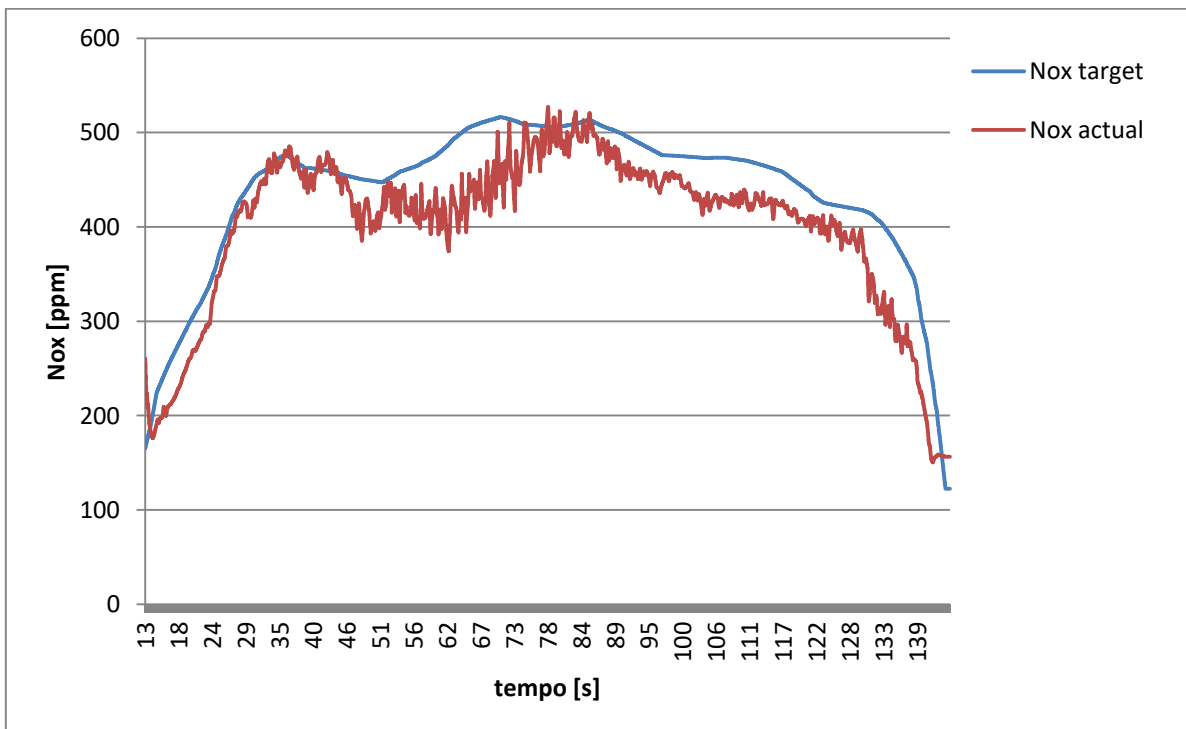


Figure 7.3: Model Based/Closed Loop Control, NO_x result.

Results of hardware in the loop phase show that BMEP accurately follows the target trend while NO_x deviates slightly from it. The reason why NO_x does not reach the target value, as it was during the model in the loop phase, is linked to the simplified engine model that was used.

An important parameter that has been determined during this phase is the NetRunTime that is the time necessary for the control system to evaluate the control parameters, i.e. SOI and q . This value fluctuates between a maximum and a minimum because the number of iterations required by the controller varies from one cycle to another.

i min	2
i max	10
i average	8

Table 7.1: Number of cycle iterations.

NetRunTime max [s]	0.0127
NetRunTime min [s]	0.0023
NetRunTime average [s]	0.0079

Table 7.2: NetRunTime.

The average NetRunTime is approximately 8 ms and the average number of cycle iterations is about 8. The average time required for iteration is calculated as ratio between the average NetRunTime and the average iterations for cycle. The result is about 1 ms at iteration.

Average iteration time	0.001
------------------------	-------

Table 7.3: Average iteration time.

Chapter

8 Conclusion

The goal of this study has been the development of an algorithm that controls brake mean effective pressure and nitrogen oxide emissions in a 3.0L compression ignition engine; for this purpose the parameters on which it acts are the start of injection of the main pulse and the injected fuel quantity. The control system consists of:

- Model Based Control of NO_x and BMEP.
- Closed Loop Control of NO_x .

The closed loop control has been added with the intention of improving the nitrogen oxide emissions as the model based control is not able to guarantee the imposed tolerance.

In this study, the algorithm validation procedure followed two phases and in both of them the engine is virtual. The two stages are:

- Model in the Loop.
- Hardware in the Loop.

During the Model in the loop phase, the algorithm has been tested at different speed and load conditions to prove its validity under different working conditions. During the Hardware in the loop phase, the controller has been implemented onto a rapid prototyping device to simulate its real time behavior. In the absence of neural networks, in the HiL phase, a Simulink engine model was used instead of the GT Power mean value model.

The results show that the developed algorithm is able to effectively control both nitrogen oxides and brake mean effective pressure and it has been discovered that each iteration requires a computational time of 1 ms on the ETAS ES910 device in agreement with the maximum engine speed constraint.

In the near future, the hardware in the loop phase will be repeated using a mean value engine model in order to obtain even more precise results. Subsequently the controller will be tested on the engine installed at the test bench through rapid prototyping. Furthermore, the controller will be further modified by increasing the number of control variables, for example EGR and boost pressure.

9 Bibliography

- [1] H. Gilles, "Model-Based Control of BMEP and NO_x Emissions in a Euro VI 3.0L Diesel Engine," 2017.
- [2] F. Millo, "Material of the Thermic Engines course".
- [3] E. Spessa, "Material of the Polluting Emissions course".
- [4] M. Brunello, "Development of a pressure-based algorithm to control IMEP and MFB₅₀ in a heavy-duty diesel engine and assessment by means of the HiL methodology".
- [5] R. Finesso, "A New Control-Oriented Semi-Empirical Approach to Predict Engine-Out NO_x Emissions in a Euro VI 3.0 L Diesel Engine".
- [6] R. Finesso, " HRR and MFB₅₀ Estimation in a Euro 6 Diesel Engine by Means of Control-Oriented Predictive Models".
- [7] J. Heywood, "Internal Combustion Engine Fundamentals".
- [8] S. D'Ambrosio, "A Control Oriented Real-Time Semi-Empirical Model for the Prediction of NO_x Emissions in Diesel Engines".
- [9] R. Finesso, ""Development and Validation of a Real-Time Model for the Simulation of the Heat Release Rate, InCylinder Pressure and Pollutant Emissions in Diesel Engines".